

**STRUCTURAL DAMAGE DETECTION USING FREQUENCY
RESPONSE FUNCTIONS**

A Thesis

by

SELCUK DINCAL

Submitted to the Office of Graduate Studies of
Texas A&M University
in partial fulfillment of the requirements for the degree of

MASTER OF SCIENCE

December 2005

Major Subject: Civil Engineering

**STRUCTURAL DAMAGE DETECTION USING FREQUENCY
RESPONSE FUNCTIONS**

A Thesis

by

SELCUK DINCAL

Submitted to the Office of Graduate Studies of
Texas A&M University
in partial fulfillment of the requirements for the degree of

MASTER OF SCIENCE

Approved by:

Chair of Committee, Anne M. Raich
Committee Members, Harry L. Jones
N.K. Anand
Head of Department, David V. Rosowsky

December 2005

Major Subject: Civil Engineering

ABSTRACT

Structural Damage Detection Using Frequency

Response Functions. (December 2005)

Selcuk Dincal, B.S., Osmangazi University, Eskisehir, Turkey

Chair of Advisory Committee: Dr. Anne M. Raich

This research investigates the performance of an existing structural damage detection method (SDIM) when only experimentally-obtained measurement information can be used to calculate the frequency response functions used to detect damage. The development of a SDIM that can accurately identify damage while processing measurements containing realistic noise levels and overcoming experimental modeling errors would provide a robust method for identifying damage in the larger, more complex structures found in practice. The existing SDIM program, GaDamDet, uses an advanced genetic algorithm, along with a two-dimensional finite element model of the structure, to identify the location and the severity of damage using the linear vibration information contained in frequency response functions (FRF) as response signatures. Datagen is a Matlab program that simulates the three-dimensional dynamic response of the four-story, two-bay by two-bay UBC test structure built at the University of British Columbia. The dynamic response of the structure can be obtained for a range of preset damage cases or for any user-defined damage case. Datagen can be used to provide the FRF measurement information for the three-dimensional test structure. Therefore, using the FRF measurements obtained from the UBC test structure allows for a more realistic evaluation of the performance of the SDIM provided by GaDamDet as the impact on performance of more realistic noise and model errors can be investigated. Previous studies evaluated the performance of the SDIM using only simulated FRF measurements obtained from a two-dimensional structural model. In addition, the disparity between the

two-dimensional model used by the SDIM used to identify damage and the measurements obtained from the three-dimensional test structure is analyzed.

The research results indicate that the SDIM is able to accurately detect structural damage to individually damaged members or to within a damaged floor, with few false damages identified. The SDIM provides an easy to use, visual, and accurate algorithm and its performance compares favorably to performance of the various damage detection algorithms that have been proposed by researchers to detect damage in the three-dimensional structural benchmark problem.

DEDICATION

To my parents Sevki and Ayla Dincal,
and my dear Paola

ACKNOWLEDGEMENTS

I would like to thank to Dr. Anne M. Raich, for the guidance and support that she has given me throughout the research and Dr. Harry Jones and Dr. N.K. Anand for their willingness to be on the advisory committee as well as the contributions they have made. Special thanks to Dr. Tamas Liskai and Dr. Norris Stubbs for their inspiring advice and critiques. This research wouldn't have been completed without their valuable suggestions.

Finally, I would like to thank and dedicate this work to my parents Sevki and Ayla Dincal and my dear Paolita that always has been there for me.

TABLE OF CONTENTS

	Page
ABSTRACT	iii
DEDICATION	v
ACKNOWLEDGEMENTS	vi
TABLE OF CONTENTS	vii
LIST OF FIGURES.....	x
LIST OF TABLES	xvi
1 INTRODUCTION.....	1
1.1 Overview	1
1.2 Research Objectives	1
1.3 Background.....	2
1.3.1 Frequency Response Functions for Damage Detection	3
1.3.2 Description of UBC Structural Benchmark Problem	4
1.4 Organization of the Thesis.....	6
2 HYBRID STRUCTURAL DAMAGE IDENTIFICATION METHODOLOGY.....	8
2.1 Description of the Structural Damage Identification Program GaDamDet.....	8
2.1.1 Detecting Structural Damage Using GaDamDet.....	8
2.1.2 Running GaDamDet	11
2.2 Description of the Experimental Response Measurement Program Datagen.....	16
2.2.1 Definition of UBC Test Structure	19
2.3 Discussion of the Hybrid Structural Damage Identification Method Proposed	21
2.3.1 Modifications Required in the Finite Element Model Used by GaDamdet.....	22
2.3.2 Modifications Required in the Measurement/Excitation Pairs.....	24
2.3.3 Required Input/Output Parameters in Datagen	25
3 FREQUENCY RESPONSE FUNCTIONS	28
3.1 Random Data	28
3.1.1 Stationary Random Data	29

	Page
3.1.1.1 Ergodic Stationary Random Data	30
3.2 Analysis of Random Data.....	30
3.3 Input/Output Relations	33
3.4 Basic Dynamic Characteristics.....	34
3.5 Frequency Response Functions	37
3.6 Single-Input/Output Relationships	38
3.6.1 Single-Input/Single-Output Models	38
3.6.2 Single-Input/Multiple-Output Models.....	43
3.7 Multiple-Input/Output Relationships	45
3.7.1 Multiple-Input/Single-Output Models.....	45
3.7.1.1 Two-Input/One-Output Models	50
3.7.1.2 Multiple Coherence Functions.....	53
3.7.1.3 Conditioned Spectral Density Functions	54
3.7.1.4 Partial Coherence Functions	58
3.7.2 General and Conditioned Multiple-Input Models	59
3.7.2.1 Algorithm for Conditioned Spectra and Frequency Response Functions	62
Spectral Density and Frequency Response Functions Using Matrix Calculations	65
3.7.2.3 Partial and Multiple Coherence Functions	67
4 ANALYSIS MODELS FOR BENCHMARK TEST CASES	70
4.1 Single-Input/Multiple-Output Model	73
4.2 Multiple-Input/Multiple-Output Model.....	76
5 RESULTS AND DISCUSSIONS	84
5.1 Single-Input/Multiple-Output Model	85
5.1.1 Case 3: 1 st Story Braces Are Damaged	85
5.1.1.1 All Four Modes Are Used for Damage Detection	87
5.1.1.2 The Last Mode Is Omitted for Damage Detection	90
5.1.2 Case 3: 1 st - 3 rd Story Braces Are Damaged	92
5.1.2.1 All Four Modes Are Used for Damage Detection	95
5.1.2.2 The Last Two Modes Are Omitted for Damage Detection	97
5.1.3 Case 3: 2 nd Story Braces Are Damaged	100
5.1.4 Case 4: 1 st Story Braces Are Damaged.....	101
5.1.5 Case 4: 1 st - 3 rd Story Braces Are Damaged	104
5.1.6 Case 5: 1 st Story Braces Are Damaged.....	106
5.1.7 Case 5: 1 st - 3 rd Story Braces Are Damaged	110
5.2 Multiple-Input/Single-Output Model	113
5.2.1 Case 1: 1 st Story Braces Are Damaged	113

	Page
5.2.1.1	The Measurement Is Taken From the First Floor (at Node 7)..... 113
5.2.1.2	The Measurement Is Taken From The Second Floor (at Node 8) 116
5.2.2	Case 1: 1 st - 3 rd Story Braces Are Damaged 118
5.3	Multiple-Input/Multiple-Output Model..... 120
5.3.1	Case 1: 1 st Story Braces Are Damaged 121
5.3.1.1	All Four Modes Are Used for Damage Detection 124
5.3.1.2	The Last Mode Is Omitted for Damage Detection 126
5.3.2	Case 1: 1 st - 3 rd Story Braces Are Damaged 127
5.3.2.1	All Four Modes Are Used for Damage Detection 130
5.3.2.2	First Two Modes Are Used for Damage Detection 132
5.3.3	Case 1: 3 rd Story Braces Are Damaged 134
5.3.4	Case 2: 1 st Story Braces Are Damaged 135
5.3.5	Case 2: 1 st - 3 rd Story Braces Are Damaged 138
5.4	Effect of Noise on Performance of the SDIM 141
5.4.1	SIMO Model: 1 st Story Braces Are Damaged Using Case 3 (10% Noise)..... 142
5.4.2	MISO Model: 1 st Story Braces Are Damaged Using Case 1 (10% Noise)..... 144
5.4.3	MIMO Model: 1 st Story Braces Are Damaged Using Case 1 (10% Noise)..... 147
6	SUMMARY AND CONCLUSIONS..... 150
6.1	Future Recommendations..... 152
	REFERENCES 154
	APPENDIX A 157
	APPENDIX B 162
	VITA 164

LIST OF FIGURES

	Page
Figure 2.1 Main Menu Structure of <i>GaDamDet</i> Program	11
Figure 2.2 Settings Menu and Its Toolbar.....	12
Figure 2.3 Finite Element Model Input and Matlab Measurement Data Files.....	13
Figure 2.4 Genetic Algorithm Parameter Sheet	14
Figure 2.5 Structure Plot Option in <i>GaDamDet</i>	15
Figure 2.6 Damage Cases Defined by <i>Datagen</i> for the UBC Benchmark Problem...	17
Figure 2.7 <i>Datagen</i> Case IDs.....	18
Figure 2.8 <i>Datagen</i> Parameter Sheet	19
Figure 2.9 UBC Test Structure.....	20
Figure 2.10 Input/Output Parameters for the Multiple-Input/Multiple-Output Model (Only in Weak Direction)	26
Figure 2.11 Input/Output Parameters for the Single-Input/Multiple-Output Model (Both in Weak and Strong Direction)	26
Figure 3.1 Single-Input/Single-Output System with Output Noise	33
Figure 3.2 Single-Input/Multiple-Output System with Output Noise.....	35
Figure 3.3 Single-Input/Multiple-Output System	44
Figure 3.4 Multiple-Input/Single-Output System	46
Figure 3.5 Two-Input/One-Output System with Output Noise.....	51
Figure 3.6 Decomposition of $x_2(t)$ from $x_1(t)$	55
Figure 3.7 Two-Input/One-Output Model with Mutually Uncorrelated Inputs	57
Figure 3.8 Multiple-Input Model for Arbitrary Inputs.....	60

	Page
Figure 3.9 Multiple-Input Model for Ordered Conditioned Inputs	61
Figure 4.1 Node Numbering for 2-D Finite Element Model.....	70
Figure 4.2 Element Numbering for 2-D Finite Element Model	70
Figure 4.3 Input/Output Locations for the Single-Input/Multiple-Output Model.....	72
Figure 4.4 Input/Output Locations for the Multiple-Input/Multiple-Output Model ..	72
Figure 4.5 Cross-Spectrum Function Between Force Input at Roof Level and Acceleration Output at the First Floor in the Weak Direction	74
Figure 4.6 Frequency Response Function Between Force Input at Roof Level and Acceleration Output at the First Floor in the Weak Direction	75
Figure 4.7 Ordinary Coherence Function Between Force Input at Roof Level and Acceleration Output at the First Floor in the Weak Direction	75
Figure 4.8 Ordinary Coherence Function Between Force Input at the First and Second Floor	76
Figure 4.9 Ordinary Coherence Function Between Force Input and Acceleration Output at the First Floor	77
Figure 4.10 Multiple Coherence Function Between the Output (First Floor Acceleration) and the Given Inputs (Forces in each Story)	78
Figure 4.11 FRF for 12/7 Excitation/Masurement Pair for the MIMO Problem	80
Figure 4.12 FRF for 13/8 Excitation/Masurement Pair for the MIMO Problem	81
Figure 4.13 FRF for 13/7 Excitation/Masurement Pair for the MISO Problem	82
Figure 4.14 FRF for 14/7 Excitation/Masurement Pair for the MISO Problem	83
Figure 5.1 FRF for the 1 st Floor – 1 st Story Braces Are Broken SIMO – 12 DOF Symmetric Model	85
Figure 5.2 FRF for the 2 nd Floor – 1 st Story Braces Are Broken SIMO – 12 DOF Symmetric Model	86

	Page
Figure 5.3 FRF for the 3 rd Floor – 1 st Story Braces Are Broken SIMO – 12 DOF Symmetric Model	86
Figure 5.4 FRF for the 4 th Floor – 1 st Story Braces Are Broken SIMO – 12 DOF Symmetric Model	87
Figure 5.5 Simulated vs. Detected Damages for Trial #1	88
Figure 5.6 Simulated vs. Detected Damages for Trial #1 with Hillclimbing #1867	90
Figure 5.7 Simulated vs. Detected Damages for Trial #2 with Hillclimbing #739	92
Figure 5.8 FRF for the 1 st Floor – 1 st - 3 rd Story Braces Are Broken SIMO – 12 DOF Symmetric Model	93
Figure 5.9 FRF for the 2 nd Floor – 1 st - 3 rd Story Braces Are Broken SIMO – 12 DOF Symmetric Model	93
Figure 5.10 FRF for the 3 rd Floor – 1 st - 3 rd Story Braces Are Broken SIMO – 12 DOF Symmetric Model	94
Figure 5.11 FRF for the 4 th Floor – 1 st - 3 rd Story Braces Are Broken SIMO – 12 DOF Symmetric Model	94
Figure 5.12 Simulated vs. Detected Damages for Trial #3 with Hillclimbing #178	96
Figure 5.13 Simulated vs. Detected Damages for Trial #4	99
Figure 5.14 Simulated vs. Detected Damages for Trial #4 with Hillclimbing #1489	99
Figure 5.15 Simulated vs. Detected Damages for Trial #5	101
Figure 5.16 FRF for the 1 st Floor – 1 st Story Braces Are Broken SIMO – 12 DOF Asymmetric Model	102
Figure 5.17 Simulated vs. Detected Damages for Trial #6 with Hillclimbing #667	104

	Page
Figure 5.18 FRF for the 1 st Floor – 1 st - 3 rd Story Braces Are Broken SIMO – 12 DOF Asymmetric Model	105
Figure 5.19 Simulated vs. Detected Damages for Trial #7 with Hillclimbing #580	107
Figure 5.20 FRF for the 1 st Floor – 1 st Story Braces Are Broken SIMO – 120 DOF Asymmetric Model	107
Figure 5.21 Simulated vs. Detected Damages for Trial #8 with Hillclimbing #519	109
Figure 5.22 FRF for the 1 st Floor – 1 st - 3 rd Story Braces Are Broken SIMO – 120 DOF Asymmetric Model	110
Figure 5.23 Simulated vs. Detected Damages for Trial #9 with Hillclimbing #1575	112
Figure 5.24 FRF for the 1 st Floor – 1 st Story Braces Are Broken MISO – 12 DOF Symmetric Model	114
Figure 5.25 Simulated vs. Detected Damages for Trial #10 with Hillclimbing #8693	116
Figure 5.26 Simulated vs. Detected Damages for Trial #11 with Hillclimbing #160	118
Figure 5.27 FRF for the 1 st Floor – 1 st - 3 rd Story Braces Are Broken MISO – 12 DOF Symmetric Model	119
Figure 5.28 Simulated vs. Detected Damages for Trial #12 with Hillclimbing #9903	121
Figure 5.29 FRF for the 1 st Floor – 1 st Story Braces Are Broken MIMO – 12 DOF Symmetric Model	122
Figure 5.30 FRF for the 2 nd Floor – 1 st Story Braces Are Broken MIMO – 12 DOF Symmetric Model	122
Figure 5.31 FRF for the 3 rd Floor – 1 st Story Braces Are Broken MIMO – 12 DOF Symmetric Model	123

	Page
Figure 5.32 FRF for the 4 th Floor – 1 st Story Braces Are Broken MIMO – 12 DOF Symmetric Model	123
Figure 5.33 Simulated vs. Detected Damages for Trial #13 with Hillclimbing #3395	125
Figure 5.34 Simulated vs. Detected Damages for Trial #14 with Hillclimbing #1232	127
Figure 5.35 FRF for the 1 st Floor – 1 st - 3 rd Story Braces Are Broken MIMO – 12 DOF Symmetric Model	128
Figure 5.36 FRF for the 2 nd Floor – 1 st - 3 rd Story Braces Are Broken MIMO – 12 DOF Symmetric Model	128
Figure 5.37 FRF for the 3 rd Floor – 1 st - 3 rd Story Braces Are Broken MIMO – 12 DOF Symmetric Model	129
Figure 5.38 FRF for the 4 th Floor – 1 st - 3 rd Story Braces Are Broken MIMO – 12 DOF Symmetric Model	129
Figure 5.39 Simulated vs. Detected Damages for Trial #15 with Hillclimbing #10511	131
Figure 5.40 Simulated vs. Detected Damages for Trial #16 with Hillclimbing #5039	133
Figure 5.41 Simulated vs. Detected Damages for Trial #17 with Hillclimbing #1266	135
Figure 5.42 FRF for the 1 st Floor – 1 st Story Braces Are Broken MIMO – 120 DOF Symmetric Model	136
Figure 5.43 Simulated vs. Detected Damages for Trial #18 with Hillclimbing #309	138
Figure 5.44 FRF for the 1 st Floor – 1 st - 3 rd Story Braces Are Broken MIMO – 120 DOF Symmetric Model	139
Figure 5.45 Simulated vs. Detected Damages for Trial #19 with Hillclimbing #58	141

	Page
Figure 5.46 FRF for the 1 st Floor – 1 st Story Braces Are Broken SIMO – 12 DOF Symmetric Model (10% Noise).....	142
Figure 5.47 Simulated vs. Detected Damages for Trial #20 with Hillclimbing #4976	144
Figure 5.48 FRF for the 1 st Floor – 1 st Story Braces Are Broken MISO – 12 DOF Symmetric Model (10% Noise).....	145
Figure 5.49 Simulated vs. Detected Damages for Trial #21 with Hillclimbing #4083	147
Figure 5.50 FRF for the 4 th Floor – 4 th Story Braces Are Broken MIMO – 12 DOF Symmetric Model (10% Noise).....	148
Figure 5.51 Simulated vs. Detected Damages for Trial #22	149
Figure A.1 Sample Input File of a SIMO Problem for the <i>ModalFEM</i> Utility Program	161

LIST OF TABLES

		Page
Table 2.1	The Section Properties of the Benchmark Structure	21
Table 5.1	GA Parameters Used	84
Table 5.2	SDIM Results for 1 st Story Braces Damaged Using 4 FRFs – SIMO Case 3, All Four Modes Are Used	88
Table 5.3	SDIM Results for 1 st Story Braces Damaged Using 4 FRFs – SIMO Case 3, All Four Modes Are Used, After Hillclimbing #1867	89
Table 5.4	SDIM Results for 1 st Story Braces Damaged Using 4 FRFs – SIMO Case 3, Last Mode Is Omitted	91
Table 5.5	SDIM Results for 1 st Story Braces Damaged Using 4 FRFs – SIMO Case 3, Last Mode Is Omitted, After Hillclimbing #739	91
Table 5.6	SDIM Results for 1 st and 3 rd Story Braces Damaged Using 4 FRFs – SIMO Case 3, All Four Modes Are Used	95
Table 5.7	SDIM Results for 1 st and 3 rd Story Braces Damaged Using 4 FRFs – SIMO Case3, All Four Modes Are Used, After Hillclimbing #178	95
Table 5.8	SDIM Results for 1 st and 3 rd Story Braces Damaged Using 4 FRFs – SIMO Case 3, Last Two Modes Are Omitted	97
Table 5.9	SDIM Results for 1 st and 3 rd Story Braces Damaged Using 4 FRFs – SIMO Case 3, Last Two Modes Are Omitted, After Hillclimbing #1489	98
Table 5.10	SDIM Results for 2 nd Story Braces Damaged Using 4 FRFs – SIMO Case 3	100
Table 5.11	SDIM Results for 1 st Story Braces Damaged Using 4 FRFs – SIMO Case 4	103
Table 5.12	SDIM Results for 1 st Story Braces Damaged Using 4 FRFs – SIMO Case 4, After Hillclimbing #1867	103
Table 5.13	SDIM Results for 1 st and 3 rd Story Braces Damaged Using 4 FRFs – SIMO Case 4	105

	Page
Table 5.14 SDIM Results for 1 st and 3 rd Story Braces Damaged Using 4 FRFs – SIMO Case 4, After Hillclimbing #580	106
Table 5.15 SDIM Results for 1 st Story Braces Damaged Using 4 FRFs – SIMO Case 5	108
Table 5.16 SDIM Results for 1 st Story Braces Damaged Using 4 FRFs – SIMO Case 5, After Hillclimbing #519	109
Table 5.17 SDIM Results for 1 st and 3 rd Story Braces Damaged Using 4 FRFs – SIMO Case 5	111
Table 5.18 SDIM Results for 1 st and 3 rd Story Braces Damaged Using 4 FRFs – SIMO Case 5, After Hillclimbing #1575	111
Table 5.19 SDIM Results for 1 st Story Braces Damaged Using 4 FRFs – MISO Case 1, Accelerometer Is at Node 7	115
Table 5.20 SDIM Results for 1 st Story Braces Damaged Using 4 FRFs – MISO Case 1, Accelerometer Is at Node 7, After Hillclimbing #8693	115
Table 5.21 SDIM Results for 1 st Story Braces Damaged Using 4 FRFs – MISO Case 1, Accelerometer Is at Node 8	117
Table 5.22 SDIM Results for 1 st Story Braces Damaged Using 4 FRFs – MISO Case 1, Accelerometer Is at Node 8, After Hillclimbing #160	117
Table 5.23 SDIM Results for 1 st and 3 rd Story Braces Damaged Using 4 FRFs – MISO Case 1, Accelerometer Is at Node 7	120
Table 5.24 SDIM Results for 1 st and 3 rd Story Braces Damaged Using 4 FRFs – MISO Case 1, Accelerometer Is at Node 7, After Hillclimbing #9903	120
Table 5.25 SDIM Results for 1 st Story Braces Damaged Using 4 FRFs – MIMO Case 1, All Four Modes Are Used	124
Table 5.26 SDIM Results for 1 st Story Braces Damaged Using 4 FRFs – MIMO Case 1, All Four Modes Are Used, After Hillclimbing #3395	124
Table 5.27 SDIM Results for 1 st Story Braces Damaged Using 4 FRFs – MIMO Case 1, The Last Mode Is Omitted.....	126

	Page
Table 5.28 SDIM Results for 1 st Story Braces Damaged Using 4 FRFs – MIMO Case 1, The Last Mode Is Omitted, After Hillclimbing #1232.....	126
Table 5.29 SDIM Results for 1 st and 3 rd Story Braces Damaged Using 4 FRFs – MIMO Case 1, All Four Modes Are Used	130
Table 5.30 SDIM Results for 1 st and 3 rd Story Braces Damaged Using 4 FRFs – MIMO Case 1, All Four Modes Are Used, After Hillclimbing #10511	131
Table 5.31 SDIM Results for 1 st and 3 rd Story Braces Damaged Using 4 FRFs – MIMO Case 1, First Two Modes Are Used	132
Table 5.32 SDIM Results for 1 st and 3 rd Story Braces Damaged Using 4 FRFs – MIMO Case 1, First Two Modes Are Used, After Hillclimbing #5039	133
Table 5.33 SDIM Results for 3 rd Story Braces Damaged Using 4 FRFs – MIMO Case 1	134
Table 5.34 SDIM Results for 3 rd Story Braces Damaged Using 4 FRFs – MIMO Case 1, After Hillclimbing #1266	134
Table 5.35 SDIM Results for 1 st Story Braces Damaged Using 4 FRFs – MIMO Case 2	136
Table 5.36 SDIM Results for 1 st Story Braces Damaged Using 4 FRFs – MIMO Case 2, After Hillclimbing #309	137
Table 5.37 SDIM Results for 1 st and 3 rd Story Braces Damaged Using 4 FRFs – MIMO Case 2.....	139
Table 5.38 SDIM Results for 1 st and 3 rd Story Braces Damaged Using 4 FRFs – MIMO Case 2, After Hillclimbing #58.....	140
Table 5.39 SDIM Results for 1 st Story Braces Damaged Using 4 FRFs (10% Noise) – SIMO Case 3	143
Table 5.40 SDIM Results for 1 st Story Braces Damaged Using 4 FRFs (10% Noise) – SIMO Case 3, After Hillclimbing #4976.....	143
Table 5.41 SDIM Results for 1 st Story Braces Damaged Using 4 FRFs (10% Noise) – MISO Case 1	146

	Page
Table 5.42 SDIM Results for 1 st Story Braces Damaged Using 4 FRFs (10% Noise) – MISO Case 1, After Hillclimbing #4083.....	146
Table 5.43 SDIM Results for 1 st Story Braces Damaged Using 4 FRFs (10% Noise) – MIMO Case 1	149
Table A.1 Cards That Can be Used in the Text Input File (*.inp) for the <i>ModalFEM</i> Utility Program	157
Table B.1 List of Files in the Datagen Package	162
Table B.2 List of Input Parameters in the Datagen Package.....	162
Table B.3 List of Output Parameters in the Datagen Package	163

1 INTRODUCTION

1.1 Overview

Detecting structural damage using the information contained in vibration signatures has become more widely accepted by researchers and practitioners due to the availability of efficient and economical analysis methods and measurement systems. Vibration-based structural identification methods (SDIM) can provide global identification methods that also minimize the level of destructive impact on structural integrity that may occur in the search for damage. In comparison, often only limited information can be obtained concerning structural damage using local non-destructive damage detection techniques, which include radiographs, magnetic and ultrasonic methods. In addition, in order to use local techniques for health monitoring, typically the approximate damage location must be known which makes these methods highly unsuitable for automated health monitoring systems. Global damage detection methods have the potential to provide information throughout the life-cycle of a structure, while local damage methods are usually suited to checking the immediate condition of specific structural members or connections after a natural hazard like an earthquake or hurricane.

1.2 Research Objectives

This research evaluates the performance of an existing structural damage identification program, GaDamDet, in identifying damage globally for a large-scale experimental structure. The hybrid SDIM proposed uses the frequency response functions (FRF) obtained from the first phase of the benchmark structural health monitoring (SHM) problem as input parameters in the GaDamDet structural damage detection program.

Therefore, this research investigates several complex issues related to signal processing, including input/output relationships and data processing.

Different analytical models of the three-dimensional test structure are examined in order to study the effects that model complexity and model error have on the SDIM's performance. The loss or gain of useful information is also examined by choosing partial or full sensor locations in the system. The performance of the proposed hybrid SDIM is compared to the performance of different SDIMs developed by other researchers on the same benchmark problem and to the performance of GaDamDet using the program's original features and models. The measurements taken from the UBC damaged structure are available and are used to validate the responses obtained by Datagen. Evaluating the performance of the SDIM using the FRFs obtained from the UBC test structure will allow conclusions to be made concerning the potential benefits of using the GaDamDet SDIM in real-time monitoring applications of large, more realistic structural systems.

This thesis also provides useful tools regarding random data analysis by developing methods for obtaining frequency response functions from the force and response records provided by the UBC benchmark problem for any damage condition.

1.3 Background

A vibration-based damage detection algorithm is used in this research. The idea behind this technique is that the changes in a structure's physical properties will cause changes in the structure's dynamic response properties, which include natural frequencies, modal shapes and frequency response functions of the structure.

A literature review of vibration-based damage identification methods was provided by Doebling *et al* in 1996 and 1998. Several methods that include using changes in mode shapes, changes in natural frequencies, measurements of flexibility to detect damage in structures are explained in these research reviews.

Rytter (1993) provided a system in which a SDIM can be classified into one of four levels according to their capabilities. Level 1 concerns the capability to detect

damage but only by relaying information about the existence of damage in structures. Level 2 concerns damage localization. A Level 2 method provides information about the possible damage locations. Level 3 concerns assessment and these methods are capable of estimating the severity of the damage in addition to the previous information. Level 4 methods involve prediction. These methods would be capable of estimating the remaining life of a structure in addition to locating and quantifying the damage.

In addition to the level of damage detection provided, different SDIMs can also be classified according to the parameters used such as the response or static measurement information used (either in time domain or frequency domain), the type of excitation or loading provided (known or unknown), and the type of optimization method or direct method used to identify the location and/or extent of damage.

Liszkai and Raich (2003) proposed a FRF-based SDIM which is examined further in this thesis for damage detection. The advantages of using FRF data over modal parameters are that FRF data can be measured directly on structures without any intermediate steps and that it provides information over a frequency range instead of only at certain frequencies. In the FRF-based SDIM program, the damage detection problem is formulated as an optimization problem, which is solved using an Implicit Redundant Representation (IRR) GA due to the unstructured nature of damage detection (Liszkai, 2003). The unstructured problem stems from not knowing a priori the number of damages in addition to the location and severity of the damages.

1.3.1 Frequency Response Functions for Damage Detection

Several researchers have relied on the used of FRF information for system identification and damage detection. Wang et al. (1997) used measured FRF data obtained before and after damage to develop an SDIM algorithm based on nonlinear perturbation equations. This method determined a damage vector that indicated both the location and magnitude of damage. The perturbation equations were weighted at selected locations and frequencies in order to reduce the effect of measurement errors. An iterative version of

the SDIM algorithm was also introduced to handle incomplete measurement cases. Lee and Shin (2002) introduced a FRF-based SDIM for beam structures using the dynamic equation motion for the intact and damaged beams in the continuous domain. Damages throughout the beam were described by a damage distribution function, which was assumed to have non-zero values at the damage locations. Instead of examining the whole domain of the problem, a reduced domain strategy was also developed that eliminated regions of possibly undamaged areas from the solution using an iterative technique. Thyagarajan et al. (1998) investigated the optimization of FRFs to diagnose damage using a minimum number of sensors. The proposed optimization problem was solved using a gradient-based optimization subroutine contained in the MATLAB (1999a) optimization toolbox. The SDIM technique developed is limited mainly to small structures due to its large computational expense. Sampaio et al. (1999) introduced the FRF Curvature Method as an extension of the Mode Shape Curvature Method proposed by Pandey et al. (1991). In the FRF Curvature Method damage is assessed by identifying the largest computed absolute difference between the mode shape curvatures of the damaged and undamaged structure. The difference between FRFs curvatures is used to detect, localize and quantify the damage. Marwala and Heyns (1998) used a combination of objective functions that used both FRF and modal information to minimize an error function using the MATLAB (1999a) optimization toolbox. Marwala (2000) presented a SDIM defined using a committee of neural networks that employed FRFs, modal parameters and wavelet transform data simultaneously to identify structural damage.

1.3.2 Description of UBC Structural Benchmark Problem

The joint International Association for Structural Control - American Society of Civil Engineers (IASC-ASCE) Structural Health Monitoring Task Group investigated a series of benchmark problem structures in order to provide a consistent forum to allow researchers to evaluate the performance of different SDIMs. Phase I of the study

involved simulating structural response using an analytical structural model subjected to different damage scenarios. Phase II considered the application of the proposed SDIMs to detect damage based on structural response data obtained experimentally. The test model used in both phases is a four-story, two-bay by two-bay steel-frame structure. Results obtained by different SDIMs have been presented in the literature and are collected on the Structural Health Monitoring Committee ASCE website. A special session was held to discuss the benchmark problem at the 14th ASCE Engineering Mechanics Conference in 2000 and at the Joint ASME-ASCE Mechanics and Materials Conference in 2001. A special issue in the Journal of Engineering Mechanics was prepared to present research results concerning the benchmark identification problem. An overview of the SDIMs previously researched for the benchmark problem is provided in the next few paragraphs.

Johnson, Lam, Katafygiotis and Beck (2000) presented detailed information concerning the properties of the structural members, imposed damage scenarios as well as detailed information concerning the simulation cases. Analysis of two different finite element models (12 and 120 DOF) was performed and the natural frequencies of the analytical models were presented in this study.

Au, Yuen and Beck (2000) applied a two-stage approach to identify damage. Natural Excitation Technique (NExT) was used to obtain the modal parameters of the system. An a priori probability density function (PDF) was first assumed for the mass and stiffness of the structure. A Bayesian statistical approach and the modal parameters obtained previously were used to update this prior PDF. By comparing the PDF of the stiffness of the system before and after damage, it was possible to detect the location and severity of the damage in a probabilistic manner.

The Damage Index Method is a SDIM developed by Park, Stubbs and Bolton (1998). This method detects, locates, and estimates the severity of damage using a damage indicator based on the relationship between the material stiffness properties of the undamaged and the damaged member of the structure. This method was used by Rodriguez and Barroso (2002) in conjunction with their proposed stiffness-mass ratios

method to estimate baseline modal parameters from damaged response data when a shear-beam model is used. These methods can identify damage locations in a structure to specific stories within the structure, since shear-beam models work with story stiffness changes.

Bernal and Gunes (2000) applied a multi-stage approach for detecting damage in the benchmark structure. As the first step, the modal characteristics were identified by using an Eigen System Realization Algorithm (ERA) with a Kalman observer or a subspace identification algorithm. The second and third steps involve locating damaged regions based on the identified flexibility matrix of the structure. Damage was then quantified by comparing the undamaged structure with the damaged structure.

Corbin, Hera and Hou (2000) proposed an application of wavelet analysis for damage detection in order to locate damage regions in structures. Damage and the moment that the damage occurred were detected by a spike or an impulse in a wavelet decomposition of the acceleration data. Quantification of the damage was not presented.

Dyke, Caicedo and Johnson (2000) used a combination of NExT and ERA methods for identification of modal parameters. Then, the optimal stiffness of structural elements was obtained using unconstrained nonlinear optimization. Changes in the stiffness coefficients indicated the location of damage, but the severity was difficult to quantify using this method.

1.4 Organization of the Thesis

This thesis is divided into six sections. Section 2 discusses the two programs used for evaluating the performance of the SDIM. Since the hybrid approach presented combines two programs, it is necessary to provide information about the parameters and input/output relationships of the programs. The finite element model used to define the benchmark structure is also explained in this section. Section 3 discusses how to obtain frequency response functions (FRF) from random data. After defining some basic concepts, mathematical formulations of the FRFs will be given. A simple algorithm is

also introduced in this section in order to compute FRFs for different input/output models. Section 4 focuses on how the force and acceleration signals obtained from Datagen are processed and how either a single input/multiple output (SIMO) or multiple input/multiple output (MIMO) problem is defined and solved in GaDamDet. Section 5 presents the SDIM results for the proposed hybrid approach and compares the results with other SDIMs developed by other researchers involved in the benchmark problem. The discussion includes an analysis of the SDIMs features, benefits, and limitations. In Section 6, a summary of the results is provided along with the conclusions made within the scope of this research. Future recommendations and future research extensions are also identified and discussed in this section.

2 HYBRID STRUCTURAL DAMAGE IDENTIFICATION METHODOLOGY

The hybrid structural damage identification methodology proposed links the FRF-based damage identification method provided by GaDamDet with measurement information obtained through Datagen for the UBC benchmark test structure. Before discussing the proposed hybrid approach in detail, the features and implementation details of the GaDamDet and the Datagen programs are discussed. Understanding the inputs and outputs of each program as well as parameters used will provide a better understanding and limitations of the hybrid SDIM methodology developed.

2.1 Description of the Structural Damage Identification Program GaDamDet

The SDIM provided by GaDamDet is based on the assumption that damage affects the stiffness of structural members. Therefore, damage can be detected globally by identifying changes in member stiffness, as any stiffness changes also affect the global dynamic response of the structure. A linear finite element model of the undamaged structure is also defined through a simple input card and is used as the baseline model for the SDIM. To detect damage, the stiffness parameters of the intact model are updated by the SDIM using an optimization method that seeks to match the analytically computed FRFs obtained from the updated baseline model to the measured FRFs obtained from the damaged structure.

2.1.1 *Detecting Structural Damage Using GaDamDet*

The theory behind the SDIM provided by GaDamDet is that minimizing the difference between the FRF matrices of the undamaged and the damaged structure captures both

the location and extent of damage. In order to formulate the damage detection problem as an optimization problem, an objective function is defined, that is minimized.

$$f = \sum_{k=k_1}^{k_n} \left(\int_{\varpi_0}^{\varpi} |\bar{A}_{jk}(\omega) - A_{jk}(\omega)| d\omega \right)^2 \quad (2.1)$$

where j is the excitation degree of freedom (DOF), k is the DOF where the response is measured, A_{jk} is the jk^{th} accelerance FRF in the finite element model, \bar{A}_{jk} is jk^{th} measured accelerance FRF, $k_1 \dots k_n$ are the DOF where measurements are taken, ϖ_0 and ϖ are the lower and upper frequencies of the measured frequency range, and the symbol $||$ indicates complex magnitude (Liszkai, 2003).

The analytical FRFs are found by inverting the dynamic stiffness matrix of the structure. If the system is excited by a set of sinusoidal forces with ω circular frequency, but with different amplitudes and phases, then the equations of motion can be written as:

$$\mathbf{M}\ddot{\mathbf{u}} + \mathbf{C}\dot{\mathbf{u}} + \mathbf{K}\mathbf{u} = \mathbf{f}_0 e^{-i\omega t} \quad (2.2)$$

where \mathbf{M} , \mathbf{C} and \mathbf{K} are the mass, damping, and stiffness matrices of the undamaged structure, \mathbf{u} is the displacement vector, ω is the circular natural frequency of excitation, \mathbf{f}_0 is the vector of complex forcing amplitudes, i is the imaginary unit, and t is time.

It is assumed that the solution of the above set of differential equations exists in the form

$$\mathbf{u} = \mathbf{z} e^{-i\omega t} \quad (2.3)$$

where \mathbf{z} is the vector of time independent complex amplitudes. The formal solution of equation (2.2) is obtained in the form.

$$\mathbf{z} = (\mathbf{K} - i\omega\mathbf{C} - \omega^2\mathbf{M})^{-1}\mathbf{f}_0 \equiv \mathbf{R}\mathbf{f}_0 \quad (2.4)$$

where the receptance matrix \mathbf{R} is defined as a function of ω .

$$\mathbf{R} = \mathbf{R}(\omega) \equiv (\mathbf{K} - i\omega\mathbf{C} - \omega^2\mathbf{M})^{-1} \quad (2.5)$$

The jk^{th} member of the receptance matrix represents the displacement response of the j^{th} DOF when the excitation is applied at the k^{th} DOF.

Each entry of the matrix of equation (2.4) is a function of ω and is also known as a frequency response function (FRF). Consequently, the receptance is a type of FRF too. From equation (2.3)

$$\dot{\mathbf{u}} \equiv \mathbf{v}e^{-i\omega t} = -i\omega\mathbf{z}e^{-i\omega t} \quad (2.6)$$

$$\ddot{\mathbf{u}} \equiv \mathbf{a}e^{-i\omega t} = -i\omega\mathbf{v}e^{-i\omega t} = -\omega^2\mathbf{z}e^{-i\omega t}$$

Using the above equations, the relationship between the receptance, mobility and accelerance matrices can be shown as:

$$\mathbf{V}(\omega) = -i\omega\mathbf{R}(\omega) \quad (2.7)$$

$$\mathbf{A}(\omega) = -\omega^2\mathbf{R}(\omega)$$

FRF matrices are commonly denoted with the notation of $\mathbf{H}(\omega)$. Receptance $\mathbf{R}(\omega)$, mobility $\mathbf{V}(\omega)$ or accelerance $\mathbf{A}(\omega)$ can be used as FRF matrices. The equations

derived for damage detection using the general FRF matrix are valid for any of the particular FRF matrices. Accelerance (inertance) will be used in this research in order to be consistent with the benchmark problem.

2.1.2 Running *GaDamDet*:

The *GaDamDet* program consists of three major modules:

1. Preprocessor for incorporating structural model, damage, and noise level information
2. Processor that includes the finite element, genetic algorithm (GA) and hillclimbing implementations,
3. A Postprocessor that include an easy to use graphical user interface.

These three modules were combined into a single program. The utility program, which generated simulated measurement data, is a separate program. The main program menu, settings menu and settings toolbar from *GaDamDet* are shown in Figures 2.1 and 2.2.



Figure 2.1 Main Menu Structure of *GaDamDet* Program
(Adapted from Lizskai, 2003)

The utility program, ModalFEM, simulates the measurement data and generates FRF input files for different finite element models. The user provides an input text file (*.inp) containing the finite element model of the structure. Using the input file, the utility program generates a binary MATLAB data file (*.mat) that contains simulated

measurement data for specific excitation and measurement locations and a specific imposed noise level.

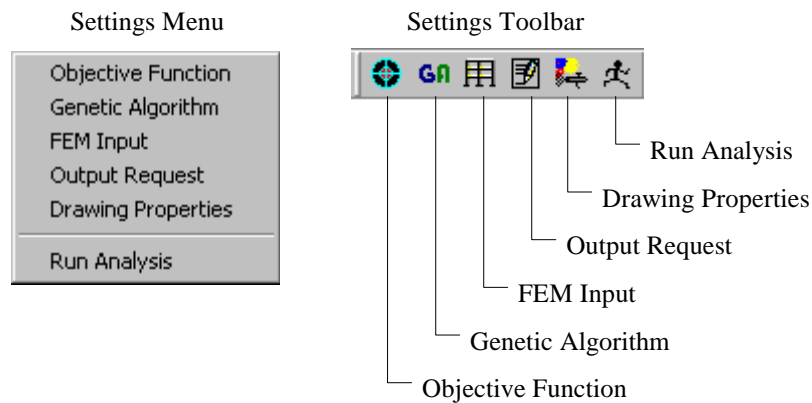


Figure 2.2 Settings Menu and Its Toolbar (Adapted from Lizskai, 2003)

The finite element model (FEM) input of the program opens a screen to let the user input two files:

1. Undamaged Finite Element Input File,
2. Matlab File containing measurement data.

The user is asked to input the undamaged finite element input card directly into the program. In comparison, the user prepares the damaged element input file and runs it in the utility program ModalFEM. The FEM input screen is shown in Figure 2.3.

ModalFEM provides the FRF of the defined damaged structure considering the location and severity of the damage provided by the damaged input file. Damage is imposed with a reduction in the stiffness for the desired element. This is done by reducing the Young Modulus of the damaged member by the percentage amount of the damage that is proposed. As stated before, all the information necessary to define the finite element model of any trial is stored in an input card. . The element numbers and

definitions (which ones are columns, beams or braces), dimensions and properties of these elements (Young Modulus, area, moment of inertia, Poisson's ratio, etc.), support conditions, etc. are defined with this input card. A sample input card with explanation of each parameter is provided in Appendix A.

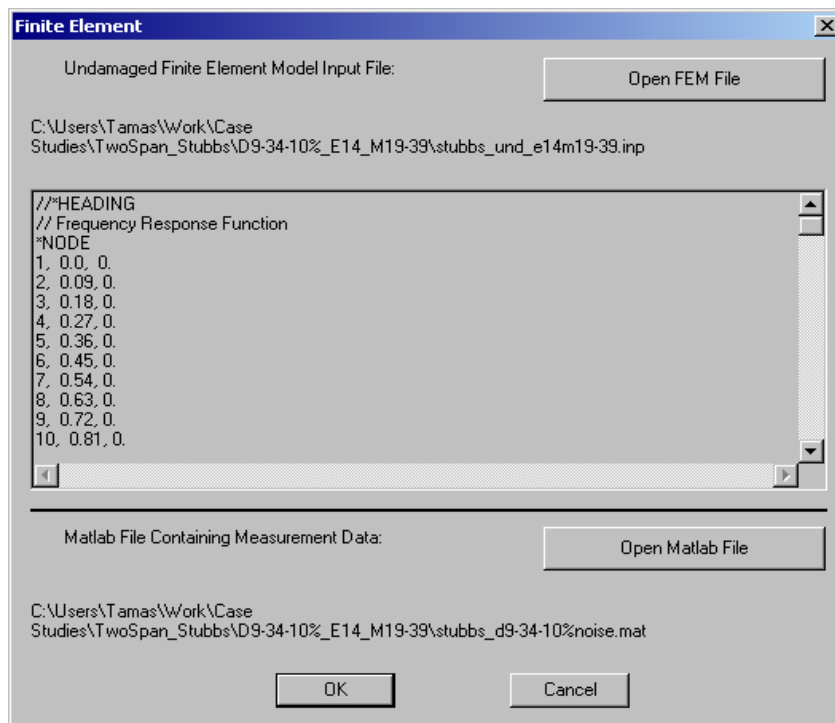


Figure 2.3 Finite Element Model Input and Matlab Measurement Data Files
(Adapted from Lizskai, 2003)

ModalFEM constructs the FRF measurements as MATLAB arrays. This MATLAB file is selected by the user in the FEM input screen as the damaged structure's input card, which is named as the "Matlab File Containing Measurement Data" in Figure 2.3.

Before running GaDamDet and performing structural damage detection, the user is able adjust any GA parameter, such as population size, crossover sides, coding type (binary or gray), mutation rate, variables (IRR or Fixed-Length), and set the optional process switches (Hillclimbing, Binary or Gray Coding, Elitism-on/off). The dialog box to input or change the genetic algorithm parameters is shown in Figure 2.4.

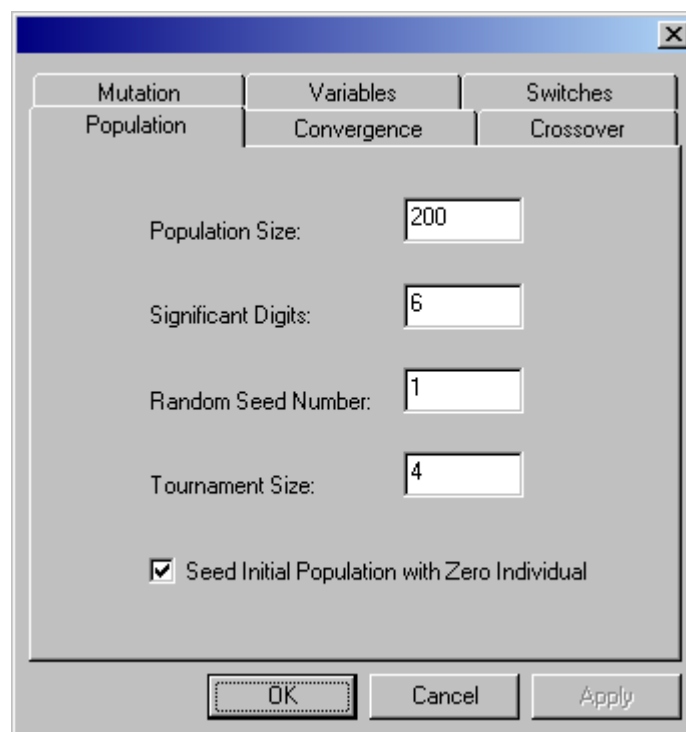


Figure 2.4 Genetic Algorithm Parameter Sheet
(Adapted from Lizskai, 2003)

The “Results” menu and its submenus offer two graphical output windows that show the genetic algorithm process results as either a “Structure Plot” or “Individual Plot”. The “Individual Plot” contains crucial information about the individual genetic

algorithm string encoding, including the fitness value, representation type, generation number, and number of gene instances. The “Structure Plot” shows the location of the damaged elements along with the damage severity directly on the structure by visually showing the two-dimensional structure and results. The severity of damage can be viewed by opening a small rectangular window showing the percent damage indicator when an element is highlighted with the cursor. The graphical output window of the “Structure Plot” menu is shown in Figure 2.5. The excitation and measurement locations and element numbers with corresponding damages (as a percentage) can be viewed in the output window.

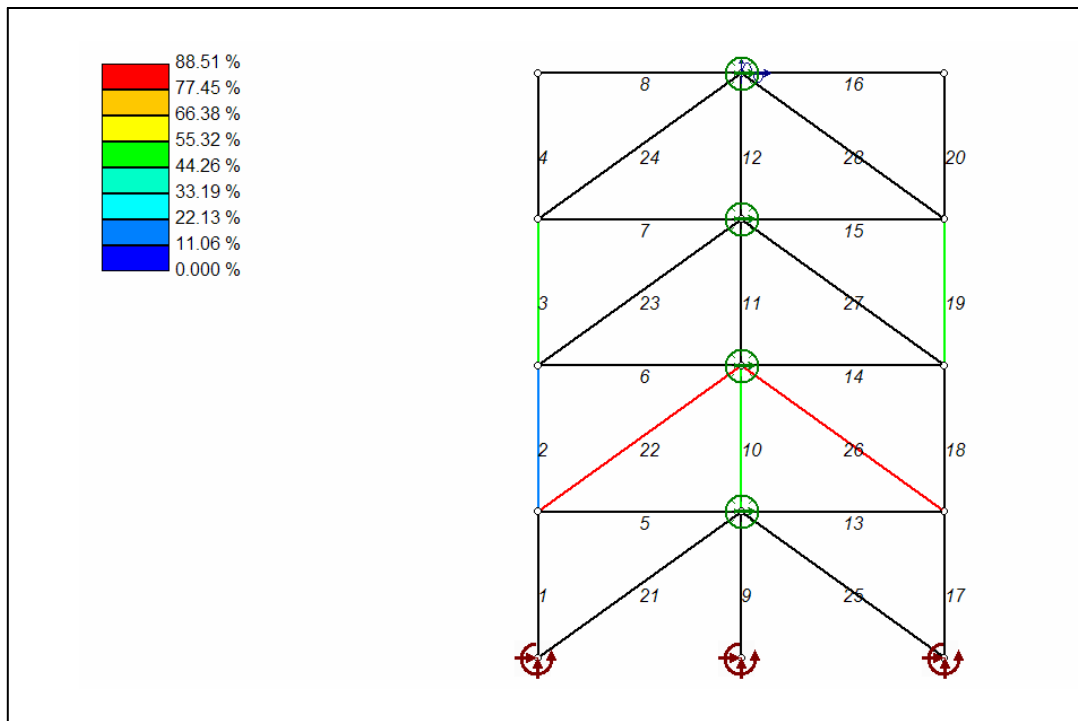


Figure 2.5 Structure Plot Option in GaDamDet

Before closing this section concerning the features of GaDamDet, a discussion of the “Hillclimbing” optimization option of the program is provided. Hillclimbing is an easy optimization method to implement as it only uses the information contained in the objective function to improve the current solution iteratively. Hillclimbing uses a single solution (point) during the search process. At each iteration, new solutions (points) are selected from the neighborhood of the current (best) solution. If the best among the newly selected points is better than the current point, then that solution becomes the current point and a new iteration starts. If there is no better point found among the new solutions, then another neighborhood is selected and tested. The process terminates if no further improvements are possible or another termination condition is satisfied, such as the number of iterations to be performed (Lizskai, 2003). The GA program employs the local hillclimber as described above in order to try to improve upon the solution obtained by the GA. The solution returned by the GA may be near-optimal due to the population converging or the GA process stopping because the maximum number of generations is exceeded. The local hillclimber is often effective in improving the GA solution toward the global optimum. The performance of the hillclimber in this research is discussed in the Results and Discussions (Section 5).

2.2 Description of the Experimental Response Measurement Program Datagen

Datagen is a Matlab program developed during Phase I of the IASC-ASCE benchmark problem. Datagen can be used to simulate the dynamic response of the 3-D four-story, two-bay by two-bay steel UBC Test Structure under various damage cases. The first version of Datagen (called Datagen version 1999.08.28) was developed on 28-August-1999 after a meeting of the ASCE Task Group on Structural Health Monitoring at California Institute of Technology. After that, the program was continuously updated according to the requirements of the ASCE task group.

The Datagen user is able to select any of the 6 damage scenarios defined officially as part of the benchmark problem using the dialog boxes that appear after

running the program in Matlab environment. A user-defined damage case can also be specified in Datagen that allows the user to specify any member or members as damaged, which allows other damage cases to be investigated. Simulated noise can also be introduced to the measurements obtained. The dialog box used to input damage scenarios is shown in Figure 2.6. A reference undamaged case is also available in order to simulate the behavior of the undamaged structure.

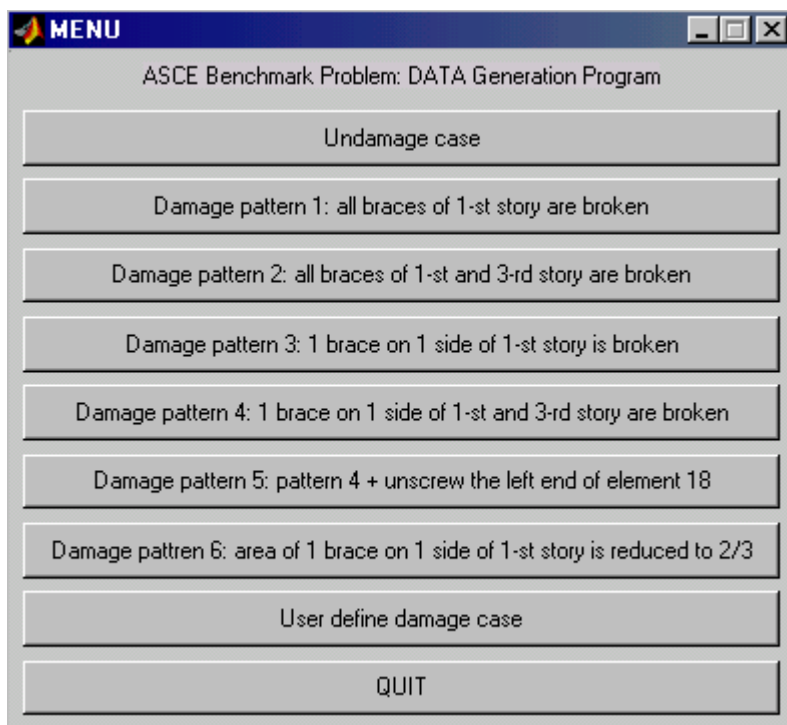


Figure 2.6 Damage Cases Defined by Datagen for the UBC Benchmark Problem

The program determines the forcing function and corresponding acceleration measurements for two main cases. These are forcing vectors in the y direction on each floor or in the x and y directions at the roof, with the option of using either 12 or 120

DOF model. The 12 DOF model is a shear-building model that constrains all DOFs except for two translations and one rotation per floor. The 120 DOF model only requires the floor nodes to have same horizontal translation and in-plane rotation. This model is used to simulate the response measurements, while the model used in the identification analyses remains simpler (12 DOF). The horizontal slab panels are assumed to contribute only towards in-plane stiffness making the floor behave as a rigid plate with respect to in-plane motions only. The remaining out of plane degrees of freedoms (vertical motion, pitching/rolling of the floor) are active. The columns and beams are modeled as Euler Bernoulli beams in both the 12 and 120 DOF finite element models. The braces are modeled as bars with no bending stiffness. Different case numbers are given to each combination of model and load in the program which can be seen in Figure 2.7.

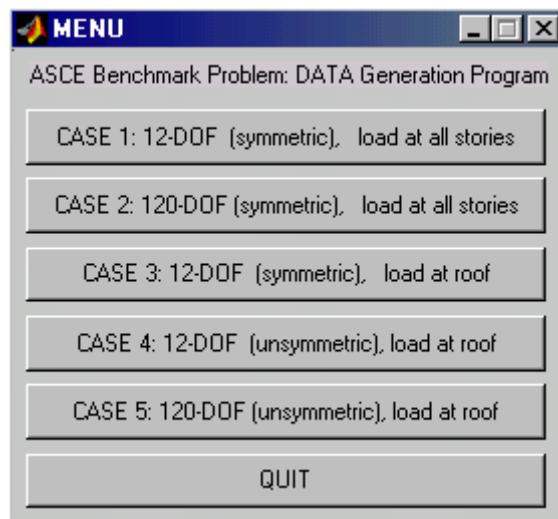
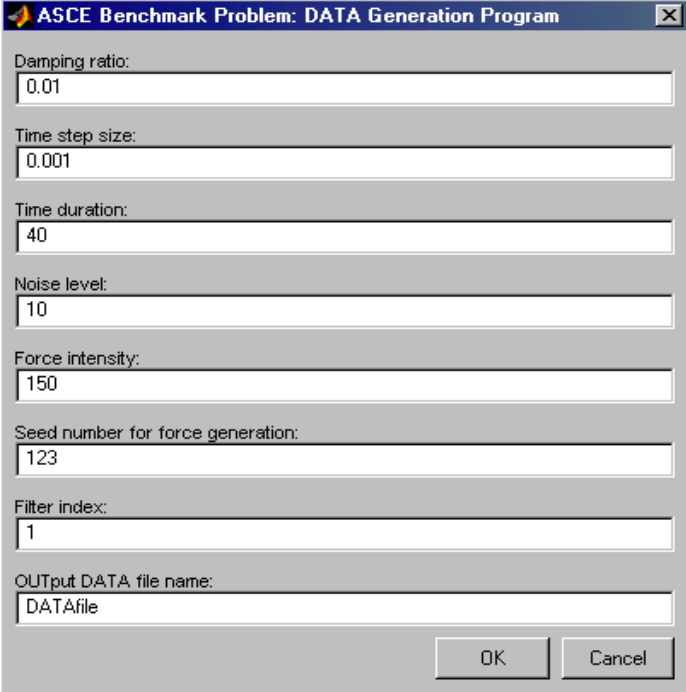


Figure 2.7 Datagen Case IDs

Datagen allows the user to adjust the set of model parameters, including the damping ratio, time duration and step size, noise level, and force intensity. The parameter sheet to input these parameters can be seen in Figure 2.8. The list of all input and output parameters as well as the files in Datagen Package are given in Appendix B.



The image shows a dialog box titled "ASCE Benchmark Problem: DATA Generation Program". It contains several input fields for parameters:

- Damping ratio: 0.01
- Time step size: 0.001
- Time duration: 40
- Noise level: 10
- Force intensity: 150
- Seed number for force generation: 123
- Filter index: 1
- OUTPUT DATA file name: DATAfile

At the bottom right, there are "OK" and "Cancel" buttons.

Figure 2.8 Datagen Parameter Sheet

2.2.1 Definition of UBC Test Structure:

The Benchmark Structure was built in one-third scale at the University of British Columbia. It is a two-bay by two-bay, four-story, rectangular steel structure, which is 3.6 m tall and 2.5 m wide. Each bay is 1.25 m x 0.9 m. Hot rolled B100 x 9 members are used for the columns, and S75 x 11 members are used for the floor beams. L25 x 25 x 3

sections are used for the bracing members on each floor. There is one floor slab per bay on each floor: four 800 kg slabs at the first floor, four 600 kg slabs at the second and third floor and four 400 kg slabs at the fourth floor. In order to simulate an asymmetric mass distribution, one of the 400 kg slabs is replaced with a 550 kg one in Cases 4 and 5 of the benchmark problem. UBC Test Structure is shown in Figure 2.9, while section properties can be seen in Table 2.1. This photograph was taken by the participants of the benchmark problem during the experimental stage (Phase II) and is taken directly from the IASC-ASCE SHM Task Group website (<http://wusceel.cive.wustl.edu/asce.shm>).



Figure 2.9 UBC Test Structure
(Adapted from the IASC-ASCE SHM Task Group Web Site)

Table 2.1 The Section Properties of the Benchmark Structure

Property	Columns	Beams	Braces
Section Type	B x 100 x 9	S x 75 x 11	1.25 x 25 x 3
Cross Sectional Area [m ²]	1.133 x 10 ⁻³	1.43 x 10 ⁻³	0.141 x 10 ⁻³
Moment of Inertia (Strong) [m ⁴]	1.97 x 10 ⁻⁶	1.22 x 10 ⁻⁶	0
Moment of Inertia (Weak) [m ⁴]	0.664 x 10 ⁻⁶	0.249 x 10 ⁻⁶	0
St. Ven. Torsion Constant [m ⁴]	8.01 x 10 ⁻⁹	38.2 x 10 ⁻⁹	0
Young's Modulus [Pa]	2 x 10 ¹¹	2 x 10 ¹¹	2 x 10 ¹¹
Mass per unit length [kg/m]	8.89	11.0	1.11

2.3 Discussion of the Hybrid Structural Damage Identification Method Proposed

In Cases 1 and 2 of ASCE benchmark problem, the structure's 3-D response is measured under ambient vibration, while in Cases 3, 4 and 5, the structure's response to a diagonally placed shaker is simulated. These models are analyzed as multiple input/multiple output and single input/multiple output problems, respectively. The input to the system is a forcing function vector in the x or y direction and the output from the system is 16 acceleration measurements. In comparison, the SDIM provided by GaDamDet uses a 2-D model (one of the perimeter frames can be chosen), which allows only 4 of these acceleration records to be used. For all the trials performed, four of the FRF s in either the weak - y or strong - x direction are computed, which corresponds to a FRF at each floor level for the 2-D frame modeled.

Instead of using the utility program ModalFEM to simulate the damaged structure's FRFs as was done in the previous research effort, the results of the ASCE Benchmark problem are used to provide the information required for the damaged structure input card by GaDamDet. In the simplest terms, the utility program ModalFEM, is replaced with the simulated results obtained from the first phase of the ASCE benchmark problem. The SDIM provided by GaDamDet changes the stiffness values of the baseline (undamaged) structural model until the differences between the

measured responses provided by Datagen and those predicted by the undated baseline model are minimized. The stiffness values in the updated model found by GaDamDet can be used to identify the severity and the location of the damage. This hybrid procedure will provide the capability to identify damage in more realistic structures since the measurement information of the damaged structure is collected experimentally from the complete three-dimensional structure and the FRFs can be easily calculated using a simple data processing algorithm, which will be defined in Section 3. The program assumes that a finite element model of the intact structure is present. However, it does not require having any records taken from the undamaged structure which may not be available most of the time. Thus, by leaving ModalFEM out, measurement information for a structure without any indication of damage location or quantity is collected, which is the case of all real-world applications.

2.3.1 Modifications Required in the Finite Element Model Used by GaDamDet

Processing the measurement information data obtained from Datagen, however, is not the only procedure required in replacing the utility program ModalFEM. Since a finite element model of the structure must be available for the SDIM to work, the model has to be defined that reflects the behavior of the structure defined in the benchmark experiment as accurately as possible. This is a challenging process, since the simulated model of the UBC structure is a 3-D model with slab elements defined at each floor, while the input card used to construct the finite element models in GaDamDet can only build simpler 2-D frame models. The difficulty with this reduction in the dimensions of the models is that the dynamic behavior of the real structure is dominated by the floor slabs due to their large mass compared to other structural elements and due to the lateral stiffness the slabs add to each floor. To overcome this problem, the weight of the slabs is computed using the *DENSITY card in order to create the 2-D model of the structure. In addition the total weight of the structure is loaded to one perimeter frame only.

The masses distributed to the floors are:

1st floor: 4 – 800 kg slabs

2nd floor: 4 – 600 kg slabs

3rd floor: 4 – 600 kg slabs

4th floor: 4 – 400 kg slabs

The volume of a beam is calculated:

$$\text{Volume} = (1.43 \times 10^{-3}) \cdot (1.25) = 0.0017875 \text{ m}^3 \quad (2.8)$$

The modified density of each beam at each floor can be defined as:

$$D1 = \frac{\text{Mass}}{\text{Volume}} = \frac{1600}{0.0017875} = 895106 \text{ kg/m}^3 \quad (2.9)$$

$$D2 = \frac{\text{Mass}}{\text{Volume}} = \frac{1200}{0.0017875} = 671328 \text{ kg/m}^3 \quad (2.10)$$

$$D3 = \frac{\text{Mass}}{\text{Volume}} = \frac{800}{0.0017875} = 447552 \text{ kg/m}^3 \quad (2.11)$$

The density of the steel (7500 kg/m^3) is kept for defining the columns and braces in the structure. The damping ratio is set at 0.01 for the first four modes and then increased to 0.015 for the other modes extracted, which is typically 4 modes. The moment of inertia of the beams is doubled to $2.44 \times 10^{-6} \text{ m}^4$ in order to simulate the same rigid effect in the 2-D structural frame as they provide in the real 3-D structure. Columns have the same moment of inertia in both models, which is $1.97 \times 10^{-6} \text{ m}^4$ in the strong and $0.664 \times 10^{-6} \text{ m}^4$ in the weak directions.

2.3.2 *Modifications Required in the Measurement / Excitation Pairs*

The number of FRF measurements used depends on the number of available measurement/excitation pairs. Ideally, one should obtain an FRF matrix that has a size equal to the product of number of measurements and number of excitations. For example with four measurements and four excitations, sixteen different FRFs should be obtained as a function of frequency. However, ModalFEM only takes the number of measurements into account when FRFs are calculated, which means it assumes a single excitation force. As an example, the following input card will produce an FRF matrix with four arrays. (Each of the array columns is a function of frequency)

```
*NSET, NSET=MEAS
    21, 24, 27, 30
*NSET, NSET=EXC
    42
```

The calculated FRFs should relate the excitation with each of the measurements obtained from imposing the excitation. Thus, EXC 1- MEAS 1 (42-21) , EXC 1- MEAS 2 (42-24), EXC 1- MEAS 3 (42-27), EXC 1- MEAS 4 (42-30) is the set of excitation/measurement pairs for this set of FRFs. It should be noted that the FRF measurements are obtained by inverting the dynamic stiffness in ModalFEM instead of processing the excitation/measurement pairs. However, this kind of a logical argument is defined in order to understand the information provided by the program algorithm. Furthermore, the same process will need to be applied with in order to obtain the damaged structures' FRFs from simulated data later on.

Using a different input card produces the following results:

*NSET, NSET=MEAS

21, 24, 27, 30

*NSET, NSET=EXC

42, 45, 48, 51

Sixteen FRFs are expected in this type of an input. However an FRF matrix with 4 arrays is obtained using ModalFEM and each excitation is related with its corresponding measurement in the program. Thus, EXC 1- MEAS 1 (42-21), EXC 2- MEAS 2 (45-24), EXC 3- MEAS 3 (48-27), EXC 4- MEAS 4 (51-30) is the set of excitation/measurement pairs for this set of FRFs. This can easily be proved if one tries to obtain excitation/measurement pairs by inputting the excitations one by one instead of applying them all simultaneously.

Thirteen different trials were run using a simple cantilever beam to prove this algorithm. The results obtained above were supported and the same technique will be used throughout the research in order to obtain the FRF measurements.

2.3.3 *Required Input/Output Parameters in Datagen:*

There are two cases that will be considered for the simulated stage of the experiment.

1. Force input (in y direction at each floor) / acceleration output (in x and y direction at each floor).
2. Force input (in x and y direction at the roof) / acceleration output (in x and y direction at each floor.)

In both cases, the system appears to be a multiple input/multiple output model; although it will be proved that the second case should be analyzed as a single input/multiple output case later in this thesis.

Since GaDamDet uses a 2-D model of the system currently, one of the four perimeter frames is chosen for analysis. Because of this feature, only four of the sixteen acceleration measurements will be used as the output parameters in the first case. Four inputs are applied to the edge columns and four outputs are taken from the middle columns (all in y direction). Input/output parameters and their locations for the first case can be seen in Figure 2.10. Only the four acceleration measurements taken weak direction are shown for simplicity. These are the records that will be used in frequency response function calculations in the following sections. The second case defines two inputs and sixteen outputs. The two inputs are at the roof level in the x and y directions while outputs are taken from the middle columns in y direction like the first case. Figure 2.11 shows the input/output parameters and locations both in weak and strong directions.

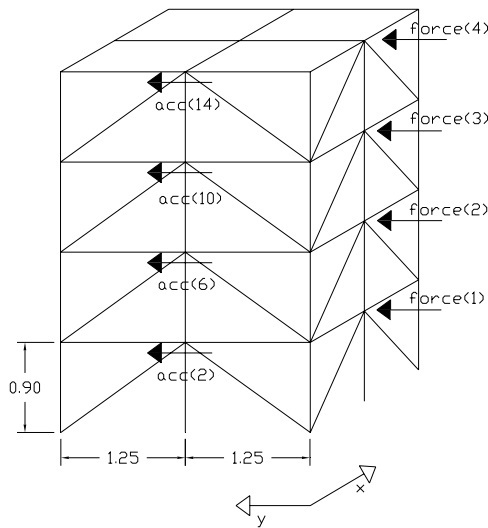


Figure 2.10 Input/Output Parameters for the Multiple-Input/Multiple-Output Model (Only in Weak Direction)

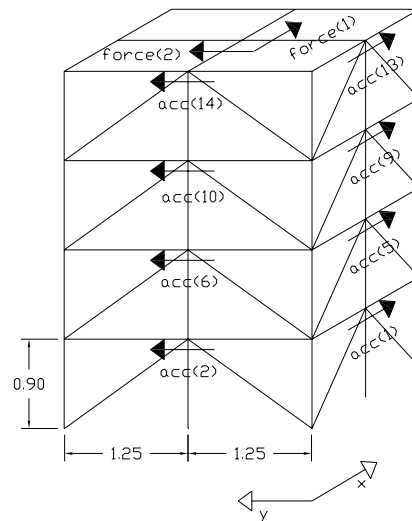


Figure 2.11 Input/Output Parameters for the Single-Input/Multiple-Output Model (Both in Weak and Strong Direction)

Only four acceleration records in each direction are shown for simplicity. The second case actually simulates a diagonally placed shaker's responses on the structure.

For the first case, the excitations applied at each floor in weak (y) direction are designed as Gaussian white noise (Gaussian white noise processes passed through a 6th order low-pass Butterworth filter with a 100-Hz cutoff). The accelerometers return noisy sensor measurements where noise is defined as Gaussian pulse processes with RMS %10 of the RMS of the roof acceleration. The data generation uses a discrete-time integration at 1 KHz and provides the sensor measurements at 1 KHz with an option of user defined lower sampling rates. The first case was actually designed to simulate the response of the structure to ambient vibration (wind loading at each floor in y-direction), but in order to simulate a process like this, a forcing function must be defined. The second case simulates a diagonally placed shaker's responses. The force in the shaker is also designed as a Gaussian white noise process filtered with a low-pass Butterworth filter.

3 FREQUENCY RESPONSE FUNCTIONS

This section discusses how frequency response functions (FRF) can be obtained from random measurement data. The input/output models examined include single input/single output, single input/multiple output, and multiple input/output relationships. After defining the basic concepts, the section discusses the mathematical formulations of the FRFs for each type of model. A simple algorithm is then introduced that can determine FRFs for different input/output measurement response problems. All definitions, concepts and equations as well as figures are based on “Random Data Analysis and Measurement Procedures (2000)” and “Engineering Applications of Correlation and Spectral Analysis (1980)” by Julius S. Bendat and Allan G. Piersol.

3.1 Random Data

A physical phenomenon, along with the data representing it, is considered random when a future time history record from an experiment cannot be predicted within a reasonable experimental error. Each observation of the phenomenon will be unique and, therefore, cannot be described by an explicit mathematical relationship. A single time history representing a random phenomenon is called a sample function, whereas the collection of all possible sample functions that the random phenomenon might have produced is called a random process or a stochastic process. Random data can be classified in two main categories; stationary or non-stationary. Stationary random data may further be categorized as being either ergodic or nonergodic.

In this research, the records obtained from the first phase of the benchmark structure test problem are stationary. Therefore, all the formulations for FRFs discussed in this research are valid for stationary random data.

3.1.1 Stationary Random Data

When a physical phenomenon is considered in terms of a random process, the properties of the phenomenon can hypothetically be described at any instant of time by computing average values over the collection of sample functions that describe the random process. The mean value (first moment) of the random process at some time t_1 can be computed by taking the instantaneous value of each sample function of the ensemble (collection of sample functions) at time t_1 , summing the values, and dividing by the number of sample functions. In a similar manner, a correlation (joint moment) between the values of the random process at two different times (called the autocorrelation function) can be computed by taking the ensemble average of the product of instantaneous values at two times, t_1 and $t_1 + \tau$. Thus, for the random process $\{x(t)\}$, where the symbol $\{ \}$ is used to denote an ensemble of sample functions, the mean value $\mu_x(t_1)$ and the autocorrelation function $R_{xx}(t_1, t_1 + \tau)$ are given by

$$\mu_x(t_1) = \lim_{N \rightarrow \infty} \frac{1}{N} \sum_{k=1}^N x_k(t_1) \quad (3.1)$$

$$R_{xx}(t_1, t_1 + \tau) = \lim_{N \rightarrow \infty} \frac{1}{N} \sum_{k=1}^N x_k(t_1) x_k(t_1 + \tau) \quad (3.2)$$

where the final summation assumes each sample function is equally likely.

For the general case where $\mu_x(t_1)$ and $R_{xx}(t_1, t_1 + \tau)$ defined in equations (3.1) and (3.2) vary as time t_1 varies, the random process $\{x(t)\}$ is said to be non-stationary. For the special case where $\mu_x(t_1)$ and $R_{xx}(t_1, t_1 + \tau)$ do not vary as time t_1 varies, the random process $\{x(t)\}$ is said to be weakly stationary or stationary in wide sense. For a weakly stationary random process, the mean value is constant and the autocorrelation function is dependent only on the time displacement τ . This means that $\mu_x(t_1) = \mu_x$ and $R_{xx}(t_1, t_1 + \tau) = R_{xx}(\tau)$.

For the special case where all possible moments and joint moments are time invariant, the random process $\{x(t)\}$ is said to be strongly stationary.

3.1.1.1 Ergodic Stationary Random Data

For almost all stationary data, the average values computed over the ensemble at time t_1 will equal the corresponding average values computed over time from a single time history record. If the k^{th} sample function of the random process is considered, then the mean value $\mu_x(k)$ and the autocorrelation function $R_{xx}(\tau, k)$ of the function are given by

$$\mu_x(k) = \lim_{T \rightarrow \infty} \frac{1}{T} \int_0^T x_k(t) dt \quad (3.3)$$

$$R_{xx}(\tau, k) = \lim_{T \rightarrow \infty} \frac{1}{T} \int_0^T x_k(t) x_k(t + \tau) dt \quad (3.4)$$

If the random process $\{x(t)\}$ is stationary, and $\mu_x(k)$ and $R_{xx}(\tau, k)$ defined in equations (3.3) and (3.4) do not differ when computed over different sample functions, the random process is said to be ergodic. That is, $\mu_x(k) = \mu_x$ and $R_{xx}(\tau, k) = R_{xx}(\tau)$. Only random processes can be ergodic. All properties of ergodic random processes can be determined by performing time averages over a single sample function. For this reason, the properties of stationary random phenomena can be measured properly from a single observed time history record. In practice, random data representing stationary physical phenomena are generally ergodic.

3.2 Analysis of Random Data

It was stated in the Section 3.1 that random data can not be represented by an explicit mathematical equation. Thus, a statistical procedure must be used to define the

descriptive properties of the data. Bendat and Piersol defined the basic statistical properties for describing single stationary random records as the following:

1. Mean and mean square values
2. Probability density functions
3. Autocorrelation functions
4. Autospectral density functions

The mean value $\mu_x(k)$ and the variance σ_x^2 for a stationary record represent the central tendency and dispersion, respectively, of the data. The mean square value ψ_x^2 , which equals the variance plus the square of the mean, provides a measure of the combined central tendency and dispersion. The mean value is estimated by simply computing the average of all data values in the record. The mean square value is similarly estimated by computing the average of all squared data values. By first subtracting the mean value estimate from all the data values, the mean square value computation yields a variance estimate.

The probability density function $p(x)$ for a stationary record represents the rate of change of probability with data value. The function $p(x)$ is generally estimated by computing the probability that the instantaneous value of the single record will be in a particular narrow amplitude range centered at various data values, and then dividing by the amplitude range. The total area under the probability density function over all data values will be unity. This indicates the certainty of the fact the data values fall between $-\infty$ and $+\infty$. The partial area under the probability density function from $-\infty$ to some given value x represents the probability distribution function, $P(x)$. The area under the probability density function between any two values x_1 and x_2 is given by $P(x_2) - P(x_1)$. This area defines the probability that any future data values at a randomly selected time will fall within this amplitude interval.

The autocorrelation function $R_{xx}(\tau)$ for a stationary record is a measure of time-related properties in the data that are separated by fixed time delays. The level of autocorrelation can be estimated by delaying the record relative to itself by some fixed

time delay τ , and then multiplying the original record by the delayed record and taking the average of the resulting product values over the available record length or over some desired portion of this record length. The procedure is repeated for all time delays of interest.

The autospectral (also called power spectral) density function $G_{xx}(f)$ for a stationary record represents the rate of change of the mean square value with respect to frequency. This measure is estimated by computing the mean square value in a narrow frequency band at various center frequencies, and then dividing by the frequency band. The total area under the autospectral density function over all frequencies will be the total mean square value of the record. The partial area under the autospectral density function from f_1 to f_2 represents the mean square value of the record associated with that frequency range.

For pairs of random records taken from two different stationary random processes, there are several joint statistical properties of importance and can be stated as the following:

1. Joint probability density functions
2. Cross-correlation functions
3. Cross-spectral density functions
4. Frequency response functions
5. Coherence functions

The first three functions measure fundamental properties shared by the pair of records in the amplitude, time, or frequency domains. From knowledge of the cross-spectral density function between the pair of records, as well as their individual autospectral density functions, one can compute theoretical linear response functions (gain factors and phase factors) between the two records. The coherence function is a measure of the accuracy of the assumed linear input/output model, and can be computed from the measured autospectral and cross-spectral density functions.

3.3 Input/Output Relations

Input/output cases of common interest can usually be considered as combinations of one or more of the following linear system models:

1. Single-input/single-output model
2. Single-input/multiple-output model
3. Multiple-input/single-output model
4. Multiple-input/multiple-output model

In all cases, there may be one or more parallel transmission paths with different time delays between each input point and output point. For the multiple input cases, the various inputs may or may not be correlated with each other.

For a single-input/single-output model, $x(t)$ and $y(t)$ are the measured input and output stationary random records, and $n(t)$ is the unmeasured extraneous output noise. The quantity $H_{xy}(f)$ is the frequency response function of a constant-parameter linear system $x(t)$ and $y(t)$. This simple system is shown in Figure 3.1.

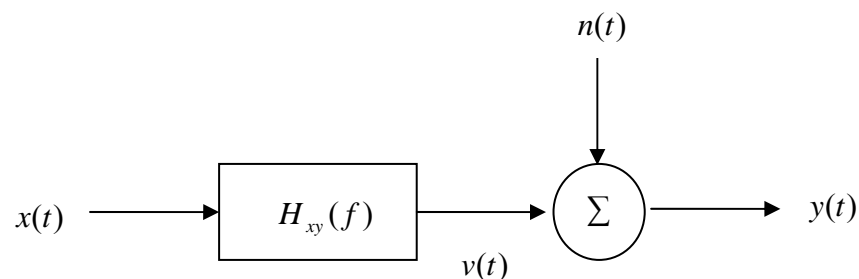


Figure 3.1 Single-Input/Single-Output System with Output Noise
(Adapted from Bendat/Piersol, 2000)

As an extension of this system, a single-input/ multiple-output model is shown in Figure 3.2. The frequency response function (FRF) $H_{xi}(f)$ is defined as the constant-parameter linear system between the input $x(t)$ and the output $y_i(t)$. There are as many frequency response functions as the number of outputs in the system in the multiple output case. The noise terms $n_i(t)$ represent unmeasured extraneous output noise at the different output measurement points.

Single-input models can be solved using measured autospectral and cross-spectral density functions. Multiple-input/multiple-output models are analyzed using two different techniques derived from an extension of the simple single-input case.

3.4 Basic Dynamic Characteristics

Before finishing the discussion of the basic concepts, several fundamental definitions related to the dynamic behavior of physical systems will be summarized. An ideal system has constant parameters, is stable, and is linear between two clearly defined points called the input or excitation and the output or response point. A simple has constant parameters if all fundamental properties of the system are time invariant. A linear system is one in which the response characteristics of the system are additive and homogenous.

The term *additive* means that the output to a sum of units is equal to the sum of the outputs produced by each input individually. The term *homogenous* means that the output produced by a constant times the input is equal to the constant times the output produced by the input alone. If x represents the input and $f(x)$ represents the output, then the system is said to be linear if for any two inputs x_1, x_2 , and a constant c satisfies the following:

$$f(x_1 + x_2) = f(x_1) + f(x_2) \quad \text{additive property} \quad (3.5)$$

$$f(cx) = cf(x) \quad \text{homogeneous property} \quad (3.6)$$

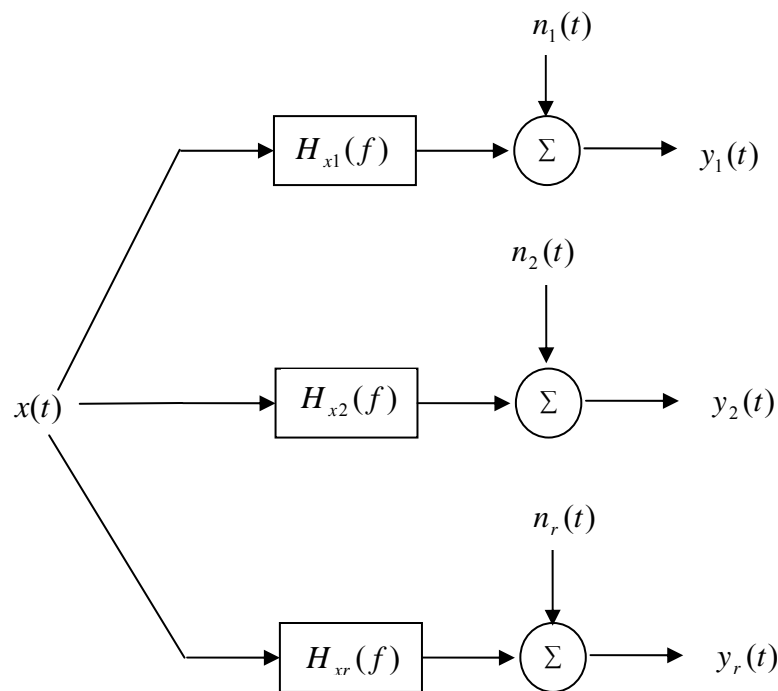


Figure 3.2 Single-Input/Multiple-Output System with Output Noise
(Adapted from Bendat/Piersol, 2000)

The response characteristics for many physical systems may be assumed to be linear over at least a limited range of inputs without involving any unreasonable errors.

The dynamic characteristics of a constant-parameter linear system can be described by an impulse response function $h(\tau)$, also called the weighting function, which is defined as the output of the system at any time to a unit impulse input applied a

time τ before. For any arbitrary input $x(t)$, the system output $y(t)$ is given by the *superposition or convolution integral*:

$$y(t) = \int_{-\infty}^{\infty} h(\tau)x(t-\tau)d\tau \quad (3.7)$$

In order for a constant-parameter linear system to be physically realizable (causal), it is necessary that the system respond only to past inputs. Therefore the following constraint must be satisfied,

$$h(\tau) = 0 \quad \text{for } \tau < 0 \quad (3.8)$$

For physical systems, the effective lower limit of the integration in Equation (3.7) is zero other than negative infinity ($-\infty$).

A constant-parameter linear system is said to be stable if every possible bounded input function produces a bounded output function. Thus, from Equation (3.7):

$$|y(t)| = \left| \int_{-\infty}^{\infty} h(\tau)x(t-\tau)d\tau \right| \leq \int_{-\infty}^{\infty} |h(\tau)||x(t-\tau)|d\tau \quad (3.9)$$

When the input $x(t)$ is bounded, there exists some finite constant A such that

$$|x(t)| \leq A \quad \text{for all } t \quad (3.10)$$

Hence from Equation (3.9)

$$|y(t)| \leq A \int_{-\infty}^{\infty} |h(\tau)|d\tau \quad (3.11)$$

Thus if the constant-parameter linear weighting function $h(\tau)$ is absolutely integrable,

$$\int_{-\infty}^{\infty} |h(\tau)| d\tau < \infty \quad (3.12)$$

then the output will be bounded and the system is stable.

3.5 Frequency Response Functions

If a constant-parameter linear system is physically realizable and stable, then the dynamic characteristics of the system can be described by a *frequency response function* $H(f)$, which is defined as the Fourier transform of weighting function $h(\tau)$.

$$H(f) = \int_0^{\infty} h(\tau) e^{-j2\pi f\tau} d\tau \quad (3.13)$$

In constant-parameter linear systems, if Fourier transform of both sides of Equation (3.7) is taken, then an important relationship is obtained:

$$Y(f) = H(f)X(f) \quad (3.14)$$

where, $X(f)$ is the Fourier transform of an input $x(t)$ and $Y(f)$ is the Fourier transform of the resulting output $y(t)$. This equation assumes that these forms exist.

The frequency response function (FRF) is generally a complex-valued quantity that may be thought of in terms of a magnitude and a phase angle. If $H(f)$ is written in complex polar notation, then the following equation is obtained.

$$H(f) = |H(f)|e^{-j\phi(f)} \quad (3.15)$$

where, the absolute value $|H(f)|$ is called the system gain factor, and the phase angle $\phi(f)$ is called the system phase factor.

A FRF is a function of only frequency in a constant-parameter linear system. If the system is nonlinear, then $H(f)$ will also be a function of the applied input (excitation). If the parameters of the system are not constant, $H(f)$ will also be a function of time.

3.6 Single-Input/Output Relationships

The theory and formulations of input/output relationships for single-output problems are discussed in this section using the concepts defined in “Random Data Analysis and Measurement Procedures (2000)” by Bendat and Piersol. It is assumed that the records involved are obtained from stationary random process with zero mean values and that the system is a constant-parameter linear system.

3.6.1 Single-Input/Single-Output Models

Consider a constant-parameter linear system with a weighting function $h(\tau)$ and frequency response function $H(f)$ that is subjected to a well-defined single input $x(t)$ from a stationary random process $\{x(t)\}$, which produces a well-defined output $y(t)$.

Under ideal conditions, the output $y(t)$ is given by the convolution integral defined in Equation (3.7) with its boundaries switched to zero to positive infinity.

$$y(t) = \int_0^{\infty} h(\tau)x(t-\tau)d\tau \quad (3.16)$$

where $h(t) = 0$ for $\tau < 0$ when the system is physically realizable. The product $y(t)y(t + \tau)$ is given by

$$y(t)y(t + \tau) = \int_0^{\infty} \int_0^{\infty} h(\alpha)h(\beta)x(t - \beta)x(t + \tau - \alpha)d\alpha d\beta \quad (3.17)$$

Taking the expected values of both sides yields the *input/output autocorrelation* relation.

$$R_{yy}(\tau) = \int_0^{\infty} \int_0^{\infty} h(\alpha)h(\beta)R_{xx}(\tau + \beta - \alpha)d\alpha d\beta \quad (3.18)$$

Similarly, the product $x(t)y(t + \tau)$ is given by

$$x(t)y(t + \tau) = \int_0^{\infty} h(\alpha)x(t)x(t + \tau - \alpha)d\alpha \quad (3.19)$$

Taking the expected values of both sides yields the *input/output cross-correlation* relation.

$$R_{xy}(\tau) = \int_0^{\infty} h(\alpha)R_{xx}(\tau - \alpha)d\alpha \quad (3.20)$$

Equation (3.20) is a convolution integral of the same form as Equation (3.16).

Taking the direct Fourier transforms of Equations (3.18) and (3.20) after various algebraic steps yields the set of two-sided spectral density functions $S_{yy}(f)$, $S_{xx}(f)$ and $S_{xy}(f)$.

$$S_{xx}(f) = \int_{-\infty}^{\infty} R_{xx}(\tau) e^{-j2\pi f\tau} d\tau \quad (3.21)$$

$$S_{yy}(f) = \int_{-\infty}^{\infty} R_{yy}(\tau) e^{-j2\pi f\tau} d\tau \quad (3.22)$$

$$S_{xy}(f) = \int_{-\infty}^{\infty} R_{xy}(\tau) e^{-j2\pi f\tau} d\tau \quad (3.23)$$

where Equation (3.23) is called the *cross-spectral density function*, or simply *cross-spectrum* between $x(t)$ and $y(t)$. Equation (3.21) and (3.22) are called *autospectral density functions of $\{x_k(t)\}$ and $\{y_k(t)\}$* (which are often called as *autospectrum* or sometimes the *power spectral density functions*). Spectral density functions satisfy the following important formulas

$$S_{yy}(f) = |H(f)|^2 S_{xx}(f) \quad (3.24)$$

$$S_{xy}(f) = H(f) S_{xx}(f) \quad (3.25)$$

Equation (3.24) is called the *input/output autospectrum relation*, while Equation (3.25) is called the *input/output cross-spectrum relation*. Equation (3.24) is a real-valued relation containing only the gain factor $|H(f)|$ of the system. Equation (3.25) is a complex-valued relation, which can be broken down into a pair of equations to give both the gain factor $|H(f)|$ and the phase factor $\phi(f)$ of the system.

The given equations apply only to ideal situations where no extraneous noise exists at input or output points, and the systems must have no time-varying or nonlinear characteristics.

In terms of one-sided spectral density functions $G_{xx}(f)$, $G_{yy}(f)$ and $G_{xy}(f)$, where $G(f) = 2S(f)$ for $f > 0$, Equations (3.24) and (3.25) becomes

$$G_{yy}(f) = |H(f)|^2 G_{xx}(f) \quad (3.26)$$

$$G_{xy}(f) = H(f)G_{xx}(f) \quad (3.27)$$

An alternative direct transform is available to derive Equations (3.26) and (3.27) without first computing the correlation expressions of Equations (3.18) and (3.20). For any pair of long but finite records of length T, Equation (3.16) is equivalent to Equation (3.14). Using Equation (3.14), the following expression can be obtained:

$$Y^*(f) = H^*(f)X^*(f) \quad (3.28)$$

where, [*] denotes complex conjugates of the expressions. It follows that,

$$|Y(f)|^2 = |H(f)|^2 |X(f)|^2 \quad (3.29)$$

$$X^*(f)Y(f) = H(f)|X(f)|^2 \quad (3.30)$$

By taking the expectation of the last two equations over different independent records, multiplying by (2/T), and letting T increase without bound yields the same equations as Equation (3.26) and (3.27). Using these expressions, the frequency response function, $H(f)$ can be calculated:

$$H(f) = \frac{G_{xy}(f)}{G_{xx}(f)} \quad (3.31)$$

Another formula for $H(f)$ can be obtained by considering the complex conjugation of Equation (3.27).

$$G_{xy}^*(f) = G_{yx}(f) = H^*(f)G_{xx}(f) \quad (3.32)$$

where

$$G_{yx}(f) = |G_{xy}(f)|e^{j\phi_{xy}(f)} \quad (3.33)$$

$$H^*(f) = |H(f)|e^{j\phi(f)} \quad (3.34)$$

To determine the phase factor of the system, the following formula can be used

$$\frac{G_{xy}(f)}{G_{yx}(f)} = \frac{H(f)}{H^*(f)} = e^{-j2\phi(f)} \quad (3.35)$$

Using Equations (3.26) and (3.32), the complete FRF of the system, can be obtained as:

$$G_{yy}(f) = H(f)[H^*(f)G_{xx}(f)] = H(f)G_{yx}(f) \quad (3.36)$$

Thus, the frequency response function can be obtained as:

$$H(f) = \frac{G_{yy}(f)}{G_{yx}(f)} \quad (3.37)$$

Equation (3.37) will give the same FRF functions as (3.31) in ideal situations (noise free environment and infinite number of measurements).

Assuming $G_{xx}(f)$ and $G_{yy}(f)$ are both different from zero, the coherence function between the input $x(t)$ and the output $y(t)$ can be defined as:

$$\gamma^2_{xy}(f) = \frac{|G_{xy}(f)|^2}{G_{xx}(f)G_{yy}(f)} \quad (3.38)$$

The ordinary coherence function is a real-valued quantity that satisfies the following equation for all f .

$$0 \leq \gamma^2_{xy}(f) \leq 1 \quad (3.39)$$

For the ideal case of a constant-parameter linear system with a single clearly defined input and output, the coherence function will be unity. If the input and output are completely unrelated, then the coherence function will be zero. Having a coherence function value other than zero or one may indicate that one or more of the following situations exist:

- a. Extraneous noise is present in the measurements.
- b. The system relating $x(t)$ and $y(t)$ is not linear.
- c. The output $y(t)$ is due to other inputs besides $x(t)$.

3.6.2 Single-Input/Multiple-Output Models

Some of the basic principles obtained in the previous section will be used to formulate the FRF responses for single-input/multiple-output problems. It is assumed that the records used are from stationary random process with zero mean values and that the systems are constant-parameter linear systems. Figure 3.3 shows an example of a single-input/multiple-output system with extraneous output noise.

When the input signal $x(t)$ and the output signals $y_i(t)$ (where i is the number of output records in the system) are measured simultaneously, Bendat and Piersol defined the system response equation as:

$$G_{xy_i}(f) = H_i(f)G_{xx}(f) \quad (3.40)$$

where $G_{xy_i}(f)$ is the cross-spectral density of the input $x(t)$ and output $y_i(t)$, $G_{xx}(f)$ is the autospectral density of the input $x(t)$ and $H_i(f)$ is the frequency response function.

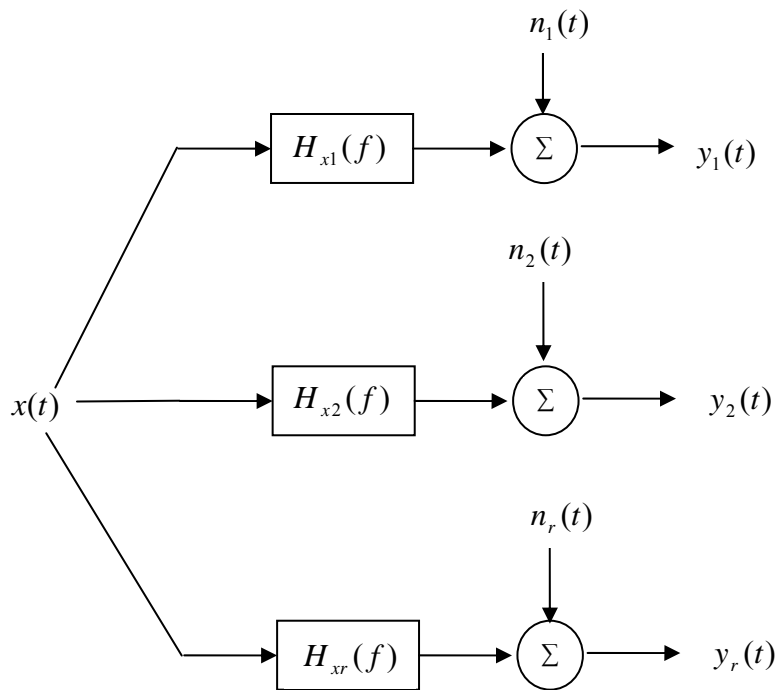


Figure 3.3 Single-Input/Multiple-Output System
(Adapted from Bendat/Piersol, 2000)

Thus, the FRFs for the system are obtained from:

$$H_i(f) = \frac{G_{xy_i}(f)}{G_{xx}(f)} \quad (3.41)$$

And the ordinary coherence function is defined as:

$$\gamma^2_{xy_i}(f) = \frac{|G_{xy_i}(f)|^2}{G_{xx}(f)G_{yiy_i}(f)} \quad (3.42)$$

3.7 Multiple-Input/Output Relationships

The previous system formulations and equations discussed will be extended to multiple-input/output problems in this section. It is assumed that all records are from stationary random process with zero mean values and that the systems are constant-parameter linear systems.

3.7.1 Multiple-Input/Single-Output Models

A set of q constant-parameter linear systems $H_i(f)$, $i = 1, 2, \dots, q$ with q clearly defined and measurable inputs $x_i(t)$, where $i = 1, 2, \dots, q$, and one measured output $y(t)$ is considered. Inputs may be mutually correlated. The output noise term $n(t)$ accounts for all deviations from the ideal model. These deviations may be due to unmeasured inputs, nonlinear operations, and instrument noise. Multiple-input/multiple-output models may be treated as a combination of separate and simpler multiple-input/single-output problems and can be solved using direct extensions of the techniques developed in this section. A multiple-input/single-input model is shown in Figure 3.4.

Four conditions must be satisfied in order to claim that the model is well-defined. These are stated by Bendat and Piersol as:

1. None of the ordinary coherence functions between any pair of input records should equal unity. If this occurs, the two input records contain redundant information and one of the input records should be eliminated from the model.
2. None of the ordinary coherence functions between any input and the total output should equal unity. If this occurs, then the other inputs are not contributing to this output and the model should be considered as a single-input/single-output model.

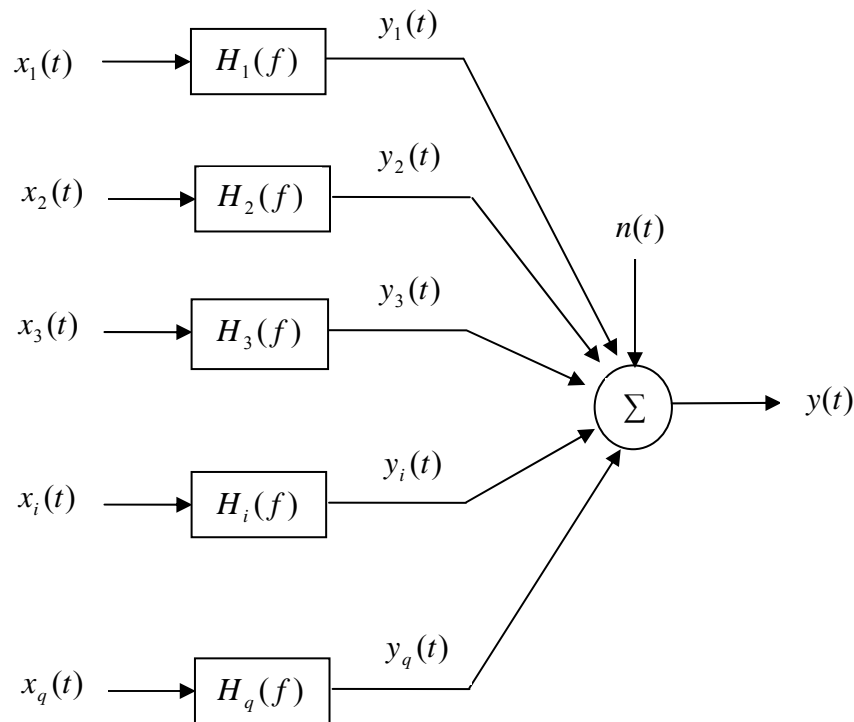


Figure 3.4 Multiple-Input/Single-Output System
(Adapted from Bendat/Piersol, 2000)

3. The multiple coherence function between any input and other inputs, excluding the given input, should not equal unity. If this occurs, then this input can be obtained by linear operations from the other inputs. Thus, this input is not providing any new information to the output and should be eliminated from the model.
4. The multiple coherence function between the output and the given inputs, in a practical situation, should be significantly high, which means above 0.50.

The output $y(t)$ may be considered to be the sum of the unmeasured q outputs $y_i(t)$, $i = 1, 2, \dots, q$ plus a noise term $n(t)$, as shown in the following equation

$$y(t) = \sum_{i=1}^q y_i(t) + n(t) \quad (3.43)$$

The corresponding finite Fourier transforms are:

$$Y(f) = \sum_{i=1}^q Y_i(f) + N(f) \quad (3.44)$$

Each output term $Y_i(f)$ for $i = 1, 2, \dots, q$ in Equation 3.44 satisfies the relationship shown:

$$Y_i(f) = H_i(f)X_i(f) \quad (3.45)$$

Therefore, the following equation can be defined

$$Y(f) = \sum_{i=1}^q H_i(f)X_i(f) + N(f) \quad (3.46)$$

where each $X_i(f)$ and $Y_i(f)$ is computed from the measured input signal $x_i(t)$ and the output signals $y(t)$.

The finite Fourier transforms for single records $x_i(t)$ and $y(t)$ of length T are

$$X_i(f) = \int_0^T x_i(t) e^{-j2\pi ft} dt \quad (3.47)$$

$$Y(f) = \int_0^T y(t) e^{-j2\pi ft} dt \quad (3.48)$$

The one-sided autospectral and cross-spectral density functions may be obtained using Finite Fourier Transforms instead of correlation functions.

$$G_{ii}(f) = G_{x_i x_i}(f) = \lim_{T \rightarrow \infty} \frac{2}{T} E[|X_i(f)|^2] \quad (3.49)$$

$$G_{ij}(f) = G_{x_i x_j}(f) = \lim_{T \rightarrow \infty} \frac{2}{T} E[X_i^*(f) X_j(f)] \quad (3.50)$$

$$G_{yy}(f) = \lim_{T \rightarrow \infty} \frac{2}{T} E[|Y(f)|^2] \quad (3.51)$$

$$G_{iy}(f) = G_{x_i y}(f) = \lim_{T \rightarrow \infty} \frac{2}{T} E[X_i^*(f) Y(f)] \quad (3.52)$$

In practice, only estimates of Equations (3.49) to (3.52) can be obtained, since T will be finite and the expected value operation $E[]$ can be taken only over a finite number of sample records.

When the records are digitized, the results will be obtained only at selected discrete frequencies. If the estimate of $G_{xy}(f)$ is denoted as $\hat{G}_{xy}(f)$, then at any frequency, f , the following relationship can be used (Bendat and Piersol):

$$\hat{G}_{xy}(f) = \frac{2}{n_d T} \sum_{k=1}^{n_d} X_k^*(f) Y_k(f) \quad (3.53)$$

where n_d is the number of different sample records $x(t)$ and $y(t)$, each of length T , so that the total record length $T_t = n_d T$. To reduce any bias errors, T should be made as large as possible. In addition, n_d should be as large as possible to reduce random errors.

Time-domain equations can be written involving the convolution integrals of the respective weighting functions $h_i(\tau)$, $i = 1, 2, \dots, q$, that are associated with the $H_i(f)$. Since using Fourier transforms in spectral relations is much simpler than using convolution integrals, Fourier transforms will now be used in order to obtain the desired quantities from this point.

For the general case of arbitrary inputs, if a different index of summation j is used instead of i in equation (3.46), then the following expression can be obtained.

$$Y(f) = \sum_{j=1}^q H_j(f) X_j(f) + N(f) \quad (3.54)$$

Multiplication of both sides by $X_i^*(f)$ for any fixed $i = 1, 2, \dots, q$ yields

$$X_i^* Y(f) = \sum_{j=1}^q H_j(f) X_i^* X_j(f) + X_i^* N(f) \quad (3.55)$$

where q is the number of inputs. If the expected values of both sides are taken then:

$$E[X^*_i(f)Y(f)] = \sum_{j=1}^q H_j(f)E[X^*_i(f)X_j(f)] + E[X^*_i(f)N(f)] \quad (3.56)$$

Multiplying the expression with a scale factor of $(2/T)$ yields the following expression:

$$G_{iy}(f) = \sum_{j=1}^q H_j(f)G_{ij}(f) + G_{in}(f) \quad (3.57)$$

If the model is well-defined, one can solve this system for $H_i(f)$ using matrix techniques.

The total autospectral density function $G_{yy}(f)$ can be written as:

$$\begin{aligned} G_{yy}(f) &= \sum_{i=1}^q \sum_{j=1}^q H^*_i(f)H_j(f)G_{ij}(f) + G_{nn}(f) \\ &+ \sum_{i=1}^q H^*_i(f)G_{in}(f) + \sum_{j=1}^q H_j(f)G_{nj}(f) \end{aligned} \quad (3.58)$$

assuming that the noise term $n(t)$ may be correlated with each input $x_i(t)$.

3.7.1.1 Two-Input/One-Output Models

The simplest case of multiple-input/single-output problems is two-input/one-output case. This case will be illustrated in this section in order to provide a better understanding of the theoretical approach presented above. A simple two-input/one-output system is

shown in Figure 3.5. The two-input/one-output system is defined by the basic transform relation

$$Y(f) = H_1(f)X_1(f) + H_2(f)X_2(f) + N(f) \quad (3.59)$$

Using the above equations, the following cross-spectral density functions between $x_1(t)$ and $y(t)$, and between $x_2(t)$ and $y(t)$, can be written as the following (dependency on frequency is omitted for simplicity).

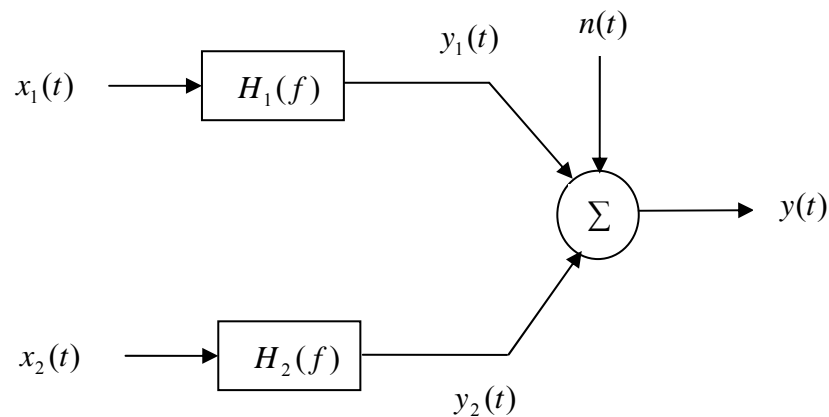


Figure 3.5 Two-Input/One-Output System with Output Noise
(Adapted from Bendat/Piersol, 2000)

$G_{11} = G_{11}(f)$ = autospectrum of $x_1(t)$

$G_{22} = G_{22}(f)$ = autospectrum of $x_2(t)$

$G_{yy} = G_{yy}(f)$ = autospectrum of $y(t)$

$G_{12} = G_{12}(f)$ = cross-spectrum between $x_1(t)$ and $x_2(t)$

$G_{1y} = G_{1y}(f)$ = cross-spectrum between $x_1(t)$ and $y(t)$

$G_{2y} = G_{2y}(f)$ = cross-spectrum between $x_2(t)$ and $y(t)$

$$G_{1y} = H_1 G_{11} + H_2 G_{12} + G_{1n} \quad (3.60)$$

$$G_{2y} = H_1 G_{21} + H_2 G_{22} + G_{2n} \quad (3.61)$$

If the noise term $n(t)$ is uncorrelated with each input $x_i(t)$, then G_{1n} and G_{2n} in Equation (3.60) and (3.61) will be zero.

The solution for $H_1(f)$ and $H_2(f)$, which assumes $\gamma^2_{12}(f) \neq 1$ and $G_{1n} = G_{2n} = 0$, is defined by Bendat and Piersol as:

$$H_1(f) = \frac{G_{1y}(f) \left[1 - \frac{G_{12}(f)G_{2y}(f)}{G_{22}(f)G_{1y}(f)} \right]}{G_{11}(f) [1 - \gamma^2_{12}(f)]} \quad (3.62)$$

$$H_2(f) = \frac{G_{2y}(f) \left[1 - \frac{G_{21}(f)G_{1y}(f)}{G_{11}(f)G_{2y}(f)} \right]}{G_{22}(f) [1 - \gamma^2_{12}(f)]} \quad (3.63)$$

with the ordinary coherence function

$$\gamma^2_{12}(f) = \frac{|G_{12}(f)|^2}{G_{11}(f)G_{22}(f)} \quad (3.64)$$

For the special case of uncorrelated inputs when $\gamma^2_{12}(f) = 0$, the terms $G_{12}(f)$ and $G_{21}(f)$ are zero also. The system can be reduced to a single-input/single-output model. For this special case, the following equations can be obtained:

$$H_1(f) = \frac{G_{1y}(f)}{G_{11}(f)} \quad (3.65)$$

$$H_2(f) = \frac{G_{2y}(f)}{G_{22}(f)} \quad (3.66)$$

3.7.1.2 Multiple Coherence Functions

A multiple coherence function is a direct extension of the ordinary coherence function. By definition, it is the ratio of the ideal output spectrum due to the measured inputs in the absence of noise to the total output spectrum, which includes the noise. In equation form, the multiple coherence function can be expressed by the following equation:

$$\gamma^2_{y:x}(f) = \frac{G_{vv}(f)}{G_{yy}(f)} = 1 - \left[\frac{G_{mm}(f)}{G_{yy}(f)} \right] \quad (3.67)$$

The ideal output spectrum may be written as $G_{vv}(f) = G_{yy}(f) - G_{mm}(f)$, where $G_{yy}(f)$ is provided in Equation (3.58).

Using Equation (3.67), the following relationship can be obtained.

$$G_{vv}(f) = \gamma^2_{y:x}(f)G_{yy}(f) \quad (3.68)$$

For all values of f , the multiple coherence function satisfies the following:

$$0 \leq \gamma^2_{y;x}(f) \leq 1 \quad (3.69)$$

If the multiple coherence function is zero, then $G_{vv}(f) = G_{yy}(f)$. This situation means that none of the output record comes from linear operations on the measured input records. The value unity indicates a perfectly linear model.

For a two-input/one-output model with uncorrelated inputs, the multiple coherence function is the sum of the ordinary coherence functions between each input and the output. This simple relation doesn't exist for correlated inputs. Thus, for uncorrelated inputs

$$\gamma^2_{y;x}(f) = \gamma^2_{1y}(f) + \gamma^2_{2y}(f) \quad (3.70)$$

3.7.1.3 Conditioned Spectral Density Functions

If correlation exists between any pair of input records, then it needs to be determined if one record causes part or all of the second record. Consider a two-input model where $x_1(t)$ and $x_2(t)$ are correlated, but not perfectly correlated, such that the coherence between them at all frequencies is $0 < \gamma^2_{12} < 1$. Turning off the first record will remove the correlated parts from the second record and leave only the part of the second record that is not due to the first record. Bendat and Piersol decomposed $x_2(t)$ into sum of two uncorrelated terms when any correlation between $x_1(t)$ and $x_2(t)$ comes from $x_1(t)$. This system can be seen in Figure 3.6.

$$x_2(t) = x_{2,1}(t) + x_{2,1}(t) \quad (3.71)$$

where $x_{2,1}(t)$ (called the residual or conditioned record) represents the part of $x_2(t)$ not due to $x_1(t)$. The optimum linear effect of $x_1(t)$ to $x_2(t)$ is denoted as $x_{2,1}(t)$.

The Fourier transform of Equation (3.71) yields

$$X_2(f) = X_{2,1}(f) + X_{2,1}(f) \quad (3.72)$$

where

$$X_{2,1}(f) = L_{12}(f)X_1(f) \quad (3.73)$$

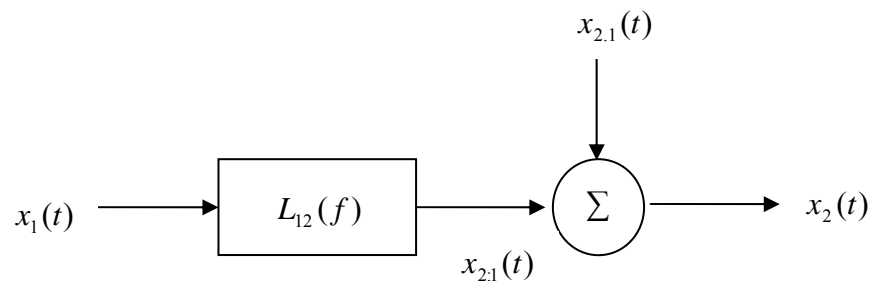


Figure 3.6 Decomposition of $x_2(t)$ from $x_1(t)$
 (Adapted from Bendat/Piersol, 2000)

Equation (3.72) may then be written as

$$X_{2,1}(f) = X_2(f) - L_{12}(f)X_1(f) \quad (3.74)$$

The constant-parameter linear system $L_{12}(f)$ represents the optimum linear system used to predict $x_2(t)$ from $x_1(t)$ taken in that order. $L_{12}(f)$ is given by the ratio of the cross-spectrum from input to output divided by the autospectrum of the input, which can be defined as:

$$L_{12}(f) = \frac{G_{12}(f)}{G_{11}(f)} \quad (3.75)$$

The spectrum of $x_2(t)$ may also be decomposed into two parts as shown

$$G_{22}(f) = G_{22,1}(f) + G_{22,2}(f) \quad (3.76)$$

where $G_{22,1}(f)$ is the coherent output spectrum

$$G_{22,1}(f) = |L_{12}(f)|^2 G_{11}(f) = \gamma^2_{12}(f) G_{22}(f) \quad (3.77)$$

and $G_{22,2}(f)$ is the noise output spectrum

$$G_{22,2}(f) = [1 - \gamma^2_{12}(f)] G_{22}(f) \quad (3.78)$$

There are two approaches that are suggested for ordering the records. When no physical basis exists, a recommended approach is to compute the ordinary coherence function between each input record and the output record. The input signal giving the highest coherence is then selected as the first one. Another approach is to compute the cross-correlation function between the records to search for relative time delay.

In order to illustrate the procedures explained until this point, a simple two-input/one-output model will be analyzed. It is assumed that the input signals are correlated and $x_2(t)$ follows $x_1(t)$. The output of the system is denoted as $y(t)$. The inputs $x_1(t)$ and $x_{2,1}(t)$ are uncorrelated in the Figure 3.7. The constant-parameter linear system $L_{1,y}(f)$ is the optimum linear system to predict $y(t)$ from $x_1(t)$, whereas the constant-parameter linear system $L_{2,y}(f)$ is the optimum linear system to predict $y(t)$ from $x_{2,1}(t)$. In equation form, Figure 3.7 can be expressed as

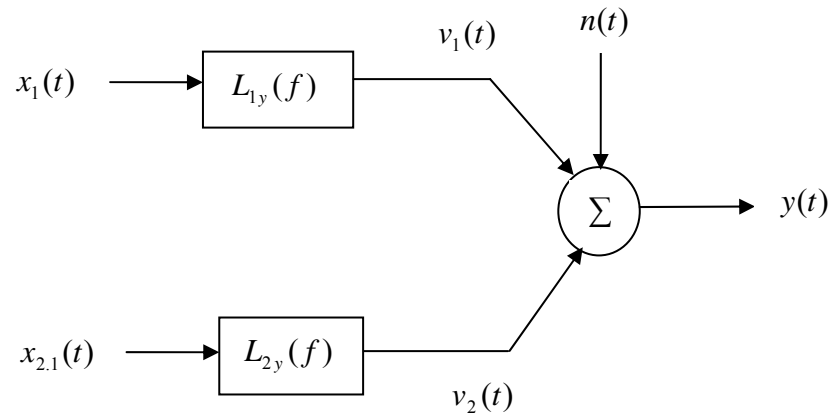


Figure 3.7 Two-Input/One-Output Model with Mutually Uncorrelated Inputs
 (Adapted from Bendat/Piersol, 2000)

$$Y(f) = L_{1y}(f)X_1(f) + L_{2y}(f)X_{2,1}(f) + N(f) \quad (3.79)$$

$$L_{1y}(f) = \frac{G_{1y}(f)}{G_{11}(f)} \quad (3.80)$$

$$L_{2y}(f) = \frac{G_{2y,1}(f)}{G_{22,1}(f)} \quad (3.81)$$

where the quantities

$G_{1y}(f)$ = cross-spectrum between $x_1(t)$ and $y(t)$

$G_{11}(f)$ = autospectrum of $x_1(t)$

$G_{2y,1}(f)$ = cross-spectrum between $x_{2,1}(t)$ and $y(t)$

$G_{22,1}(f)$ = autospectrum of $x_{2,1}(t)$

The quantity $G_{2y.1}(f)$ is called a conditioned (residual) cross-spectral density function, and $G_{22.1}(f)$ is called a conditioned (residual) autospectral density function. These functions are defined by Bendat and Piersol as

$$G_{2y.1}(f) = \frac{2}{T} E[X_{2.1}^*(f)Y(f)] \quad (3.82)$$

$$G_{22.1}(f) = \frac{2}{T} E[X_{2.1}^*(f)X_{2.1}(f)] \quad (3.83)$$

The frequency response functions for the system can then be obtained using the following relationship

$$L_{1y}(f) = H_{1y}(f) + L_{12}(f)H_{2y}(f) \quad (3.84)$$

$$L_{2y}(f) = H_{2y}(f) \quad (3.85)$$

There are only two unknowns in the above expressions ($H_{1y} = H_1$ and $H_{2y} = H_2$) and Equations (3.84) and (3.85) may be used to obtain these values. This process identified may be extended to solve multiple-input/output problems.

3.7.1.4 Partial Coherence Functions

In simplest terms, partial coherence functions play the same role as ordinary coherence functions, except that they apply to conditioned records instead of to the original records.

In partial coherence functions (the following assumes a two-input/one-output model):

1. Original records $x_1(t)$ and $y(t)$ are replaced by conditioned records $x_{2,1}(t)$ and $y_{y,1}(t)$.
2. Original spectral quantities $G_{11}(f)$, $G_{yy}(f)$ and $G_{1y}(f)$ are replaced by conditioned spectral quantities $G_{22,1}(f)$, $G_{yy,1}(f)$ and $G_{2y,1}(f)$.
3. The ordinary coherence function $\gamma^2_{1y}(f)$ is replaced by the partial coherence function $\gamma^2_{2y,1}(f)$.

Therefore, the ordinary function formula for input $x_1(t)$ and output $y(t)$ can be obtained as

$$\gamma^2_{1y}(f) = \frac{|G_{1y}(f)|^2}{G_{11}(f)G_{yy}(f)} \quad (3.86)$$

while the partial coherence function can be stated as

$$\gamma^2_{2y,1}(f) = \frac{|G_{2y,1}(f)|^2}{G_{22,1}(f)G_{yy,1}(f)} \quad (3.87)$$

For all values of f , the partial coherence function satisfies the following:

$$0 \leq \gamma^2_{2y,1}(f) \leq 1 \quad (3.88)$$

3.7.2 General and Conditioned Multiple-Input Models

The general multiple-input/output model for an arbitrary number of inputs is illustrated in Figure 3.8 and is adapted from “Random Data Analysis and Measurement Procedures (2000)” by Bendat and Piersol. The terms $X_i(f)$, $i = 1, 2, \dots, q$, where q is the number of

inputs records, represents the finite Fourier transforms of input signals $x_i(t)$. The finite Fourier transform of output record $y(t)$ is represented by $Y(f)$. The constant-parameter linear frequency response functions to be determined are represented by $H_{iy}(f), i = 1, 2, \dots, q$, while $N(f)$ represents the finite Fourier transform of the unknown extraneous output noise. It is assumed that the input and output records are measured simultaneously using a common time base.

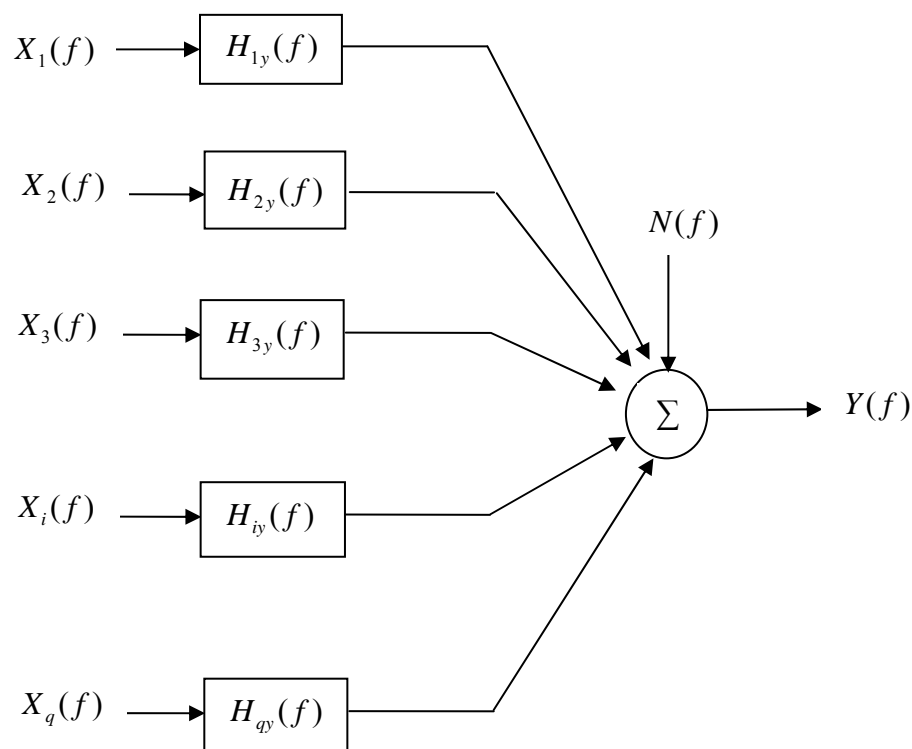


Figure 3.8 Multiple-Input Model for Arbitrary Inputs
(Adapted from Bendat/Piersol, 2000)

An alternate conditioned multiple-input/output model is shown in Figure 3.9. The original given inputs in previous figure are replaced by an ordered set of conditioned input records. For any i , the subscript notation $i.(i-1)!$ represents the i^{th} record conditioned on the previous $(i-1)$ records, which means that the linear effects of $x_1(t)$, $x_2(t)$, up to $x_{i-1}(t)$ have been removed from $x_i(t)$. These ordered conditioned input records will be mutually uncorrelated. Constant-parameter linear frequency response functions to be determined are represented by $L_{iy}(f)$, $i = 1, 2, \dots, q$, where the input precedes the output index.

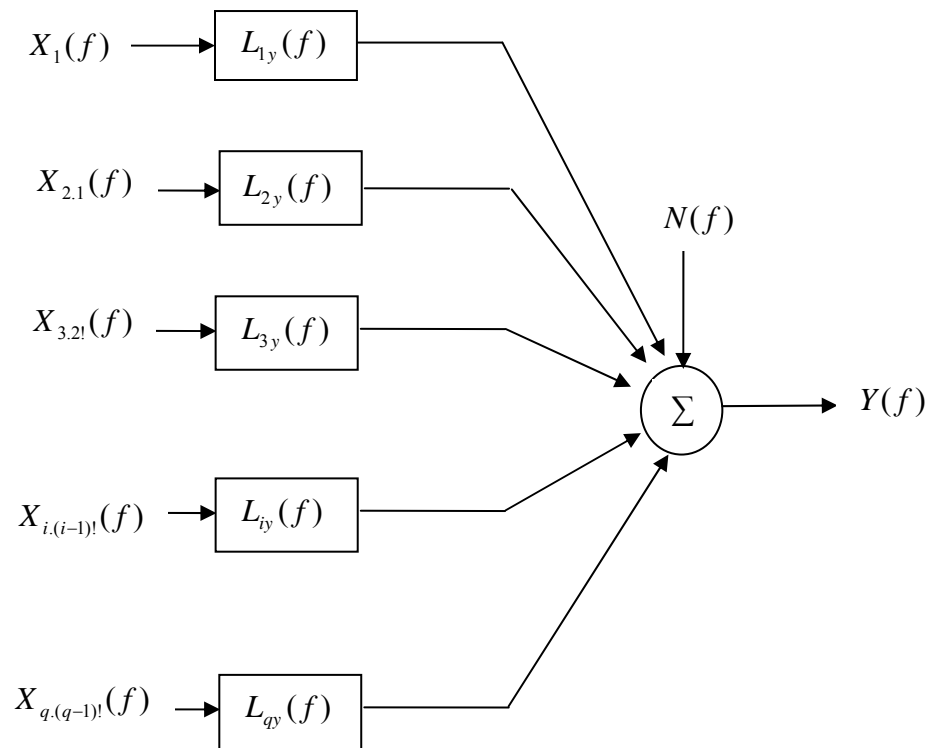


Figure 3.9 Multiple-Input Model for Ordered Conditioned Inputs
(Adapted from Bendat/Piersol, 2000)

3.7.2.1 Algorithm for Conditioned Spectra and Frequency Response Functions

A simple algorithm that computes frequency response functions from conditioned spectral densities was defined by Bendat and Piersol. A four-input/one-output problem which represents the multiple-input case of the benchmark problem is solved in order to illustrate this procedure in this section. Any multiple-input/multiple-output problem may be solved using the same algorithm by first breaking down the system into multiple-input/single-output problems and then ordering the signals using coherence functions.

The Fourier transforms of the conditioned inputs records are denoted by X_1 , $X_{2,1}$, $X_{3,2}$ up to $X_{q,(q-1)}$, where q is the number of input signals and may be calculated from the given input records by using the following formulation.

$$X_{j,r!} = X_{j,(r-1)!} - L_{rj} * X_{r,(r-1)!} \quad (3.89)$$

where j index must always be greater than r index, since only linear effects of a previous signal may be removed from a latter one. Equation (3.89) can be written for a four-input/one-output system as follows:

$$X_{2,1} = X_2 - L_{12} * X_1 \quad (3.90)$$

$$X_{3,2!} = X_{3,1} - L_{23} * X_{2,1} \quad (3.91)$$

$$X_{4,3!} = X_{4,2!} - L_{34} * X_{3,2!} \quad (3.92)$$

The constant-parameter linear system L_{qy} may be obtained as

$$L_{qy} = \frac{G_{qy,(q-1)!}}{G_{qq,(q-1)!}} \quad (3.93)$$

where the conditioned spectral density functions can be computed with the following expression

$$G_{ij,r!} = G_{ij,(r-1)!} - \left[\frac{G_{rj,(r-1)!}}{G_{rr,(r-1)!}} \right] G_{ir,(r-1)!} \quad (3.94)$$

If Equation (3.94) is examined carefully, it can be seen that the term $\frac{G_{rj,(r-1)!}}{G_{rr,(r-1)!}}$ is the same term in Equation (3.93) with different indices. Therefore, it may be calculated as

$$L_{rj} = \frac{G_{rj,(r-1)!}}{G_{rr,(r-1)!}} \quad (3.95)$$

$$\text{where} \quad r = 1, 2, \dots, (j-1) \quad (3.96)$$

$$j = 1, 2, \dots, (q+1) \quad (3.97)$$

General frequency response functions may then be found using

$$H_{iy} = L_{iy} - \sum_{j=i+1}^q L_{ij} H_{jy} \quad i = (q-1), (q-2), \dots, 1 \quad (3.98)$$

$$H_{qy} = L_{qy}$$

For a four-input/single-output model, (such as the benchmark problem analyzed in next section) frequency response functions may be obtained using the algorithm discussed above.

To Compute **L1y**:

$$L_{1y} = \frac{G_{1y}}{G_{11}} \quad (3.99)$$

To Compute **L2y**:

$$L_{2y} = \frac{G_{2y.1}}{G_{22.1}} \quad (3.100)$$

where

$$G_{2y.1} = G_{2y} - L_{1y} * G_{21} \quad (3.101)$$

$$G_{22.1} = G_{22} - L_{12} * G_{21} \quad (3.102)$$

$$L_{12} = \frac{G_{12}}{G_{11}} \quad (3.103)$$

and L_{1y} can be obtained from the previous system.

To Compute **L3y**:

$$L_{3y} = \frac{G_{3y.2!}}{G_{33.2!}} \quad (3.104)$$

where

$$G_{3y.2!} = G_{3y.1} - L_{2y} * G_{32.1} \quad (3.105)$$

$$G_{33.2!} = G_{33.1} - L_{23} * G_{32.1} \quad (3.106)$$

To Compute L_{4y} :

$$L_{4y} = \frac{G_{4y,3!}}{G_{44,3!}} \quad (3.107)$$

According to Equation (3.98), for a four-input / single-output model the relationship between constant-parameter linear systems H_{qy} and L_{qy} may be stated as:

$$H_{4y} = L_{4y} \quad (3.108)$$

$$H_{3y} = L_{3y} - L_{34}H_{4y} \quad (3.109)$$

$$H_{2y} = L_{2y} - L_{23}H_{3y} - L_{24}H_{4y} \quad (3.110)$$

$$H_{1y} = L_{1y} - L_{12}H_{2y} - L_{13}H_{3y} - L_{14}H_{4y} \quad (3.111)$$

3.7.2.2 Spectral Density and Frequency Response Functions Using Matrix Calculations

Let X be a column vector representing the Fourier transforms of the q input records $X_i = X_i(f)$, $i = 1, 2, \dots, q$ and Y be a column vector representing the Fourier transforms of the q output records $Y_k = Y_k(f)$, $k = 1, 2, \dots, q$

$$\begin{array}{r}
 X1 \\
 X2 \\
 \dots \\
 Xq
 \end{array}
 =
 \begin{array}{r}
 Y1 \\
 Y2 \\
 \dots \\
 Yq
 \end{array}
 \quad (3.112)$$

$$G_{xx} = \frac{2}{T} E\{X^* X'\} = \text{input spectral density matrix} \quad (3.113)$$

$$G_{yy} = \frac{2}{T} E\{Y^* Y'\} = \text{output spectral density matrix} \quad (3.114)$$

$$G_{xy} = \frac{2}{T} E\{X^* Y'\} = \text{input / output cross-spectral density matrix} \quad (3.115)$$

The basic matrix terms may be written using the definitions given above as follows

$$G_{xx} = \begin{matrix} G_{11} & G_{12} & \cdots & G_{1q} \\ G_{21} & G_{22} & \cdots & G_{2q} \\ \cdots & \cdots & \cdots & \cdots \\ G_{q1} & G_{q2} & & G_{qq} \end{matrix} \quad \text{input spectral density matrix} \quad (3.116)$$

$$G_{yy} = \begin{matrix} G_{y1y1} & G_{y1y2} & \cdots & G_{y1yq} \\ G_{y2y1} & G_{y2y2} & \cdots & G_{y2yq} \\ \cdots & \cdots & \cdots & \cdots \\ G_{yqy1} & G_{yqy2} & & G_{yqyq} \end{matrix} \quad \text{output spectral density matrix} \quad (3.117)$$

$$G_{xy} = \begin{matrix} G_{1y1} & G_{1y2} & \cdots & G_{1yq} \\ G_{2y1} & G_{2y2} & \cdots & G_{2yq} \\ \cdots & \cdots & \cdots & \cdots \\ G_{qy1} & G_{qy2} & & G_{qyq} \end{matrix} \quad \text{cross-spectral density matrix} \quad (3.118)$$

Without any further proof, the frequency response function matrix may be defined as follows

$$H_{xy} = G_{xx}^{-1} G_{xy} \quad (3.119)$$

where G_{xx}^{-1} is the inverse matrix of G_{xx} .

It is assumed that the number of inputs is the same as number of outputs and the inverse matrix operations can be performed.

Thus, the frequency response matrix obtained using Equation (3.119) can be shown as

$$H_{xy} = \begin{matrix} H_{1y1} & H_{1y2} & \dots & H_{1yq} \\ H_{2y1} & H_{2y2} & \dots & H_{2yq} \\ \dots & \dots & \dots & \dots \\ H_{qy1} & H_{qy2} & \dots & H_{qyq} \end{matrix} \quad \text{frequency response matrix} \quad (3.120)$$

Multiple-input/multiple-output problems can be solved easily using the matrix techniques described above. However, for the greatest physical insight into the problem, it is recommended by Bendat and Piersol that these problems be broken down into multiple-input/single-output models, and solved by the algebraic procedures outlined in section 3.7.2.1.

Matrix calculations may also be used for multiple-input/single-output and single-input/single-output problems.

3.7.2.3 Partial and Multiple Coherence Functions

Ordinary coherence functions between any input $x_i(t)$ for $i = 1, 2, \dots, q$ and the total output y are defined by

$$\gamma^2_{iy}(f) = \frac{|G_{iy}(f)|^2}{G_{ii}(f)G_{yy}(f)} \quad (3.121)$$

Partial coherence functions between any conditioned input $x_{i,2!}$ for $i = 3, 4, \dots, q$ and the output $y,2!$ may be defined by the following expression

$$\gamma^2_{iy,2!} = \frac{|G_{iy,2!}|^2}{G_{ii,2!}G_{yy,2!}} \quad (3.122)$$

up to

$$\gamma^2_{qy,(q-1)!} = \frac{|G_{qy,(q-1)!}|^2}{G_{qq,(q-1)!}G_{yy,(q-1)!}} \quad (3.123)$$

where, for a q -input/one-output model, $G_{yy,q!}$ is called the noise output spectrum, and can be defined as

$$G_{yy,q!} = G_{yy} \prod_{i=1}^q (1 - \gamma^2_{iy,(i-1)!}) \quad (3.124)$$

Thus, for a two-input/one-output model, the noise output spectrum is

$$G_{yy,2!} = G_{yy,1}(1 - \gamma^2_{2y,1}) = G_{yy}(1 - \gamma^2_{1y})(1 - \gamma^2_{2y,1}) \quad (3.125)$$

For a q -input/one-output model, the multiple coherence function is given by

$$\gamma^2_{y:q!} = 1 - \left(\frac{G_{yy,q!}}{G_{yy}} \right) = 1 - \prod_{i=1}^q (1 - \gamma^2_{iy,(i-1)!}) \quad (3.126)$$

For a two-input/one-output model, the multiple coherence function may be defined by

$$\gamma^2_{y:2!} = 1 - \left(\frac{G_{yy,2!}}{G_{yy}} \right) = 1 - (1 - \gamma^2_{1y})(1 - \gamma^2_{2y,1}) \quad (3.127)$$

4 ANALYSIS MODELS FOR BENCHMARK TEST CASES

The results available from the first phase of the UBC structural benchmark problem may be divided into two parts according to the input/output parameters involved. The force input at the roof level combined with the corresponding acceleration measurements taken at each floor level can be analyzed as a single-input/multiple-output problem. This set of measurement data will be discussed as the first case presented in this section. The force input at each floor level, along with the corresponding acceleration measurements taken at each floor level, are analyzed as a multiple-input/multiple-output problem and are discussed as the second case presented in this section.

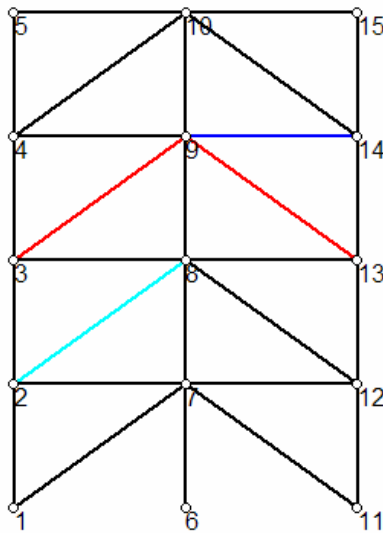


**Figure 4.1 Node Numbering for 2-D
Finite Element Model**

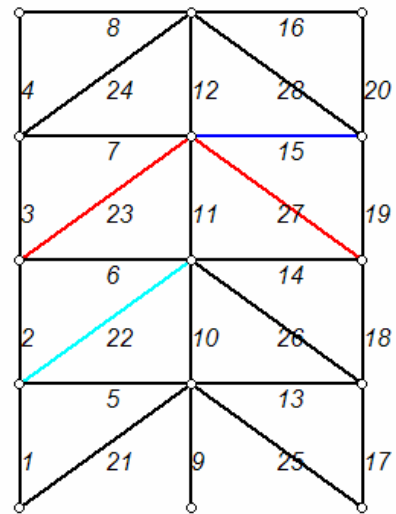


**Figure 4.2 Element numbering for 2-D
Finite Element Model**

Figure 4.1 shows the node numbering assigned for the 2-D finite element model used by the proposed SDIM. This 2-D finite element model is generated by the information provided by the input card as discussed in Section 2. The properties of the structural members, which include the columns, beams and braces, are recorded concerning the area, moment of inertia, and Young Modulus attributed to each member. The element numbering for the 2-D finite element model of the structure is shown in Figure 4.2.

The program Datagen provides the capability to examine both single and multiple excitation location cases. Case 1 simulates the effect of wind vibration by applying random forces in the y-direction (weak direction) of the structure. The structural finite element model used in Case 1 is a simple 12-DOF model. Case 2 uses a 120-DOF finite element model in order to introduce a level of modeling error to the system. Case 3 uses the 12-DOF model along with the symmetric mass distribution used in Case 1 and 2. However, the force is applied at the roof level in the weak and strong directions, which simulates the response behavior of a diagonally placed shaker. Cases 4 and 5 use an asymmetric mass distribution by replacing one of the 400-kg slab floor slabs with a 550-kg floor slab (Detailed information regarding the benchmark structure may be found in Section 2.2.1.). The 12-DOF model is used in Case 4, while Case 5 uses the 120-DOF model. All of the acceleration records are measured from the center columns along each side of the structure in both the single and multiple excitation cases.

Figure 4.3 presents the acceleration/measurement locations specified for the single-input/multiple-output problem. The measured accelerations are located at nodes 7, 8, 9 and 10, while the excitation is placed at node 10. Due to working with a 2-D finite element model for damage identification, this case may be analyzed using the response in either the strong or weak direction, even though the structure is excited in both axis directions. This is allowed because when the mass distribution in the 3-D structure is symmetric there is no torsional response due to the excitation force.

The excitation/measurement pairs used for the multiple-input/multiple-output problems (Cases 1 and 2) are presented in Figure 4.4. Accelerometers are placed at

nodes 7, 8, 9 and 10, while excitation forces are applied at nodes 12, 13, 14 and 15. The mass distribution is symmetric and the structure is only excited in the weak direction (y-axis).

There are six main damage patterns defined as part of the first phase of the UBC benchmark problem (Please refer to Section 2.2 for the input screen of these damage cases): (i) all of the first floor braces are removed, (ii) all of the first and third floor braces are removed, (iii) one brace is removed in first story, (iv) one brace is removed in each of the first and third stories, (v) one brace is removed in the first and third stories and a floor beam is loosen in the first story and (vi) area of one brace on one side of the 1st story is reduced to 2/3.

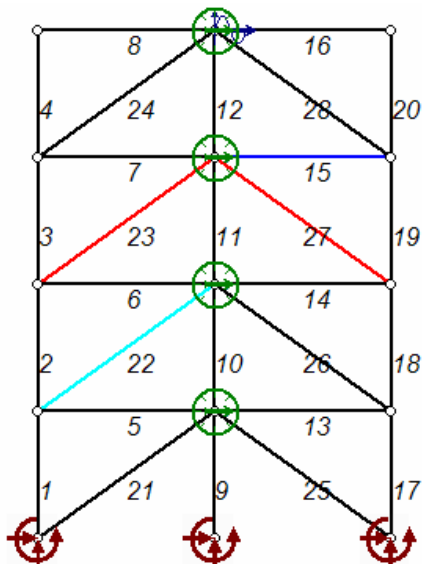


Figure 4.3 Input/Output Locations for the Single-Input/Multiple-Output Model

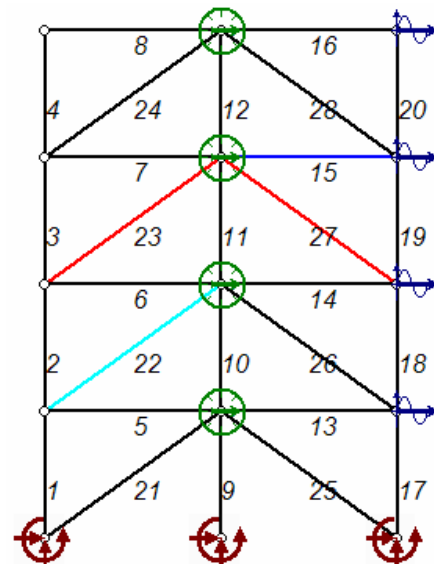


Figure 4.4 Input/Output Locations for the Multiple-Input/Multiple-Output Model

4.1 Single-Input/Multiple-Output Model

For Cases 3, 4 and 5, the FRFs will be computed using the force inputs and acceleration outputs in y-axis (weak direction). Section 3 summarizes the procedure used to obtain the FRFs for single-input/multiple-output problems. Once the power and cross-spectral density functions are determined for the given input and outputs, then the frequency response function is calculated as the ratio of the cross-spectrum between the input and output signals to power spectrum of the output signal. (Please refer to Equation 3.41 in Section 3.)

Once specific structural members are defined to be damaged (either using the pre-defined damage cases or user-defined damage case), Datagen provides the input (force) and output (acceleration) records for that particular damage case. These parameters are then used to obtain the spectral density functions required to perform the frequency response function calculations in the Matlab[®] Signal Processing Toolbox V.6 where three methods, which include nonparametric, parametric and subspace, are defined for spectrum estimation. Nonparametric methods that estimate the spectrum densities directly from the signal itself are used in this research. Using the Toolbox in this research was very effective since the formulations for calculating the FRFs presented in Section 3 are dependent on the expected value calculations, and all the calculations are based on finite set of data.

Each signal is sampled at 1 kHz and then downsampled to 125 Hz using 120 seconds as the time duration. Matlab[®] offers a function called *resample.m* that applies a low-pass, anti-aliasing filter to the records in order to avoid aliasing effects. Resampling reduces the number of points needed for the identification process. A Hanning window is also used in calculations in order to reduce the effects of leakage.

As a reference, the spectral density, frequency response, and coherence function graphs obtained from the undamaged structure using Case 3 will be presented. Noise is not present in the system for this simple case.

Figure 4.5 shows the cross-spectral density between the forcing function at the roof level and the acceleration record obtained at the first floor; hence the cross-spectral density is named G_{xy_1} which corresponds to input x and output taken from the first floor y_1 . The same naming convention of the variables will be used throughout the research unless otherwise stated. Figures 4.6 and 4.7 show the frequency response function and coherence function that correspond to the same excitation/measurement pair, respectively (the force at the roof level and the acceleration at the first floor).

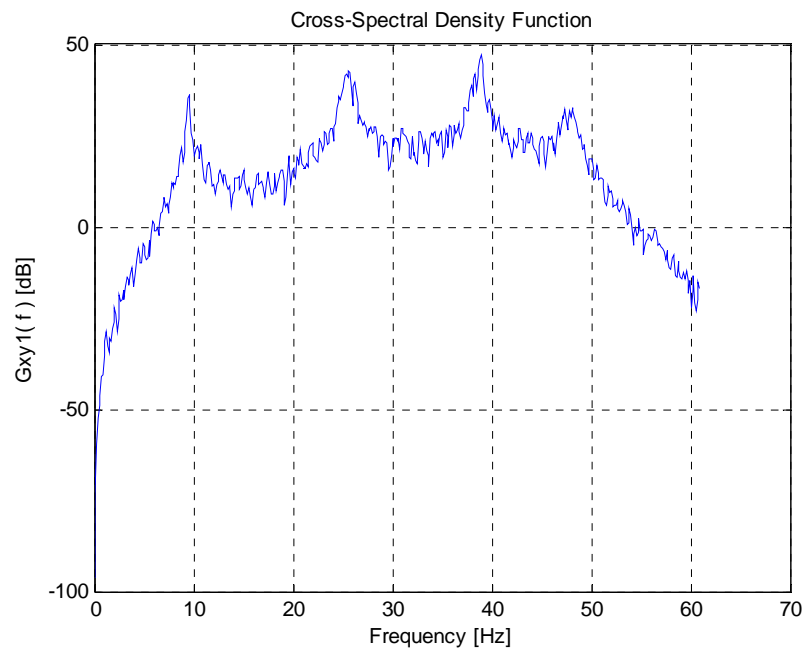


Figure 4.5 Cross-Spectrum Function Between Force Input at Roof Level and Acceleration Output at the First Floor in the Weak Direction

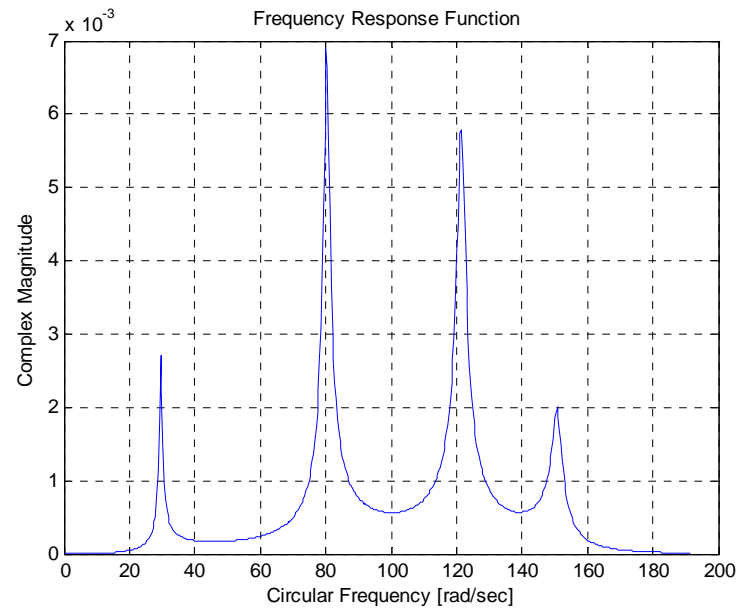


Figure 4.6 Frequency Response Function Between Force Input at Roof Level and Acceleration Output at the First Floor in the Weak Direction

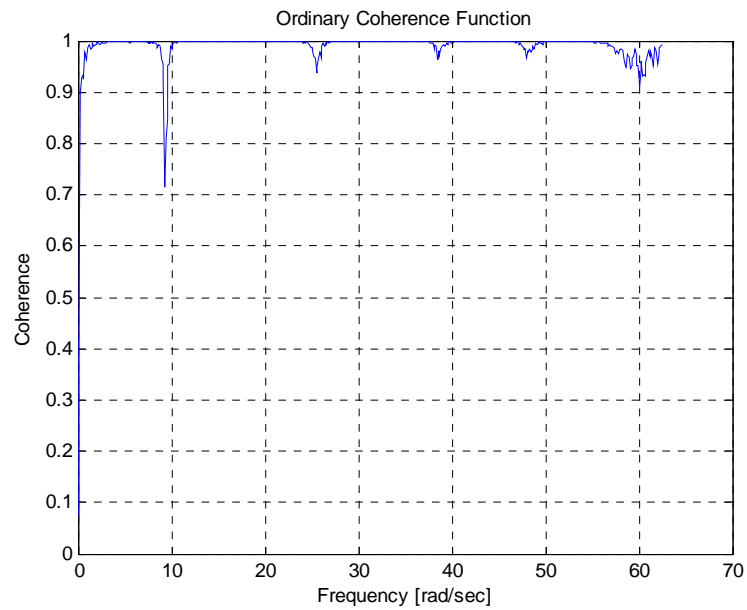


Figure 4.7 Ordinary Coherence Function Between Force Input at Roof Level and Acceleration Output at the First Floor in the Weak Direction

4.2 Multiple-Input/Multiple-Output Model

Case 1 and 2 of the first phase are analyzed as multiple-input/multiple-output problems, as stated previously. The FRFs will be computed by the procedures detailed in Section 3 using the force inputs and acceleration outputs in y-axis (weak direction). Before discussing any case, the four conditions stated in Section 7.3.1 for the multiple input system to be well-defined must be checked.

As shown in Figure 4.8, the ordinary coherence function between the force input at the first and second floor is not unity (where unity would correspond to 0 in dB-log scale). This satisfies the first condition that states that none of the ordinary coherence functions between any pair of input records should equal unity. The same results may be obtained if ordinary coherence is calculated for the other inputs.

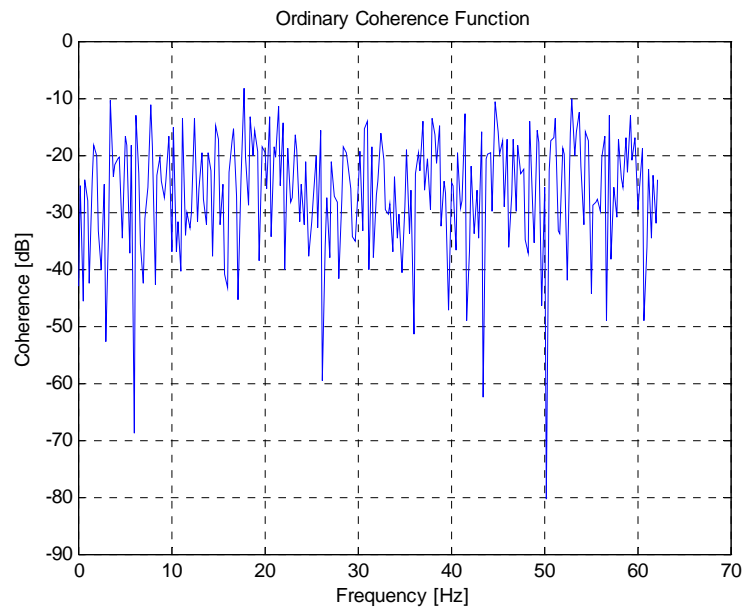


Figure 4.8 Ordinary Coherence Function Between Force Input at the First and Second Floor

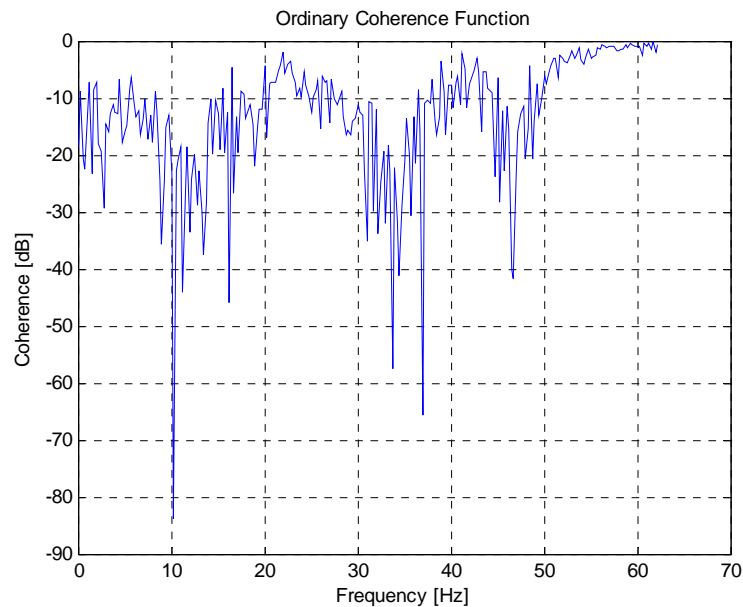


Figure 4.9 Ordinary Coherence Function Between Force Input and Acceleration Output at the First Floor

In addition to have a well-defined system, none of the ordinary coherence functions between any input and the total output should equal unity. Figure 4.9 shows the ordinary coherence function between the force input and acceleration output at the first floor and it is clear that unity hasn't been achieved in any frequency.

The multiple coherence function between the first floor acceleration and forces in each story can be seen in Figure 4.10. Coherence is significantly high, which implies the presence of an almost perfect linear model. This is an expected result if the definition of multiple coherence function is recalled. The multiple coherence function is the ratio of the ideal output spectrum due to measured inputs in the absence of noise to the total output spectrum that includes the noise. Since noise is defined to be zero for this simple model, multiple coherence values are expected to be significantly high, reaching almost unity. The multiple coherence function between the output and the given inputs, in a practical situation being significantly high is the other condition that is also satisfied.

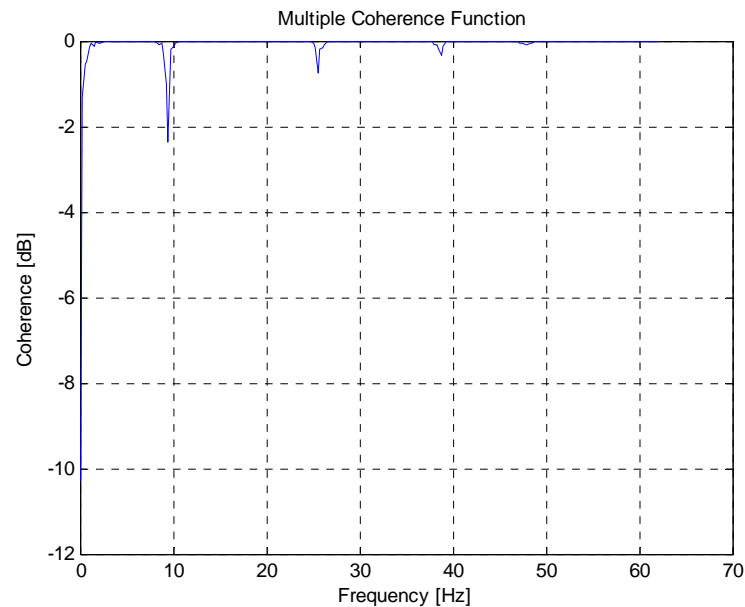


Figure 4.10 Multiple Coherence Function Between the Output (First Floor Acceleration) and the Given Inputs (Forces in Each Story)

It is worth mentioning that the procedures discussed above should be repeated for each output if the system is broken down into multiple-input/single-output systems. This process is detailed in Section 3 and is applied to all multiple-input/multiple-output problems throughout this research effort. Section 3.7.2.1 presents a straightforward algorithm that uses conditioned spectral density functions to obtain constant-parameter linear systems L_{iy} . General frequency response functions H_{iy} may then be computed using Equation 3.98. However, signals should be ordered first since the linear effects of the former input must be removed from the latter one.

The use of measurement/excitation pairs as defined in Section 2 plays a key role in using this concept. The utility program, ModalFEM, defines FRF matrices for each excitation/measurement pair as discussed in Section 2.3.2. For the sake of this argument, a simple input card will be defined again.

*NSET, NSET=MEAS

7, 8, 9, 10

*NSET, NSET=EXC

12, 13, 14, 15

These excitation/measurement pairs correspond to Figure 4.4 where multiple-input/multiple-output problem is defined. ModalFEM gives the FRFs for EXC 1- MEAS 1 (7-12), EXC 2- MEAS 2 (8-13), EXC 3- MEAS 3 (9-14), and EXC 4- MEAS 4 (10-15). Thus for the benchmark problem at hand, when the measurement is taken from the first floor the excitation/measurement pair is (7-12) - first floor acceleration to first floor force in ModalFEM, the excitation at the first floor is identified as the first input record and the linear effects of it are removed from the remaining force vectors (at nodes 13, 14 and 15). The force input at the second floor is then defined to be the second input and the linear effects of it may be removed from the other two forcing vectors (at nodes 14 and 15) using conditioned spectra. Following the same convention, when the related excitation/measurement pair is (8-13), the linear effects of the force at node 13 should be removed from the remaining force vectors such as 12, 14, and 15.

ModalFEM can only take the number of measurements into account when computing the FRFs, currently. Therefore, the number of FRF matrices depends solely on the number of accelerometers. Solving a multiple-input/single-output problem is only possible by repeating the measurement location at each different excitation node.

*NSET, NSET=MEAS

7, 7, 7, 7

*NSET, NSET=EXC

12, 13, 14, 15

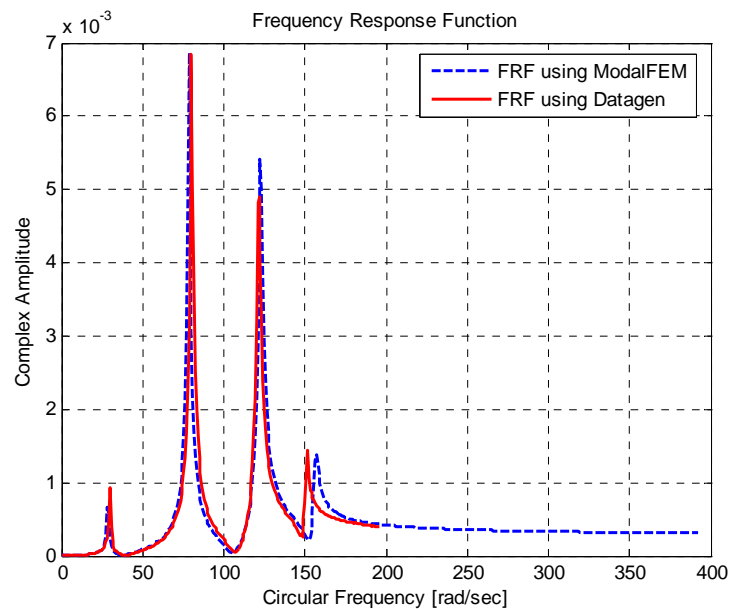


**Figure 4.11 FRF for 12/7 Excitation/Measurement Pair
for the MIMO Problem**

ModalFEM will compute the FRFs at each excitation/measurement location with these input parameters. Thus, the FRFs will correspond to these pairs: EXC 1- MEAS 1 (7-12), EXC 1- MEAS 2 (7-13), EXC 1- MEAS 3 (7-14), and EXC 1- MEAS 4 (17-15).

Figure 4.11 plots the FRF versus frequency computed for the first floor excitation and measurement pair of the multiple-input/multiple-output (MIMO) problem. This case may be defined by applying the force at node 12 and placing the accelerometer at node 7 in ModalFEM. Two graphs are plotted on the same scale in order to provide a comparison. Since the use of ModalFEM will be completely eliminated from the system when using the hybrid approach, the performance of the proposed algorithm will depend on how well Datagen captures the response that ModalFEM simulates. Thus, without running the program, one may be able to predict the success of that particular trial by just examining the graphs. Demonstrative graphs of the results obtained from

some of the test cases will be provided in the Results and Discussions Section for this reason.

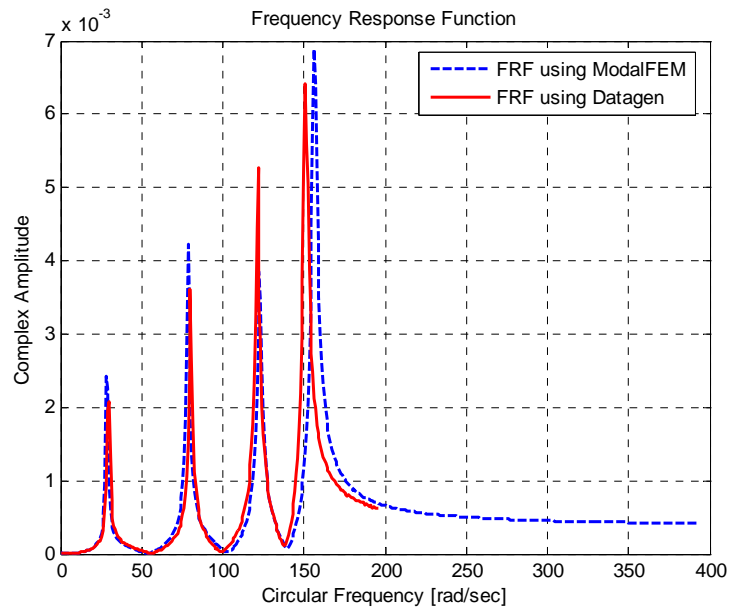


**Figure 4.12 FRF for 13/8 Excitation/Masurement Pair
for the MIMO Problem**

Figure 4.12 shows the FRF graphs computed for the second floor excitation and measurement pair of the multiple-input/multiple-output (MIMO) problem. The dashed line presents the FRF computed by ModalFEM, while the solid line is the FRF calculated using the measurement information provided by Datagen using the procedures detailed above and in Section 3. The correlation between the two FRFs is fairly strong, especially at lower frequencies, as indicated in the Figure.

The following figures highlight multiple-input/single-output cases where the forcing functions are acting on the edge columns on each floor level and the

accelerometer is placed at node 7, which corresponds to the center column at the first floor level.

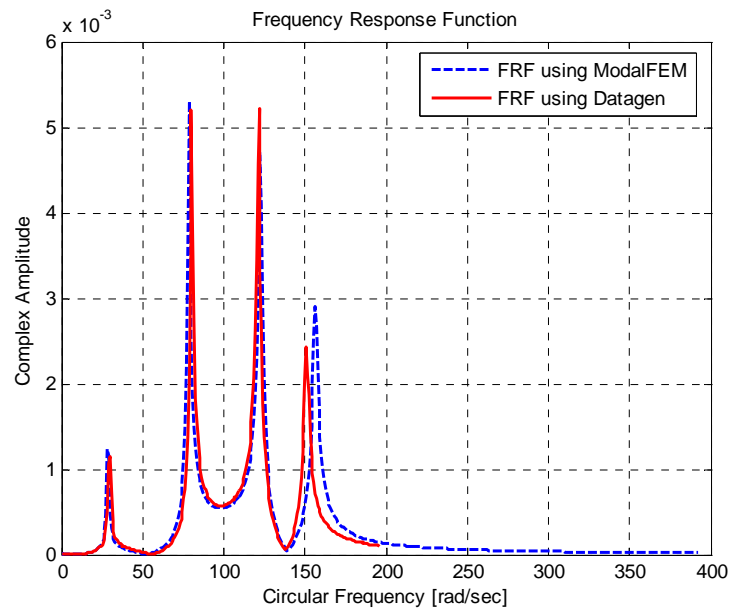


**Figure 4.13 FRF for 13/7 Excitation/Measurement Pair
for the MISO Problem**

The excitation is located at the second floor in Figure 4.13, while it acts on the edge column of the third floor in Figure 4.14.

It should be noted that the 12/7 - excitation / measurement pair would be the same in both the MIMO and MISO cases, so the results are not repeated for the MISO case. The second and third floor excitations are used instead.

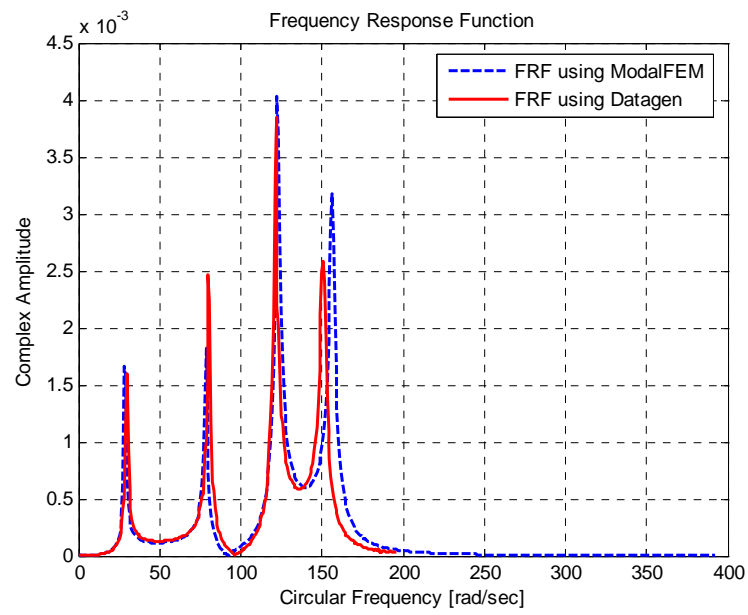


**Figure 4.14 FRF for 14/7 Excitation/Measurement Pair
for the MISO Problem**

5 RESULTS AND DISCUSSIONS

This section is divided into four sub-sections. Sections 5.1, 5.2 and 5.3 present the results obtained from considering the SIMO, MISO and MIMO problems for ideal noise free measurements. The last section, section 5.4, provides the damage detection results obtained when noisy measurements were used by the SDIM.

The results obtained from each test case are provided both in tabular format and graphically. The damage indices (percent damages) values predicted by the SDIM are presented before and after hillclimbing is applied in order to compare the performance of the local hillclimber on improving the results obtained by the SDIM proposed.

A comparison of the FRF graphs obtained using Datagen and ModalFEM is presented before any results for a particular test case are presented. In previous research, it has been shown that GaDamDet is able to locate and quantify damage using its own utility program that simulates dynamic response, thus the performance of any trial directly depends on how well Datagen replaces ModalFEM. A perfect match between the FRFs available will ensure a successful damage detection result, while any small difference in the FRFs would correspond to a possible shift from the optimal solution.

Table 5.1 defines the GA parameters used by the SDIM to perform optimization throughout this research. The same parameters will be used in each trial unless otherwise stated. These parameters are provided as the defaults of GaDamDet program (with the only exception of turning on the reduced hillclimbing option).

Table 5.1 GA Parameters Used

Population Size	200
Primary Crossover Rate	0.9
Mutation Rate	0.005
Coding Type	Binary
Variable Representation	Implicit Redundant Representation (IRR)
Seeded Initial Population	

5.1 Single-Input/Multiple-Output Model

5.1.1 Case 3: 1st Story Braces Are Damaged

Results of considering damage pattern one (all first story braces are 100% damaged) using Case 3 (12-DOF model with symmetric mass distribution) is presented in this section. This case is one of the simplest cases of the SIMO problems at hand since there is no rotational response due to the diagonally applied force at the roof when the mass distribution is symmetric. Figures 5.1 through 5.4 provide the FRF graphs obtained when the first floor braces (namely element # 21 and # 25) are defined to be 100% damaged. The solid curve represents the FRF found using Datagen, while the dashed curve is the FRF obtained using ModalFEM. An obvious difference appears in the last modes of the FRFs, which may lead into a shift from the optimal solution.

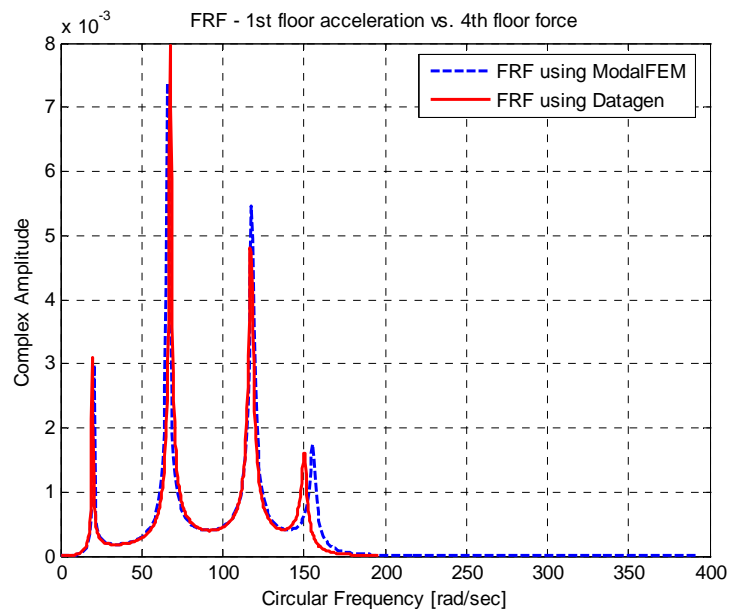


**Figure 5.1 FRF for the 1st Floor – 1st Story Braces Are Broken
SIMO - 12 DOF Symmetric Model**

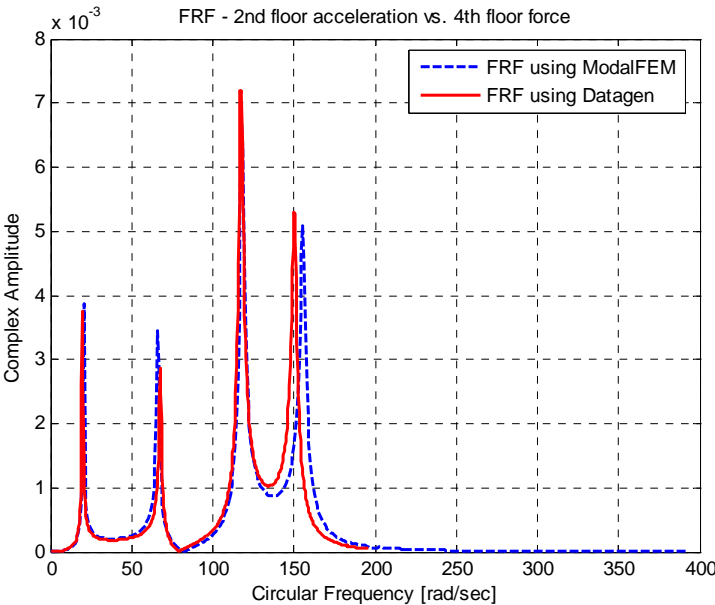


Figure 5.2 FRF for the 2nd Floor – 1st Story Braces Are Broken SIMO - 12 DOF Symmetric Model

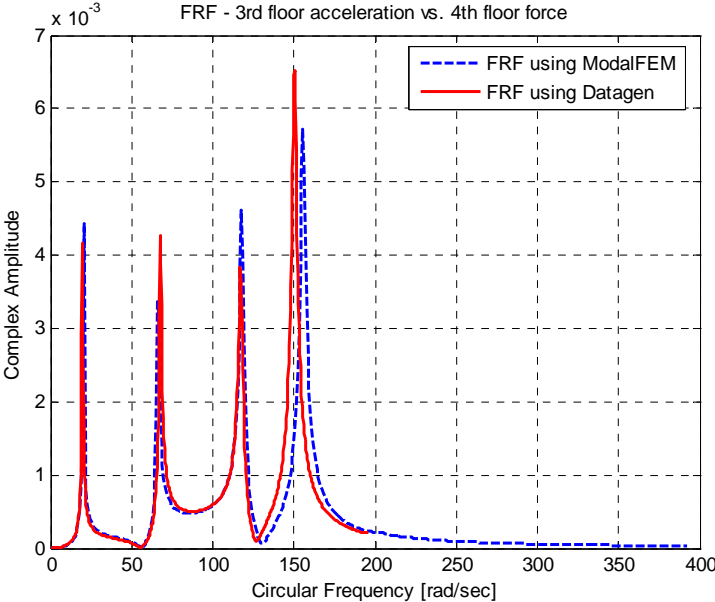
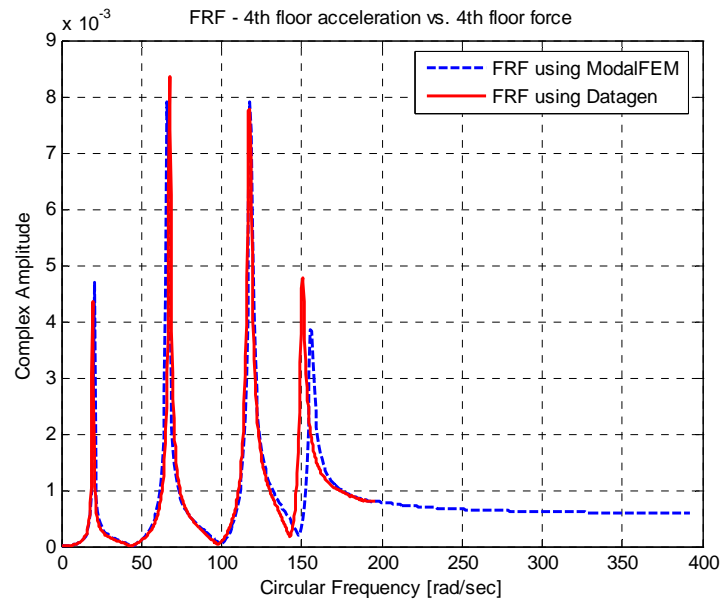


Figure 5.3 FRF for the 3rd Floor – 1st Story Braces Are Broken SIMO - 12 DOF Symmetric Model



**Figure 5.4 FRF for the 4th Floor – 1st Story Braces Are Broken
SIMO - 12 DOF Symmetric Model**

Noise is not present in the system for these trials. Two different cases are analyzed in order to examine the effects of the shifted last mode on the ability of the SDIM to detect damage.

5.1.1.1 All Four Modes Are Used for Damage Detection

If all four modes are used in damage detection algorithm, then the following results are obtained. “Full Sensor Layout” mentioned in the following tables imply the usage of all accelerometer information available. All SIMO and MIMO trials have four different accelerometer locations and FRFs will be computed using all these four measurements. However, only one accelerometer (either at the first or second floor) is available in MISO problems which simulates the usage of partial sensor layout in the system.

**Table 5.2 SDIM Results for 1st Story Braces Damaged Using 4 FRFs – SIMO
Case 3, All Four Modes Are Used**

Trial	Case	Imposed Damage	Sensor Layout	Damaged Elements	Percent
Trial #1	12 DOF-Symmetric	1 st story braces 100%	Full	1 st story brace # 21	62.01%
	Measurements are taken in y- direction			1 st story brace # 25	88.19%
				# 13	81.85%
				# 14	49.50%
				# 19	64.97%
				# 27	15.07%

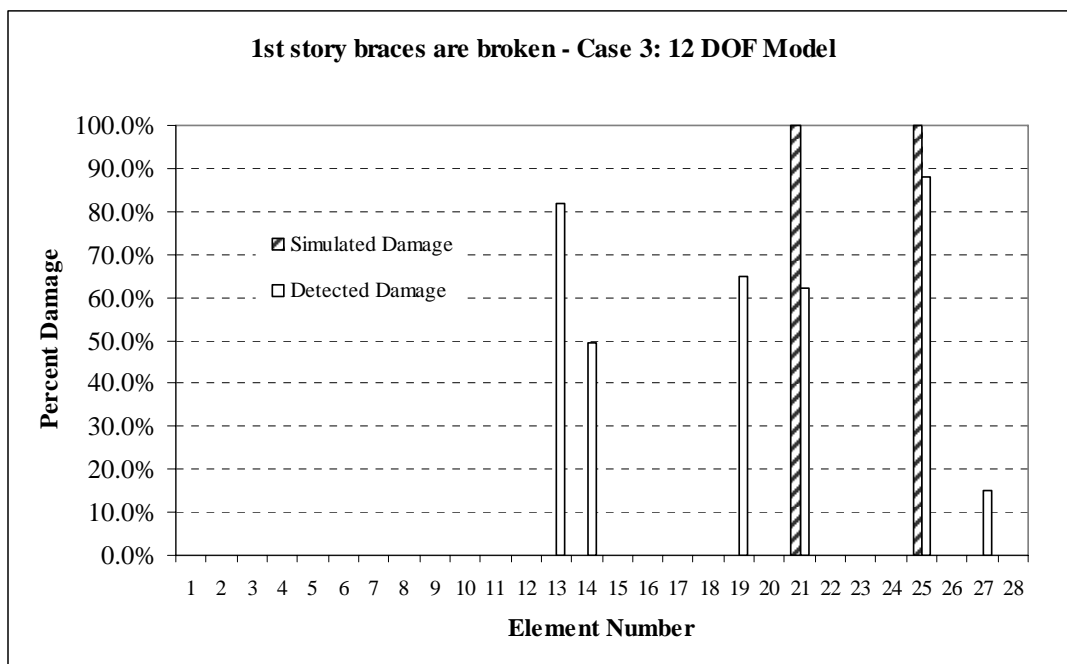


Figure 5.5 Simulated vs. Detected Damages for Trial #1

Table 5.2 and Figure 5.5 provide the results obtained by the SDIM without using the hillclimber. The proposed SDIM detected 62.01% and 88.19% damage at first floor brace #21 and #25, respectively, while the simulated damage was 100% in these braces. Moreover, four members were falsely identified as damaged in this particular trial. Table 5.3 and Figure 5.6 provide the results for Trial #1 after 1867 hillclimbing iterations. It can be seen that the hillclimbing operator was able to eliminate one falsely damage member from the solution set, although it was not able to improve the overall results significantly. Hillclimbing is not guaranteed to improve the results (and most likely will not); unless a good set of reference points – a good current solution – is provided. The hillclimber searches for better points in the neighborhood of the current solution. If the current (best) solution is near-optimal to start with, the system may iterate into a wrong solution set, thus giving more falsely damaged members or leading to a decrease in damage indices of the actual damaged elements. The hillclimbing operator, therefore, should only be considered as a fine-tuner of the program and it is not accounted for improving the results for relatively unsuccessful trials.

**Table 5.3 SDIM Results for 1st Story Braces Damaged Using 4 FRFs – SIMO
Case 3, All Four Modes Are Used, After Hillclimbing # 1867**

Trial	Case	Imposed Damage	Sensor Layout	Damaged Elements	Percent
Trial #1	12 DOF-Symmetric	1st story braces 100%	Full	1st story brace # 21	60.15%
	Measurements are taken in y- direction			1st story brace # 25	93.88%
				# 13	90.27%
				# 19	63.24%
				# 27	14.11%

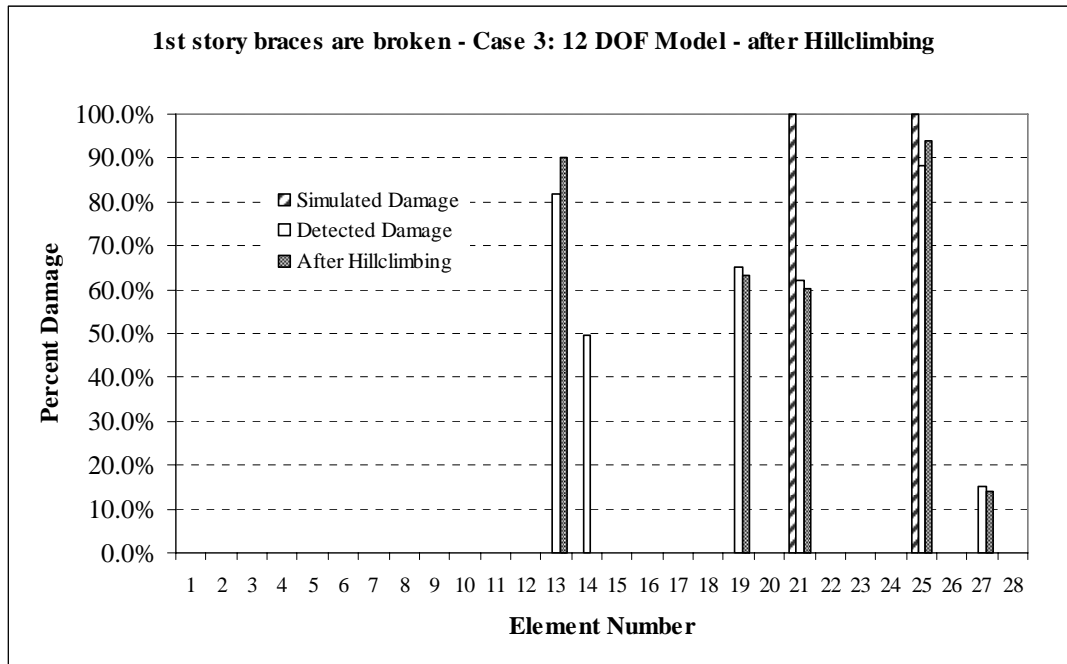


Figure 5.6 Simulated vs. Detected Damages for Trial #1 with Hillclimbing # 1867

5.1.1.2 The Last Mode Is Omitted for Damage Detection

This trial is expected to provide better damage detection results than the previous one, since the effects of the last mode are removed from the system by only using FRFs up to that point. Practically, omitting a mode from the FRF response data would be difficult to do as the user would not be able to eliminate any modes from the system without a good understanding of the natural frequencies of the system. However, these trials are performed to investigate how much information is gained (or lost) by omitting a mode from the FRF used by the SDIM.

**Table 5.4 SDIM Results for 1st Story Braces Damaged Using 4 FRFs – SIMO
Case 3, Last Mode Is Omitted**

Trial	Case	Imposed Damage	Sensor Layout	Damaged Elements	Percent
Trial #2	12 DOF-Symmetric	1st story braces 100%	Full	1st story brace # 21	82.06%
	Measurements are taken in y- direction			1st story brace # 25	89.78%
				# 5	78.22%
				# 13	86.63%

**Table 5.5 SDIM Results for 1st Story Braces Damaged Using 4 FRFs – SIMO
Case 3, Last Mode Is Omitted, After Hillclimbing # 739**

Trial	Case	Imposed Damage	Sensor Layout	Damaged Elements	Percent
Trial #2	12 DOF-Symmetric	1st story braces 100%	Full	1st story brace # 21	82.14%
	Measurements are taken in y- direction			1st story brace # 25	89.88%
				# 5	82.44%
				# 13	82.57%

Tables 5.4 and 5.5 indicate that more optimal damage indices were obtained for the actual damaged members 21 and 25 and the number of falsely damaged members was decreased compared to Trial #1. In addition, the falsely damaged members # 5 and #13 (first story beams) are at the same floor as the actually damaged members. The program seems to isolate the first floor to be damaged as a whole, thus finding the source of the loss of stiffness as the 1st floor. The improved SDIM results stem from the more accurate FRF function provided to the SDIM.

Tables 5.4 and 5.5 show the percent damages in tabular format while Figure 5.7 plots them with respect to element number. Hillclimbing does not significantly improve the current results in this trial.

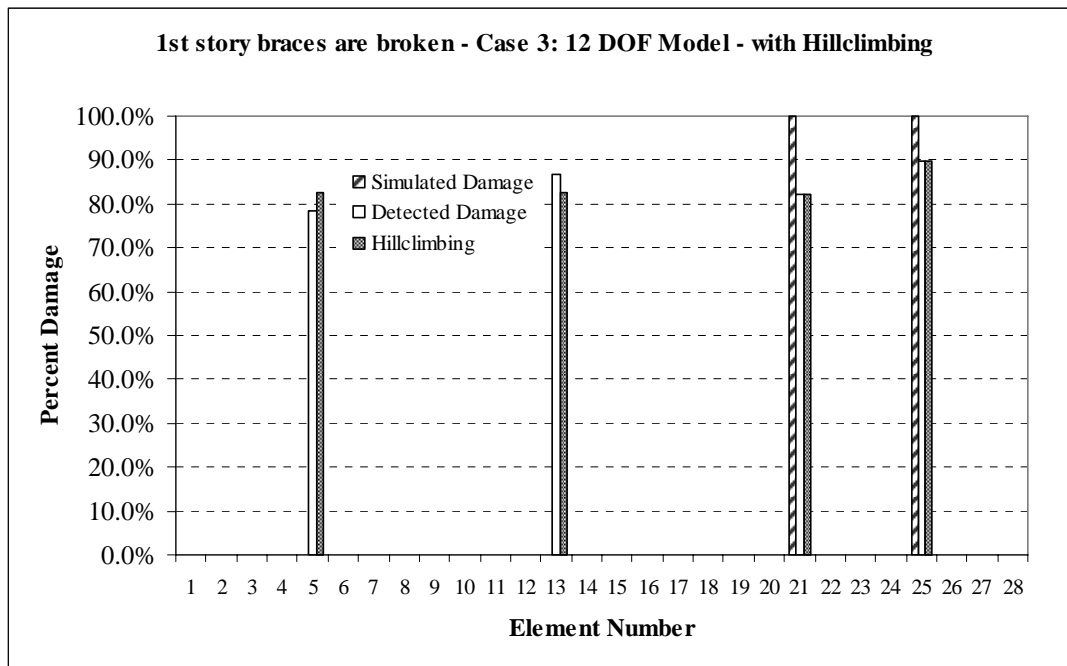
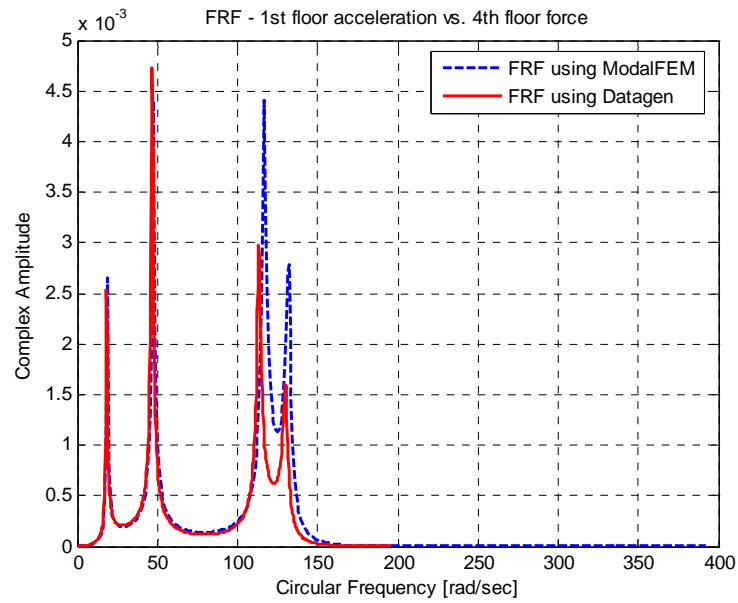


Figure 5.7 Simulated vs. Detected Damages for Trial #2 with Hillclimbing # 739

5.1.2 Case 3: 1st – 3rd Story Braces Are Damaged

The results from trials considering damage pattern two (all braces of the first and third story are broken) using Case 3 is presented in this section.

Figures 5.8 through 5.11 provide the FRF graphs for this particular damage case. The solid curve represents the FRFs found using Datagen, while the dashed curve represents the FRFs obtained using ModalFEM.



**Figure 5.8 FRF for the 1st Floor – 1st- 3rd Story Braces Are Broken
SIMO - 12 DOF Symmetric Model**

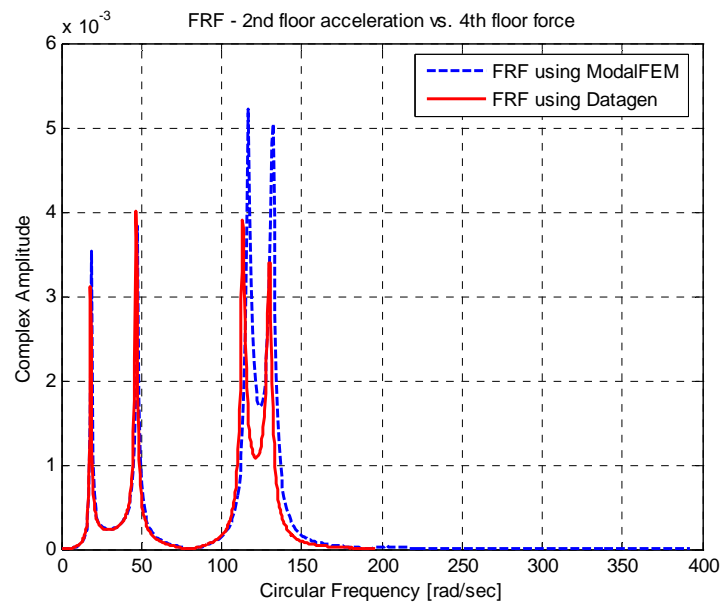


**Figure 5.9 FRF for the 2nd Floor – 1st- 3rd Story Braces Are Broken
SIMO - 12 DOF Symmetric Model**

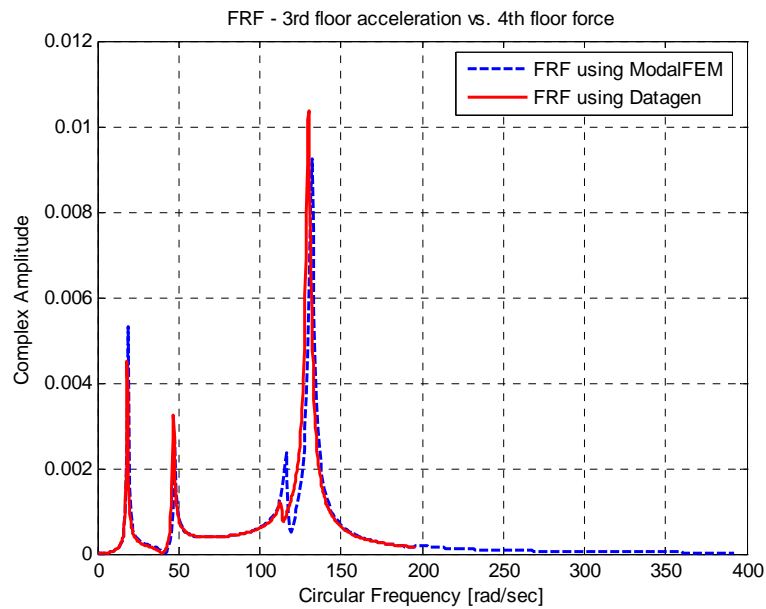


**Figure 5.10 FRF for the 3rd Floor – 1st- 3rd Story Braces Are Broken
SIMO - 12 DOF Symmetric Model**

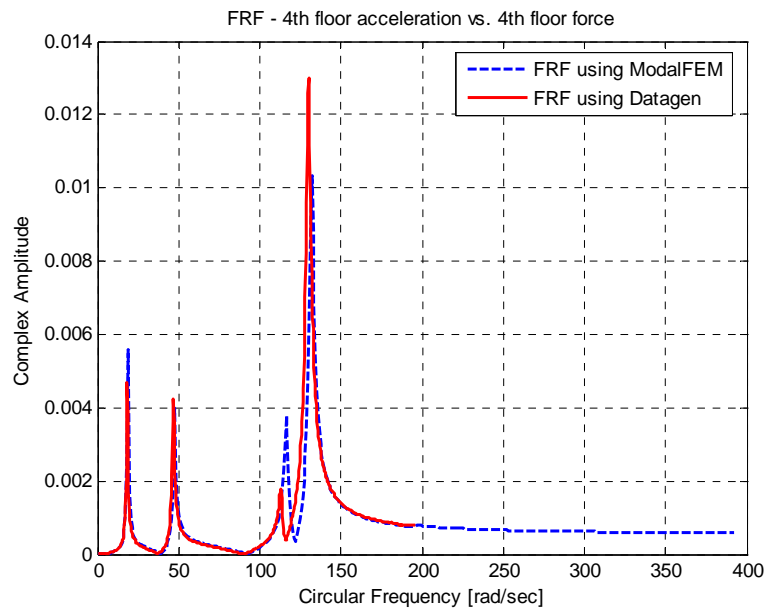


**Figure 5.11 FRF for the 4th Floor – 1st- 3rd Story Braces Are Broken
SIMO - 12 DOF Symmetric Model**

5.1.2.1 All Four Modes Are Used for Damage Detection

The correlation between the two FRFs is greater for the first two modes and then decreases with mode three and four. If all four modes are provided to the SDIM, then the following results are obtained. Tables 5.6 and 5.7 provide the results of the damage predictions obtained by the SDIM with and without using the hillclimber, respectively.

**Table 5.6 SDIM Results for 1st and 3rd Story Braces Damaged Using 4 FRFs – SIMO
Case 3, All Four Modes Are Used**

Trial	Case	Imposed Damage	Sensor Layout	Damaged Elements	Percent
Trial #3	12 DOF-Symmetric	1st- 3rd story braces 100%	Full	1st floor brace # 21	61.84%
	Measurements are taken in y-direction			1st floor brace # 25	0.00%
				3rd floor brace # 23	98.68%
				3rd floor brace # 27	94.29%
				# 5	89.88%
				# 19	49.51%
				# 22	50.22%

**Table 5.7 SDIM Results for 1st and 3rd Story Braces Damaged Using 4 FRFs – SIMO
Case 3, All Four Modes Are Used, After Hillclimbing # 178**

Trial	Case	Imposed Damage	Sensor Layout	Damaged Elements	Percent
Trial #3	12 DOF-Symmetric	1st- 3rd story braces 100%	Full	1st floor brace # 21	99.00%
	Measurements are taken in y-direction			1st floor brace # 25	0.00%
				3rd floor brace # 23	99.00%
				3rd floor brace # 27	99.00%
				# 5	91.85%
				# 19	40.44%
				# 22	39.96%

Although, the number of falsely detected members is fewer for this case compared to Trial #1 (which also uses the same excitation and mass distribution case - Case #3), one of the first floor braces (member #25) was identified to be completely undamaged. The hillclimber improves the results in a local sense for this case, since it is not expected to obtain any reasonable damage index for member #25 through hillclimbing. However, it was able to fine tune the results, thus providing member 21, 23 and 27 as 99% damage with three falsely identified damaged members.

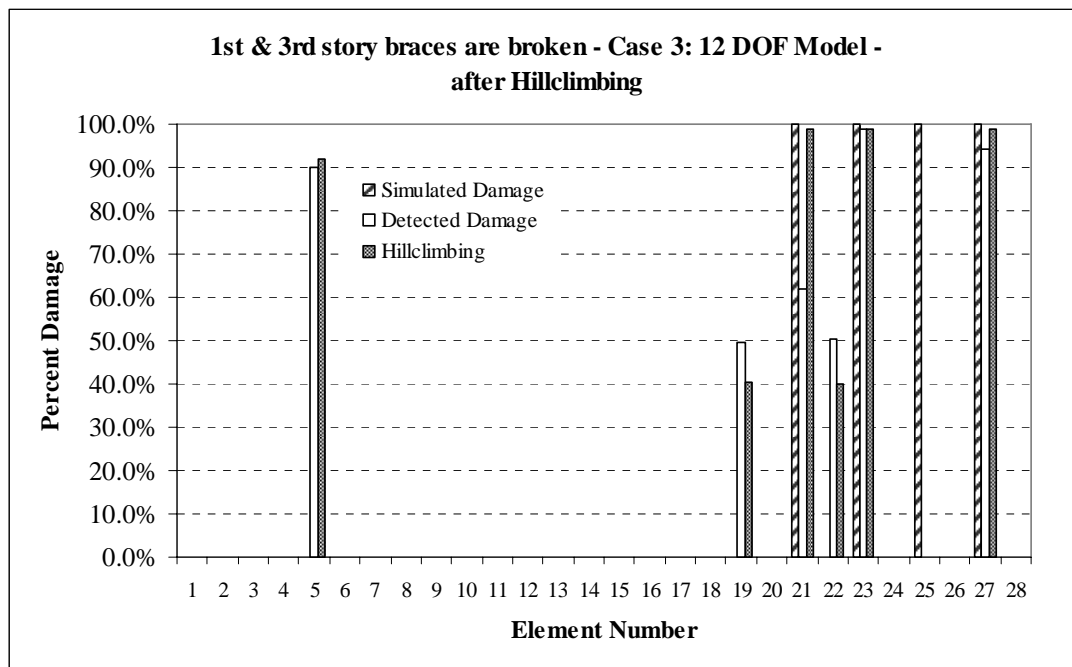


Figure 5.12 Simulated vs. Detected Damages for Trial #3 with Hillclimbing # 178

Figure 5.12 shows the SDIM results obtained for Trial #3 with and without hillclimber after 178 iterations.

5.1.2.2 The Last Two Modes Are Omitted for Damage Detection

Missing a broken member completely is an unacceptable mistake for an SDIM even if the other members were identified correctly to be damaged. The question concerns how to improve the results obtained by the SDIM. In many cases, providing more information or providing higher quality information to the SDIM results in greater accuracy in detecting damage. If Figures 5.8 to 5.11 are examined carefully, it can be seen that the first two modes of the FRF graphs obtained by Datagen are matching almost perfectly with the FRFs obtained by ModalFEM. Again to provide a comparison concerning SDIM performance, the last two modes of the FRF are omitted and additional trials are performed.

Tables 5.8 and 5.9 show the SDIM results before and after hillclimbing for Trial #4. The SDIM was able to identify the first floor brace #25 to be damaged as almost 90% for this case without using hillclimbing, while the other first floor brace #21 and the two third floor braces, #23 and #27 have 76.79%, 97.81% and 97.42% damages respectively.

**Table 5.8 SDIM Results for 1st and 3rd Story Braces Damaged Using 4 FRFs – SIMO
Case 3, Last Two Modes Are Omitted**

Trial	Case	Imposed Damage	Sensor Layout	Damaged Elements	Percent
Trial #4	12 DOF-Symmetric	1st- 3rd story braces 100%	Full	1st floor brace # 21	76.79%
	Measurements are taken in y-direction			1st floor brace # 25	89.73%
				3rd floor brace # 23	97.81%
				3rd floor brace # 27	97.42%
				# 16	85.96%
				# 17	95.93%

**Table 5.9 SDIM Results for 1st and 3rd Story Braces Damaged Using 4 FRFs – SIMO
Case 3, Last Two Modes Are Omitted, After Hillclimbing # 1489**

Trial	Case	Imposed Damage	Sensor Layout	Damaged Elements	Percent
Trial #4	12 DOF-Symmetric	1st - 3rd story braces 100%	Full	1st floor brace # 21	76.79%
	Measurements are taken in y-direction			1st floor brace # 25	80.41%
				3rd floor brace # 23	97.82%
				3rd floor brace # 27	91.27%
				# 9	35.49%
				# 15	44.05%
				# 16	77.73%
				# 17	95.96%
				# 19	0.34%

Figures 5.13 and 5.14 show the inefficiency of using hillclimbing for this particular trial. Hillclimbing not only degrades the damage indices of the actual damage members, but also creates some new falsely damaged members, thus working in the opposite direction in this case.

The unacceptable results obtained in Trial #3 and the poor convergence of hillclimber in Trial #4 may all be related to the differences between FRFs obtained from Datagen and ModalFEM. Therefore, before performing additional SDIM trials, a representative FRF graph will be provided to allow for a comparison of the two programs.

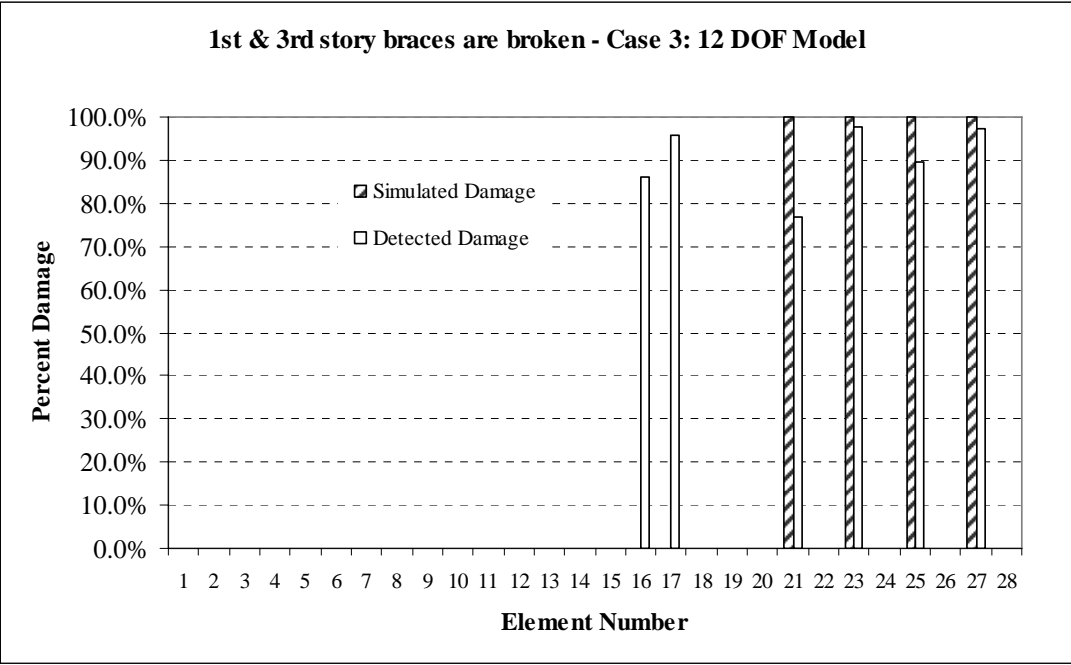


Figure 5.13 Simulated vs. Detected Damages for Trial #4

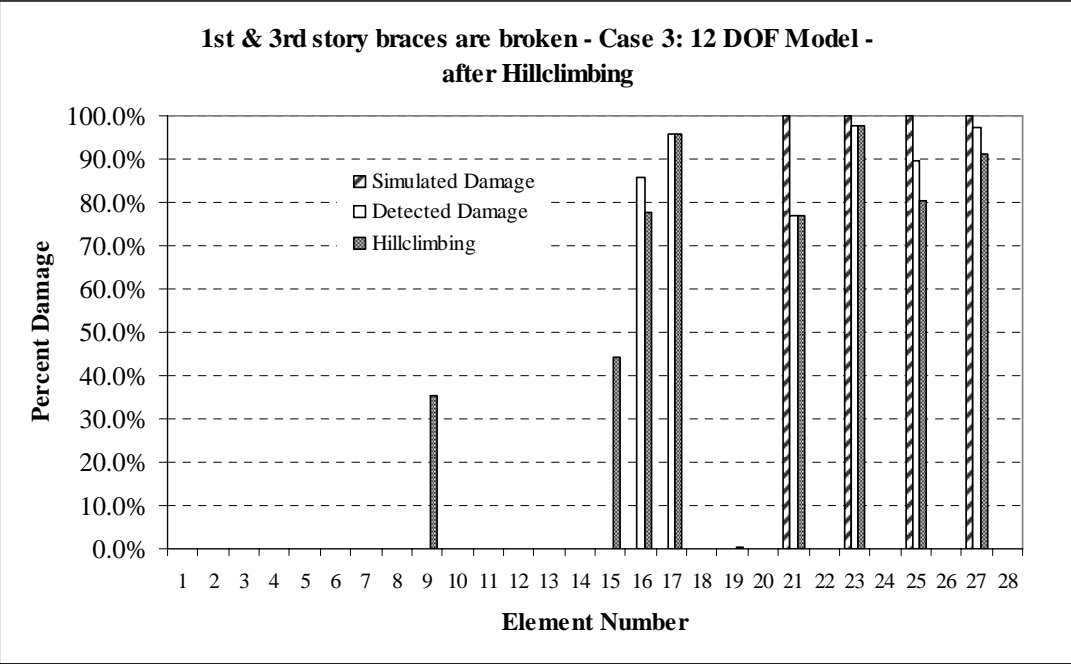


Figure 5.14 Simulated vs. Detected Damages for Trial #4 with Hillclimbing # 1489

5.1.3 Case 3: 2nd Story Braces Are Damaged

A user-defined damage case is analyzed in this section by simulating the second story braces to be damaged as 100%.

Table 5.10 shows the percent damages in tabular format, while Figure 5.15 plots them with respect to element number. Hillclimbing was not used in this particular trial.

The second story braces # 22 and # 26 were identified as 83.54% and 88.51% damaged. The falsely damaged members # 2 and #10 are on the same floor as the actual damage, while the other two falsely damaged members are at the adjacent floors of the actual damaged members. Therefore, it seems reasonable to summarize that the program tries to isolate the second floor as damaged, thus finding the source of the loss of stiffness of the whole structure as the 2nd floor.

**Table 5.10 SDIM Results for 2nd Story Braces Damaged Using 4 FRFs – SIMO
Case 3**

Trial	Case	Imposed Damage	Sensor Layout	Damaged Elements	Percent
Trial #5	12 DOF-Symmetric	2nd story braces 100%	Full	2nd floor brace #22	83.54%
	Measurements are taken in y-direction			2nd floor brace #26	88.51%
				# 2	21.18%
				# 3	48.90%
				# 10	51.81%
				# 19	50.30%

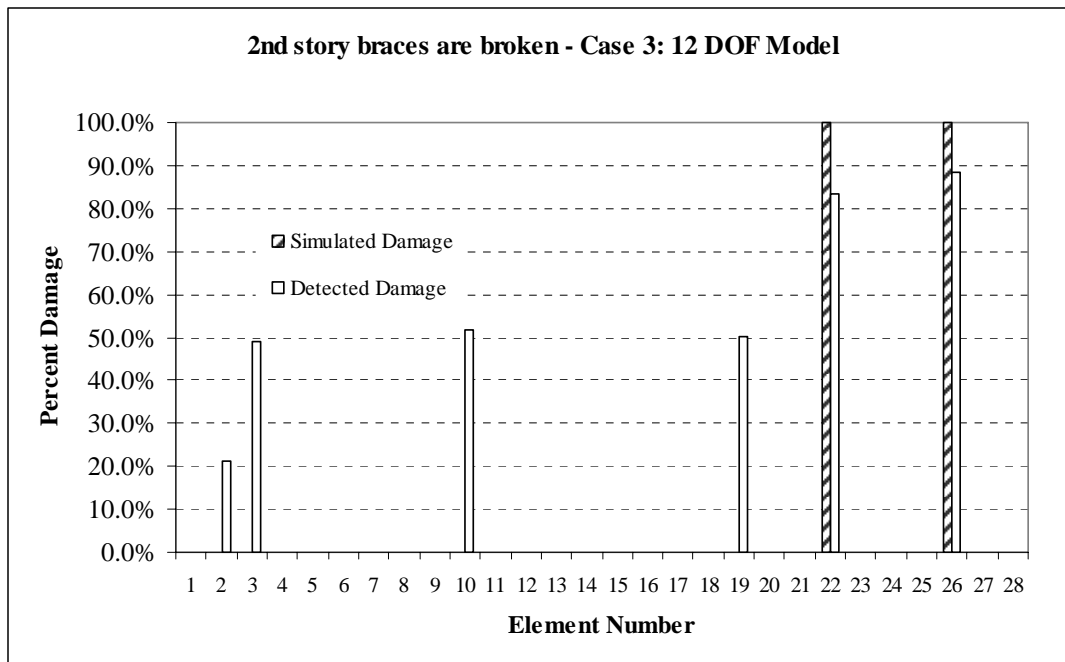
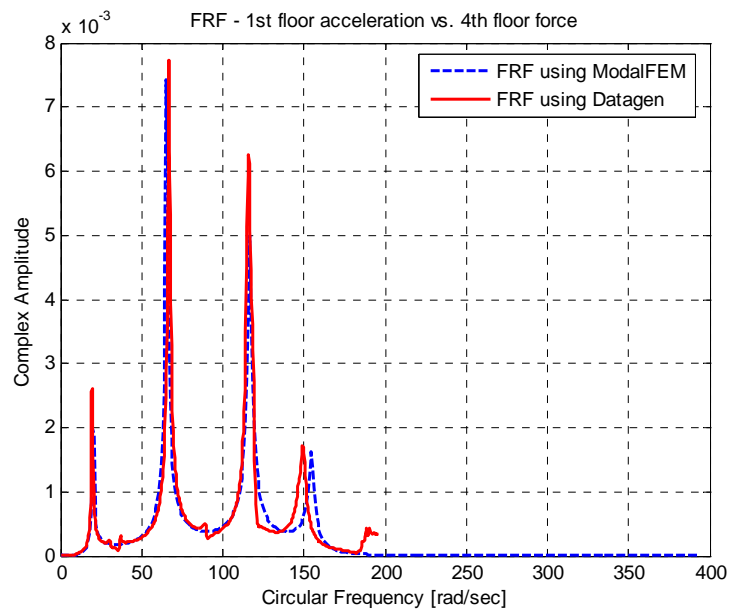


Figure 5.15 Simulated vs. Detected Damages for Trial #5

5.1.4 Case 4: 1st Story Braces Are Damaged

The results obtained for damage pattern one (all first story braces are broken) using Case 4 (12 DOF model with asymmetrical mass distribution) is presented in this section. This case is more complicated than Case 3 due to the asymmetric mass distribution (550 kg slab placed at the fourth floor). This mass distribution will result in coupling between the rotational and translational modes of vibration. Figure 5.16 shows the FRF computed between the first floor acceleration and the fourth floor force when the first floor braces (namely element # 21 and # 25) are defined to be damaged. The performance of this trial and the one given in Section 5.1.5 may also provide an indication of how well the input card information simulates (thus how well the asymmetrical intact structure represents) the real asymmetry present in the benchmark structure. Noise is not present in the system.



**Figure 5.16 FRF for the 1st Floor – 1st Story Braces Are Broken
SIMO - 12 DOF Asymmetric Model**

The number of falsely detected members is fewer for this case compared to Trial #1, which also uses same damage pattern but with symmetrical mass distribution. The actual damaged members were identified as 77.17% and 81.91% damaged while three falsely detected members, #5, #11 and #26, were also identified as 85.34%, 63.53% and 9.56% damaged respectively. An important output of this case is that, with this kind of a model, results may not be improved by just omitting the last mode as in Trial #1 which has the significant difference only in the last mode of the FRF graphs. In this case, each mode contains some new information and cannot be simulated perfectly by the ModalFEM utility program. Although the FRF obtained using Datagen contains more accurate information, GaDamDet is only able to locate and quantify damage if the FRF of the damaged structure perfectly matches with the one that ModalFEM creates.

**Table 5.11 SDIM Results for 1st Story Braces Damaged Using 4 FRFs – SIMO
Case 4**

Trial	Case	Imposed Damage	Sensor Layout	Damaged Elements	Percent
Trial #6	12 DOF-Asymmetrical	1st story braces 100%	Full	1st floor brace # 21	77.16%
	Measurements are taken in y- direction			1st floor brace # 25	81.97%
				# 5	83.47%
				# 11	64.04%
				# 26	10.28%

**Table 5.12 SDIM Results for 1st Story Braces Damaged Using 4 FRFs – SIMO
Case 4, After Hillclimbing # 667**

Trial	Case	Imposed Damage	Sensor Layout	Damaged Elements	Percent
Trial #6	12 DOF-Asymmetrical	1st story braces 100%	Full	1st floor brace # 21	77.17%
	Measurements are taken in y- direction			1st floor brace # 25	81.91%
				# 5	85.34%
				# 11	63.53%
				# 26	9.56%

However, the results obtained were not worse than the case performed for the symmetrical mass distribution. The hillclimber did not impact the results in 667 iterations.

Tables 5.11 and 5.12 provide the detailed SDIM results of Trial # 6 in tabular format obtained before and after using hillclimbing. Figure 5.17 shows graphically that the number of hillclimbing iterations were not enough to make an impact on the SDIM results of this trial.

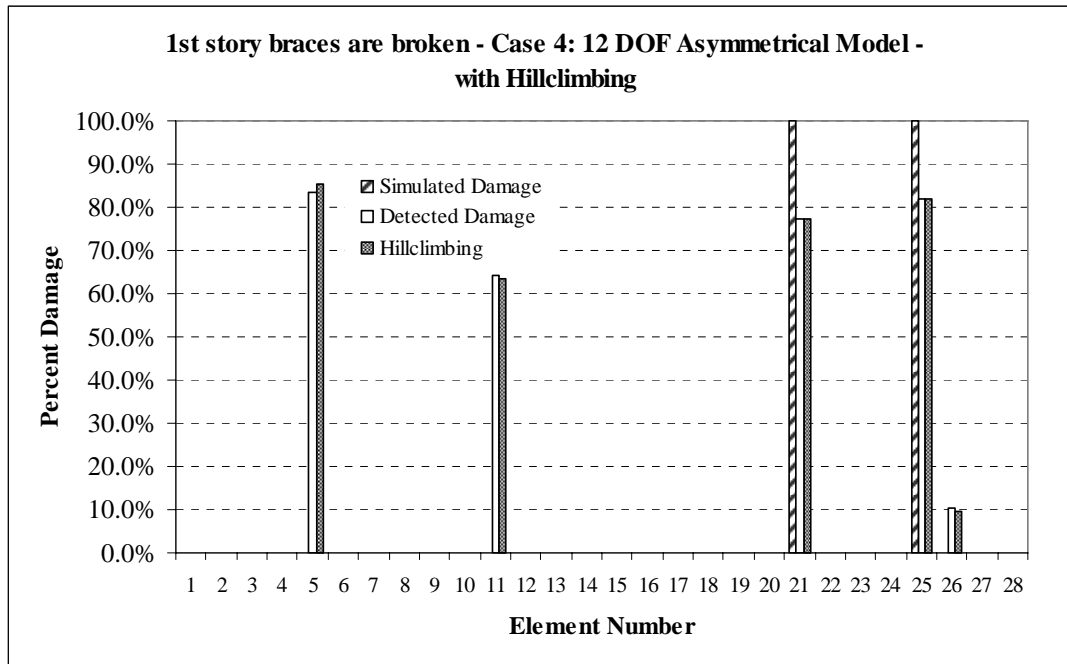
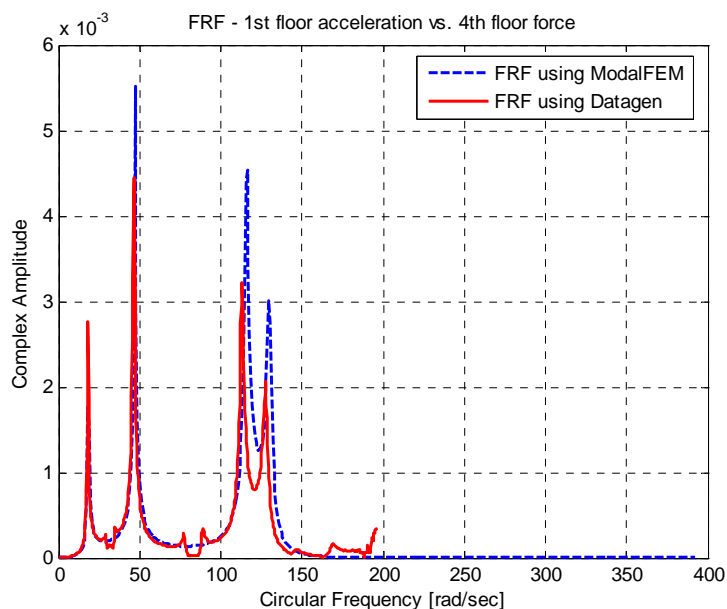


Figure 5.17 Simulated vs. Detected Damages for Trial #6 with Hillclimbing # 667

5.1.5 Case 4: 1st- 3rd Story Braces Are Damaged

The results obtained considering damage pattern two (all the first story and third braces are broken) using Case 4 is presented in this section. The results will be compared with the results obtained from Trial #3 and #4 where symmetrical mass distribution is used instead.

Figure 5.18 shows the FRF computed between the first floor acceleration and the fourth floor force for this particular damage case. The new response information is visible in the graph if it is compared with its pair – Figure 5.8 – that plots the FRF for the symmetrical mass distribution using the same damage case.



**Figure 5.18 FRF for the 1st Floor – 1st - 3rd Story Braces Are Broken
SIMO - 12 DOF Asymmetric Model**

**Table 5.13 SDIM Results for 1st and 3rd Story Braces Damaged Using 4 FRFs – SIMO
Case 4**

Trial	Case	Imposed Damage	Sensor Layout	Damaged Elements	Percent
Trial #7	12 DOF- Asymmetrical	1 st - 3 rd story braces 100%	Full	1 st floor brace # 21	73.49%
	Measurements are taken in y- direction			1 st floor brace # 25	0.00%
				3 rd floor brace # 23	98.99%
				3 rd floor brace # 27	98.95%
				# 5	74.10%
				# 11	37.10%
				# 22	49.51%

Tables 5.13 and 5.14 show the SDIM results before and after hillclimbing was applied, where the hillclimber was able to identify actually damaged members 21, 23 and 27 as 99% damaged. However, member 25 (one of the first floor braces) is found to be

completely undamaged even after hillclimbing as in Trial #3. This is an expected result, since a better solution was highly unlikely to happen for this more complicated, asymmetric case. Even the two falsely identified members (#5 and #9) with almost exact damage indices appear to be the same in both cases. Tables 5.13 and 5.14 provide the detailed SDIM results in tabular format while Figure 5.19 shows the results graphically with and without hillclimbing.

**Table 5.14 SDIM Results for 1st and 3rd Story Braces Damaged Using 4 FRFs – SIMO
Case 4, After Hillclimbing # 580**

Trial	Case	Imposed Damage	Sensor Layout	Damaged Elements	Percent
Trial #7	12 DOF- Asymmetrical	1st- 3rd story braces 100%	Full	1st floor brace # 21	99.00%
	Measurements are taken in y- direction			1st floor brace # 25	0.00%
				3rd floor brace # 23	99.00%
				3rd floor brace # 27	99.00%
				# 5	91.32%
				# 11	37.56%
				# 22	40.05%

5.1.6 Case 5: 1st Story Braces Are Damaged

The results obtained considering damage pattern one (all first story braces are 100% damaged) using Case 5 (120 DOF model with asymmetrical mass distribution) is presented in this section. This case is more complicated than Case 4 due to the model uncertainty created with using 120 DOF model. Figure 5.20 shows the FRF computed between the first floor acceleration and the fourth floor force when the first floor braces are defined to be damaged.

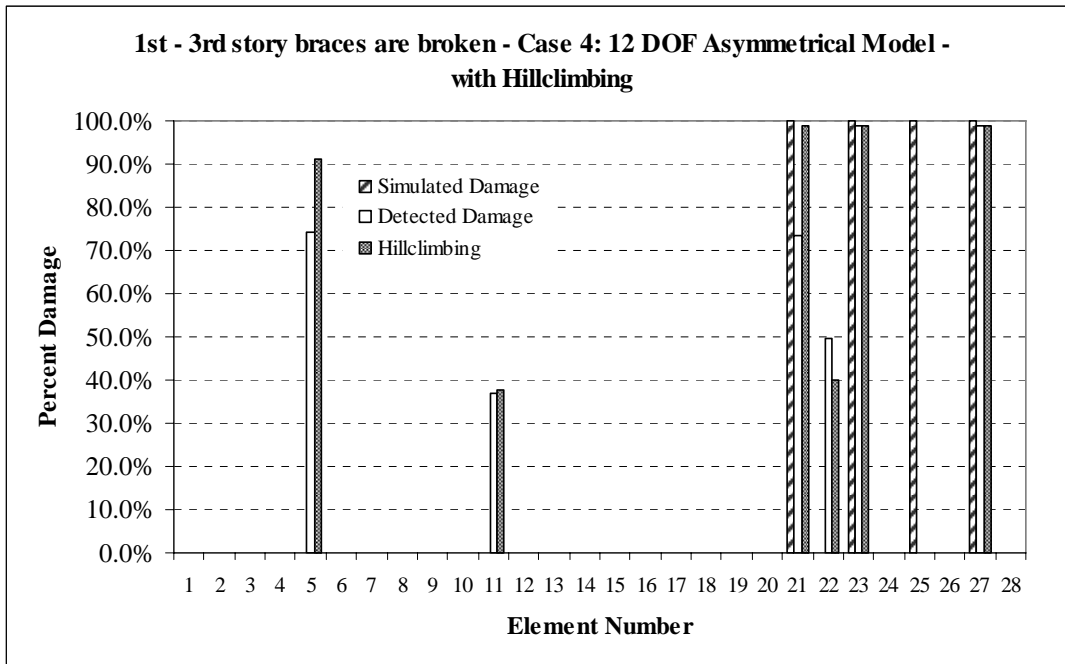


Figure 5.19 Simulated vs. Detected Damages for Trial #7 with Hillclimbing # 580

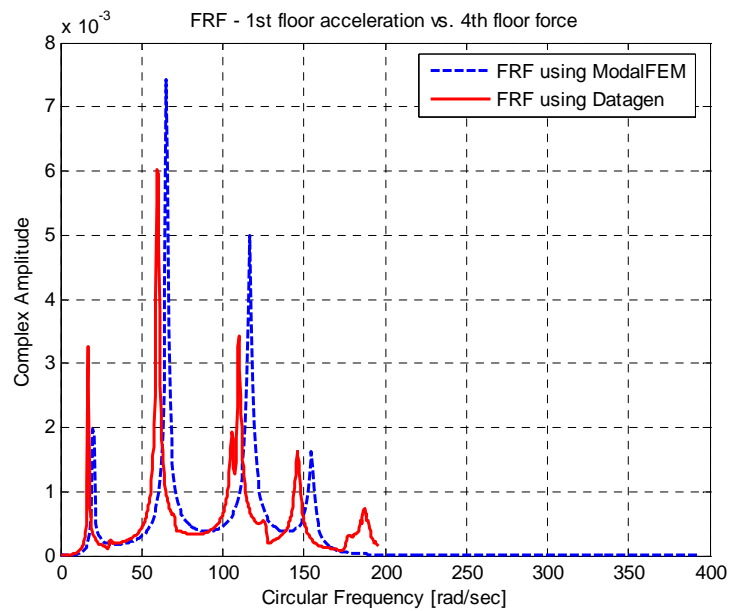


Figure 5.20 FRF for the 1st Floor – 1st Story Braces Are Broken SIMO - 120 DOF Asymmetric Model

The SDIM results for this particular trial are presented in Tables 5.15 and 5.16 before and after hillclimbing. Although one of the first floor braces (member #25) was detected as 99% damaged, the SDIM failed to locate and quantify damage in the other broken member completely. In addition, five intact members were detected as severely damaged and two of them (#14 and #17) were identified to be almost completely broken, with 95.13%, 96.70% damages. This was an expected result since Figure 5.20 already proved that the two models used by GaDamDet and Datagen have considerable differences. It is obvious that the 120 DOF model's uncertainties combined with the asymmetrical mass distribution will lead to less accurate SDIM results than those obtained in the simplest case #3.

Figure 5.21 presents the results of Trial #8 before and after hillclimbing graphically. Hillclimbing was not effective due to the inaccurate damage predictions made by the SDIM.

Table 5.15 SDIM Results for 1st Story Braces Damaged Using 4 FRFs – SIMO Case 5

Trial	Case	Imposed Damage	Sensor Layout	Damaged Elements	Percent
Trial #8	120 DOF-Asymmetrical	1st story braces 100%	Full	1st floor brace # 21	0.00%
	Measurements are taken in y-direction			1st floor brace # 25	93.63%
				# 4	68.38%
				# 8	56.68%
				# 14	95.13%
				# 17	96.70%
				# 22	74.10%

**Table 5.16 SDIM Results for 1st Story Braces Damaged Using 4 FRFs – SIMO
Case 5, After Hillclimbing # 519**

Trial	Case	Imposed Damage	Sensor Layout	Damaged Elements	Percent
Trial #8	120 DOF-Asymmetrical	1 st story braces 100%	Full	1 st floor brace # 21	0.00%
	Measurements are taken in y-direction			1 st floor brace # 25	99.00%
				# 4	63.35%
				# 8	78.26%
				# 14	95.71%
				# 17	96.37%
				# 22	72.72%

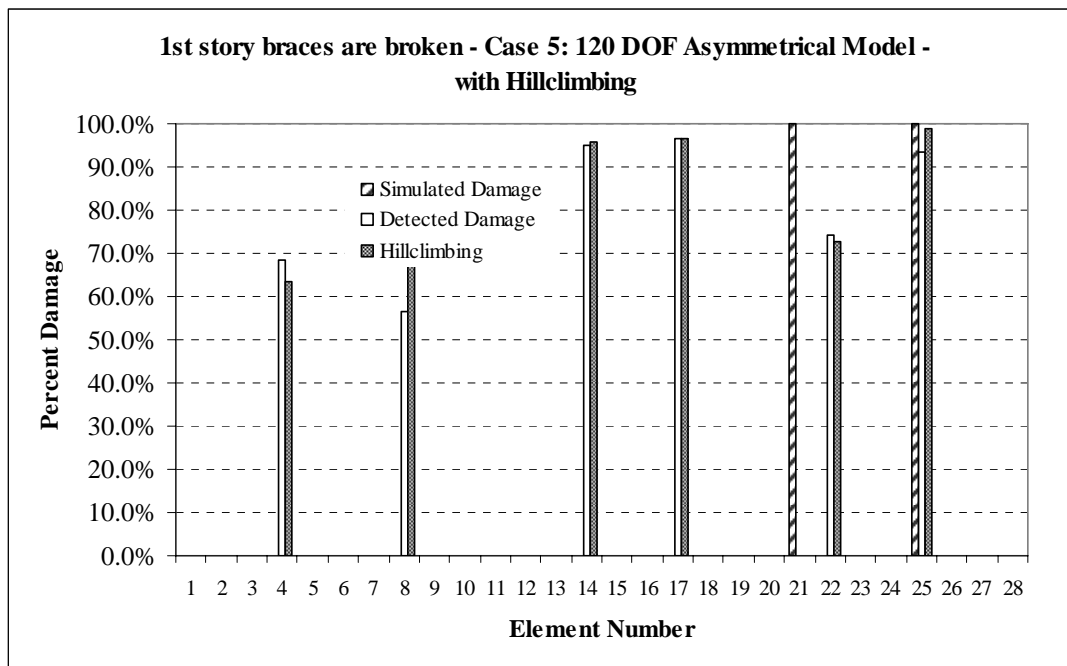
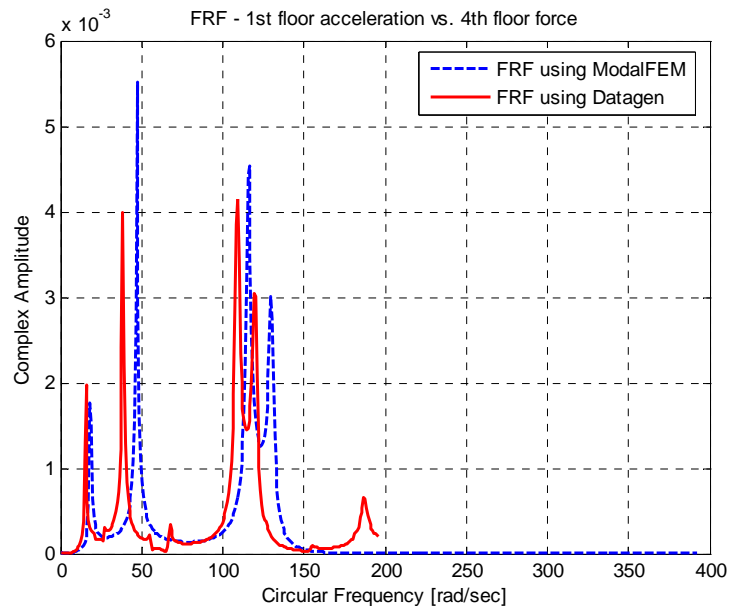


Figure 5.21 Simulated vs. Detected Damages for Trial #8 with Hillclimbing # 519

5.1.7 Case 5: 1st - 3rd Story Braces Are Damaged

The last case of single-input/multiple-output problems will be the most complicated one to be analyzed until this point due to asymmetrical mass distribution, the more sophisticated finite element mode, and having more damaged elements than considered in Case 5.1.6.



**Figure 5.22 FRF for the 1st Floor – 1st - 3rd Story Braces Are Broken
SIMO - 120 DOF Asymmetric Model**

Figure 5.22 gives sufficient information in order to predict the success of this trial. The differences between the two FRF graphs are most obvious in this case. The SDIM results for this particular trial may be seen in Tables 5.17 and 5.18 before and after hillclimbing. None of the first floor braces were detected to be damaged, while several undamaged members were falsely identified as damaged such as member #11

and #26 with 97.50% and 87.54% damages respectively. Third floor braces were identified as 72.68% and 87.47% damaged.

Table 5.17 SDIM Results for 1st and 3rd Story Braces Damaged Using 4 FRFs – SIMO Case 5

Trial	Case	Imposed Damage	Sensor Layout	Damaged Elements	Percent
Trial #9	120 DOF-Asymmetrical	1st story braces 100%	Full	1st floor brace # 21	0.00%
	Measurements are taken in y- direction			1st floor brace # 25	0.00%
				3rd floor brace # 23	72.68%
				3rd floor brace # 27	86.47%
				# 9	5.91%
				# 11	97.5%
				# 26	86.54%
				# 28	49.50%

Table 5.18 SDIM Results for 1st and 3rd Story Braces Damaged Using 4 FRFs – SIMO Case 5, After Hillclimbing # 1575

Trial	Case	Imposed Damage	Sensor Layout	Damaged Elements	Percent
Trial #9	120 DOF-Asymmetrical	1st story braces 100%	Full	1st floor brace # 21	0.00%
	Measurements are taken in y- direction			1st floor brace # 25	0.00%
				3rd floor brace # 23	72.13%
				3rd floor brace # 27	99.00%
				# 9	84.38%
				# 11	99.00%
				# 26	72.85%
				# 28	37.78%

The hillclimber was able to locate the third floor as severely damaged by also defining member #11 to be completely broken. The other highly damaged member #9 belongs to first story. Thus, what seems to have happened in this case is that, damage is mostly related to the third floor; whereas only partially related to the first floor. However, the program wasn't sensitive enough to identify each damaged member on a floor separately (due to differences between the FRFs shown in Figure 5.22)

Figure 5.23 presents the results of Trial #9 before and after hillclimbing graphically.

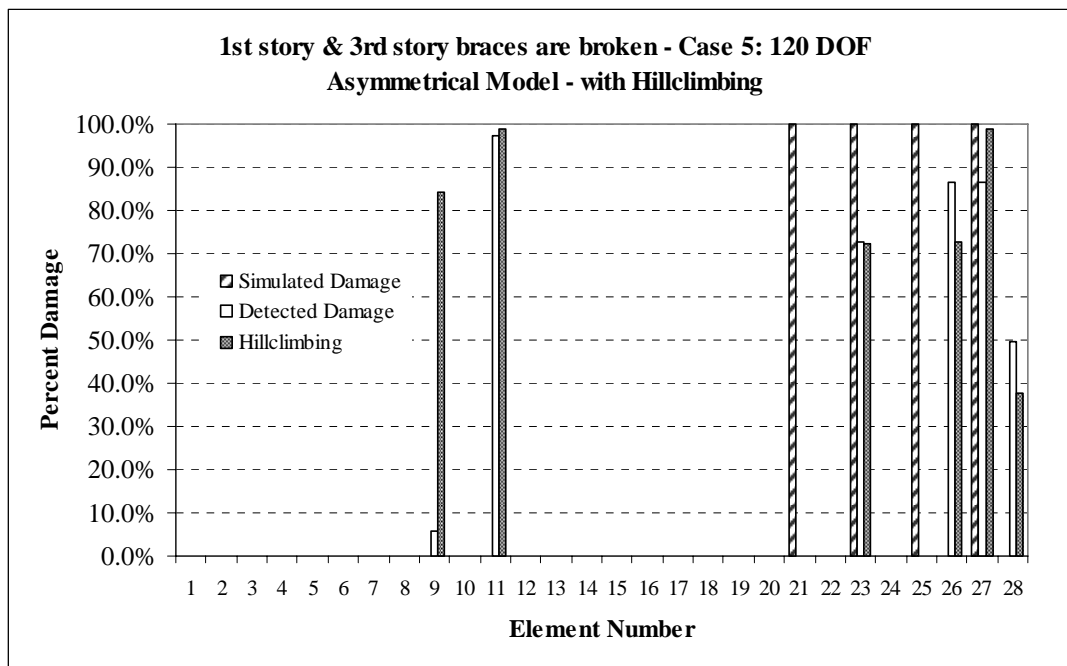


Figure 5.23 Simulated vs. Detected Damages for Trial #9 with Hillclimbing # 1575

5.2 Multiple-Input/Single-Output Model

Multiple-input/single-output problems were analyzed using the results obtained from the first case of the benchmark problem. As discussed in Section 3, MIMO problems may simply be considered as extensions of MISO problems. Thus, the same algorithm was used for obtaining the FRFs from these two cases with the only difference of acceleration and measurement locations.

The excitation/measurement pairs discussed in Section 4 simulate the effects of MISO and MIMO problems in GaDamDet, and the FRFs obtained using different pairs will lead to different results in obtained by the SDIM, although there should only be a unique solution.

5.2.1 Case 1: 1st Story Braces Are Damaged

The results obtained from considering damage pattern one (all first story braces are 100% damaged) using Case 1 (12 DOF model) is presented in this section. One advantage of using this case and Case #2 is that in both, the structure is loaded laterally in one direction (y-weak axis). Two different measurement locations were defined using the same force vectors (one at each floor along the y-axis). Ideally, the same damage indices should be obtained even if different FRFs are used as in this case.

5.2.1.1 The Measurement Is Taken From the First Floor (at Node 7)

Figure 5.24 shows the FRF computed using the first floor excitation /first floor measurement pair. The only accelerometer is placed at node 7 (first floor middle column) in this case, while multiple forces are applied at each floor on the edge columns. The FRFs obtained by Datagen and ModalFEM seem to match up well until the last frequency, which introduces the same error problem as defined at the first trial in this section.

Tables 5.19 and 5.20 provide the results obtained by the SDIM for damage pattern one before and after hillclimbing. Although the first floor braces were identified as 56.84% and 80.17% damaged, three intact members were falsely identified, while two of them (#1 and #3) almost have the same damage indices as the actually damaged members. Hillclimbing cleaned up of the falsely detected members from the solution set, although introduced a new falsely damaged element while doing that.

Figure 5.25 shows the results obtained for this trial graphically.

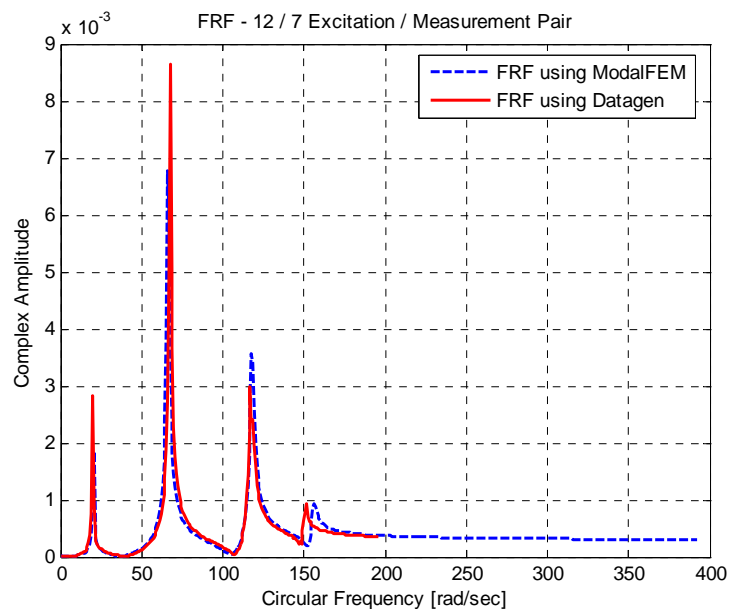


**Figure 5.24 FRF for the 1st Floor – 1st Story Braces Are Broken
MISO - 12 DOF Symmetric Model**

**Table 5.19 SDIM Results for 1st Story Braces Damaged Using 4 FRFs – MISO
Case 1, Accelerometer Is at Node 7**

Trial	Case	Imposed Damage	Sensor Layout	Damaged Elements	Percent
Trial #10	12 DOF-Symmetrical	1st story braces 100%	First Floor	1st floor brace # 21	56.84%
	Measurements are taken in y- direction			1st floor brace # 25	80.17%
				# 1	57.83%
				# 3	76.37%
				# 11	6.18%

**Table 5.20 SDIM Results for 1st Story Braces Damaged Using 4 FRFs – MISO
Case 1, Accelerometer Is at Node 7, After Hillclimbing # 8693**

Trial	Case	Imposed Damage	Sensor Layout	Damaged Elements	Percent
Trial #10	12 DOF-Symmetrical	1st story braces 100%	First Floor	1st floor brace # 21	59.24%
	Measurements are taken in y- direction			1st floor brace # 25	75.98%
				# 1	56.74%
				# 11	55.93%
				# 18	39.50%

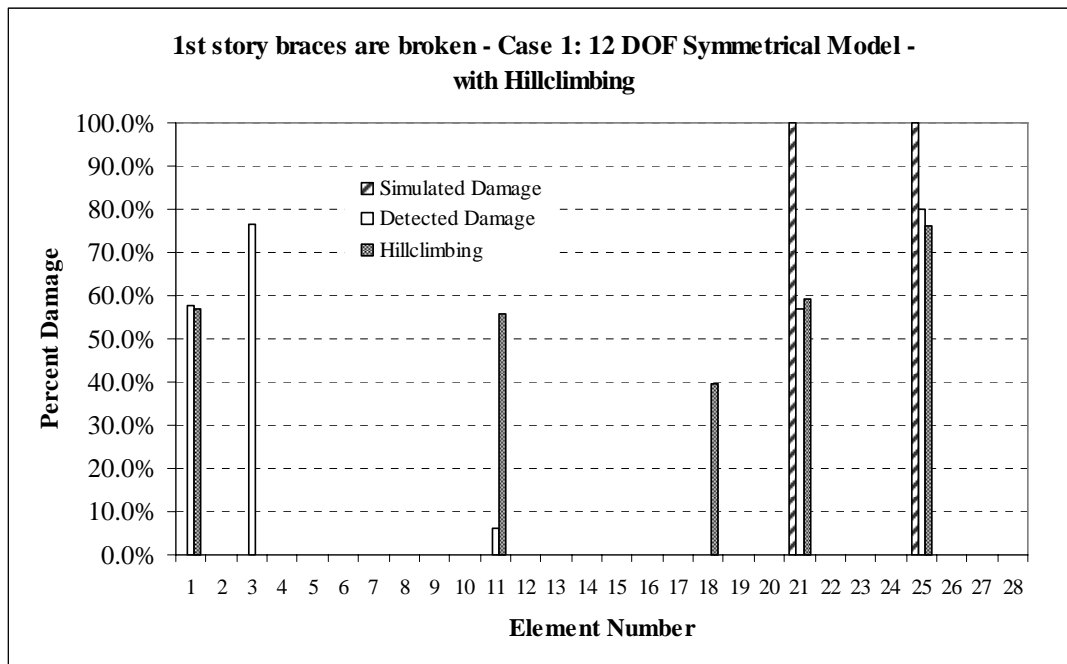


Figure 5.25 Simulated vs. Detected Damages for Trial #10 with Hillclimbing # 8693

To answer the questions concerning what would happen to the accuracy of the results if the measurement is taken from another location, additional trials were performed. It is anticipated that the FRF pairs would be different but still will contain the same information regarding the damage.

5.2.1.2 The Measurement Is Taken From the Second Floor (at Node 8)

The SDIM results for the same damage pattern with different FRFs (computed using different pairs) are presented in Tables 5.21 and 5.22 before and after hillclimbing. Slightly better results were obtained for this case, although the same damage case is analyzed. The problem is hidden in the FRF graphs presented throughout the section before each trial. For this particular case, the FRFs computed using different accelerometer locations produce different erroneous graphs where the last mode contains

the highest error between two FRFs. It should be noted that, even a small shift at the FRFs may mislead the SDIM to obtaining a different solution (different damage location and indices).

**Table 5.21 SDIM Results for 1st Story Braces Damaged Using 4 FRFs – MISO
Case 1, Accelerometer Is at Node 8**

Trial	Case	Imposed Damage	Sensor Layout	Damaged Elements	Percent
Trial #11	12 DOF-Symmetrical	1st story braces 100%	Second Floor	1st floor brace # 21	63.43%
	Measurements are taken in y- direction			1st floor brace # 25	95.87%
				# 3	82.04%
				# 13	70.82%

The proposed SDIM gave better results (compared to Trial #10) when the accelerometer was placed at node 8 (second floor) instead of node 7 (first floor). The first floor brace #25 was detected as 99% while #21 was only identified as 60% damaged. There were only two members that were falsely detected. However, they have considerably large damage indices at 82.02% and 71.36%.

**Table 5.22 SDIM Results for 1st Story Braces Damaged Using 4 FRFs – MISO
Case 1, Accelerometer Is at Node 8, After Hillclimbing # 160**

Trial	Case	Imposed Damage	Sensor Layout	Damaged Elements	Percent
Trial #11	12 DOF-Symmetrical	1st story braces 100%	Second Floor	1st floor brace # 21	60.00%
	Measurements are taken in y- direction			1st floor brace # 25	99.00%
				# 3	82.02%
				# 13	71.36%

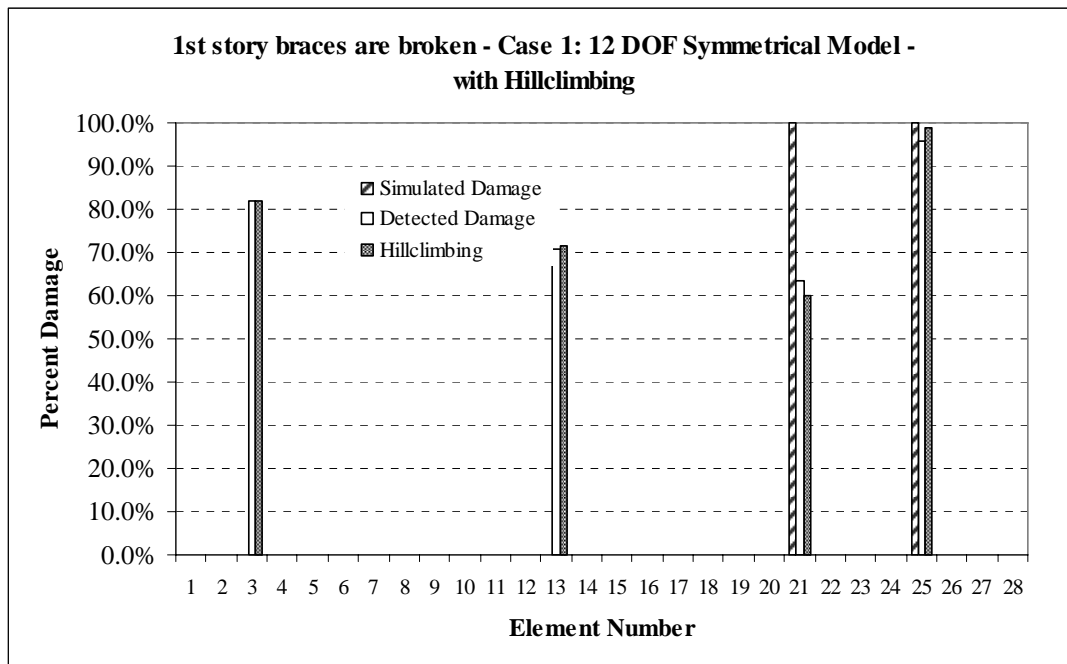
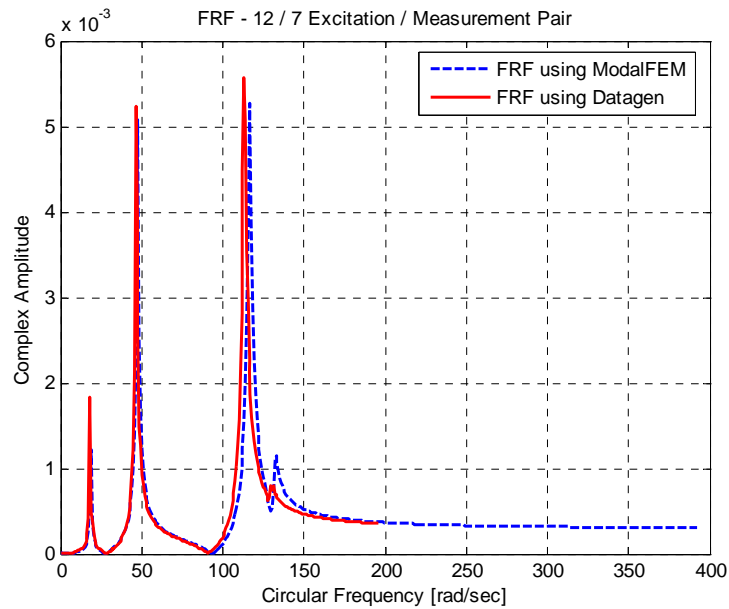


Figure 5.26 Simulated vs. Detected Damages for Trial #11 with Hillclimbing # 160

Figure 5.26 shows these results graphically with and without hillclimbing.

5.2.2 Case 1: 1st – 3rd Story Braces Are Damaged

The results obtained by the SDIM considering damage pattern two (all first and third story braces are broken) using Case 1 (12 DOF model) is presented in this section. The accelerometer is placed at node 7 again. Figure 5.27 compares the FRFs obtained using Datagen and ModalFEM.



**Figure 5.27 FRF for the 1st Floor – 1st - 3rd Story Braces Are Broken
MISO - 12 DOF Symmetric Model**

Tables 5.23 and 5.24 present the results in tabular format before and after hillclimbing. The SDIM was able to pick up two of the four damaged braces, #23 and #27 as completely broken with 99% damage, while first floor braces #21 and #25 were identified as 62.14% and 97.34% damaged respectively after hillclimbing.

Member 17 is almost broken with 96.86% damage, while the other falsely detected member has less severe damage with 19.34%.

Figure 5.28 shows the results obtained for this trial graphically.

**Table 5.23 SDIM Results for 1st and 3rd Story Braces Damaged Using 4 FRFs – MISO
Case 1, Accelerometer Is at Node 7**

Trial	Case	Imposed Damage	Sensor Layout	Damaged Elements	Percent
Trial #12	12 DOF-Symmetrical	1st – 3rd story braces 100%	First Floor	1st floor brace # 21	74.62%
	Measurements are taken in y-direction			1st floor brace # 25	74.70%
				3rd floor brace # 23	97.08%
				3rd floor brace # 27	92.80%
				# 17	98.74%
				# 26	24.78%

**Table 5.24 SDIM Results for 1st and 3rd Story Braces Damaged Using 4 FRFs – MISO
Case 1, Accelerometer Is at Node 7, After Hillclimbing # 9903**

Trial	Case	Imposed Damage	Sensor Layout	Damaged Elements	Percent
Trial #12	12 DOF-Symmetrical	1st – 3rd story braces 100%	First Floor	1st floor brace # 21	62.14%
	Measurements are taken in y-direction			1st floor brace # 25	97.34%
				3rd floor brace # 23	99.00%
				3rd floor brace # 27	99.00%
				# 17	96.86%
				# 26	19.34%

5.3 Multiple-Input/Multiple-Output Model

MIMO problems are handled as direct extensions of MISO problems while processing data obtained from Datagen. The accelerometer and excitation locations for this type of problem are detailed in Section 4. As a review in simplest terms, the first floor accelerations will be paired with first floor excitations, the second floor accelerations will be paired with second floor excitations, and so on.

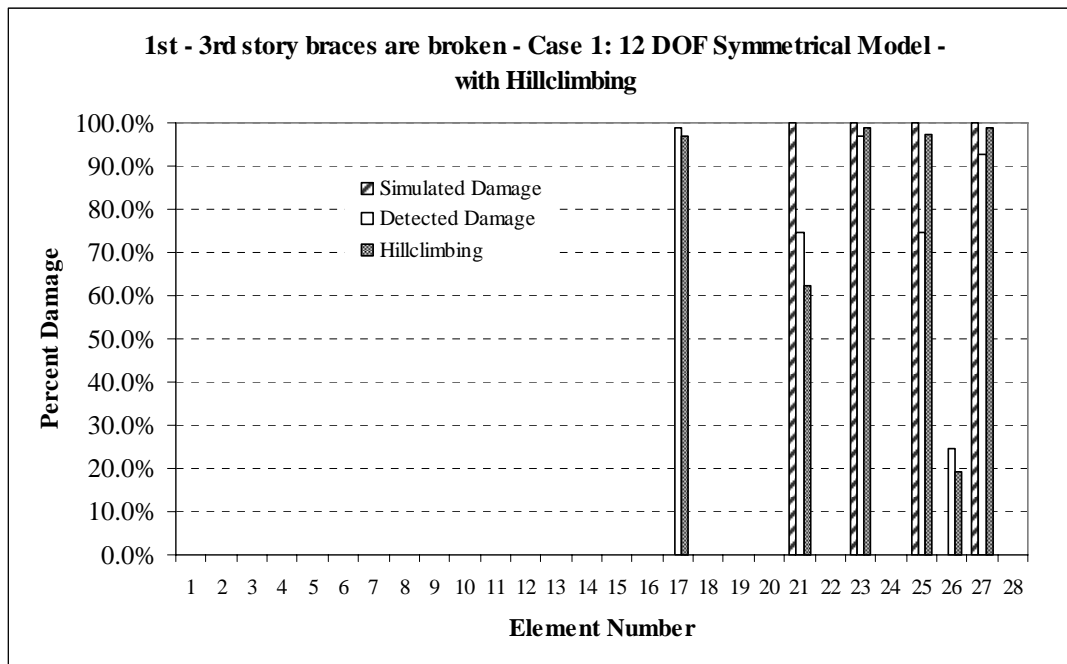
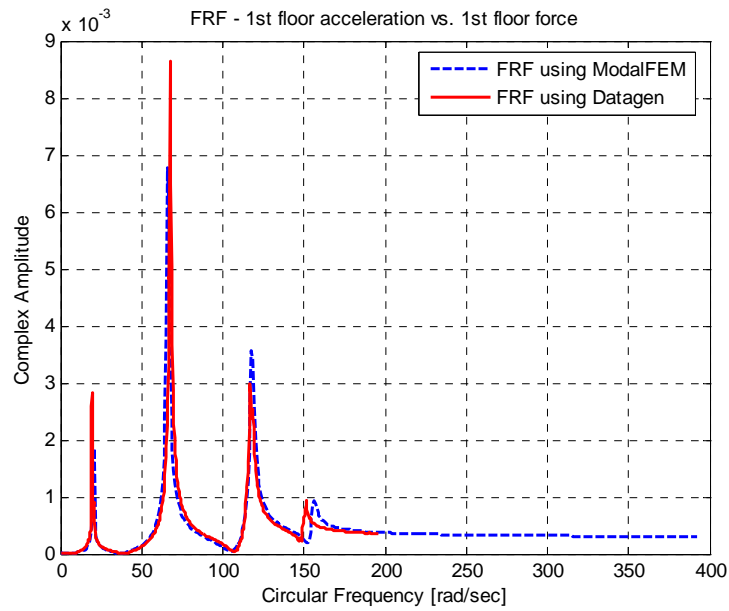


Figure 5.28 Simulated vs. Detected Damages for Trial #12 with Hillclimbing # 9903

5.3.1 Case 1: 1st Story Braces Are Damaged

The results obtained by the SDIM considering damage pattern one (all first story braces are 100% damaged) using Case 1 (12 DOF model) is presented using the MIMO approach in this section. Figures 5.29 to 5.32 show the FRF graphs for this particular damage pattern computed with different excitation/measurement pairs (than the MISO problems).



**Figure 5.29 FRF for the 1st Floor – 1st Story Braces Are Broken
MIMO - 12 DOF Symmetric Model**

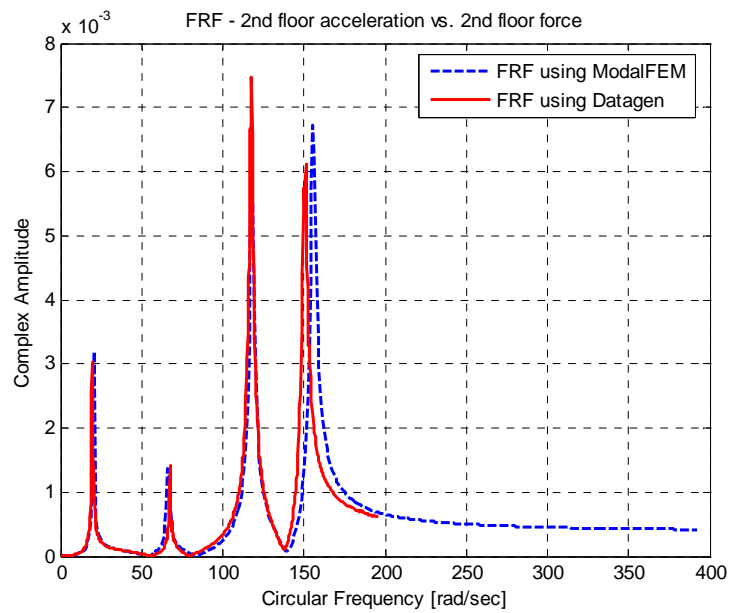


**Figure 5.30 FRF for the 2nd Floor – 1st Story Braces Are Broken
MIMO - 12 DOF Symmetric Model**

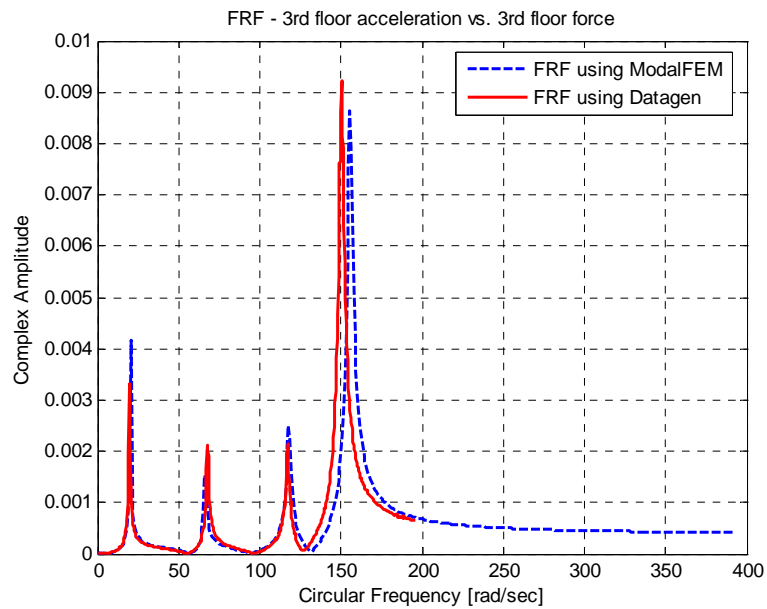


**Figure 5.31 FRF for the 3rd Floor – 1st Story Braces Are Broken
MIMO - 12 DOF Symmetric Model**

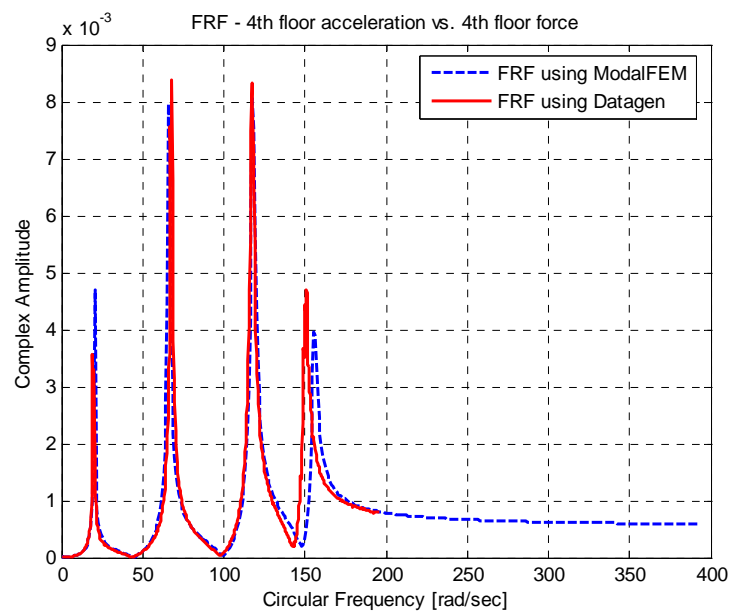


**Figure 5.32 FRF for the 4th Floor – 1st Story Braces Are Broken
MIMO - 12 DOF Symmetric Model**

5.3.1.1 All Four Modes Are Used for Damage Detection

The same kind of analysis as in SIMO problems will be followed in this section. The SDIM is run first using the whole signal length. Then one or two of the last modes shown in the FRF are omitted in order to check whether there is an improvement in the results. It is a useful exercise if one wants to show the amount of information gained (or lost) by simply running SDIM with fewer modes.

**Table 5.25 SDIM Results for 1st Story Braces Damaged Using 4 FRFs – MIMO
Case 1, All Four Modes Are Used**

Trial	Case	Imposed Damage	Sensor Layout	Damaged Elements	Percent
Trial #13	12 DOF-Symmetrical	1st story braces 100%	Full	1st floor brace # 21	65.21%
	Measurements are taken in y- direction			1st floor brace # 25	94.58%
				# 3	62.68%
				# 5	29.52%
				# 13	86.46%
				# 19	41.71%

**Table 5.26 SDIM Results for 1st Story Braces Damaged Using 4 FRFs – MIMO
Case 1, All Four Modes Are Used, After Hillclimbing # 3395**

Trial	Case	Imposed Damage	Sensor Layout	Damaged Elements	Percent
Trial #13	12 DOF-Symmetrical	1st story braces 100%	Full	1st floor brace # 21	60.53%
	Measurements are taken in y- direction			1st floor brace # 25	99.00%
				# 3	54.09%
				# 5	27.13%
				# 13	86.87%
				# 19	52.32%

Tables 5.25 and 5.26 provide the results before and after hillclimbing for this particular case. The hillclimber was able to identify the damage in one of the first story braces as 99% while the other bracing was found to have 60.53% damage. The results for this case is similar to the one obtained for the MISO (when the accelerometer was placed at node 8). Even the damage indices for falsely identified members are close. This is an encouraging result for future direction of the research as it proves that the system is consistent in itself.

Figure 5.33 shows the SDIM results for Trial #13 graphically with and without hillclimbing.

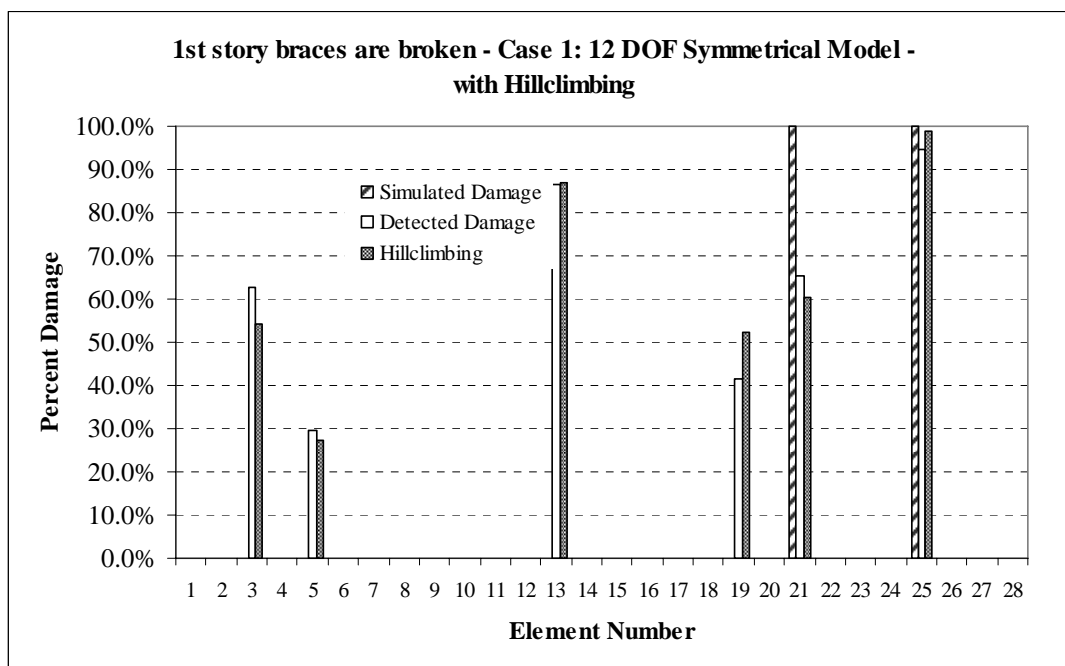


Figure 5.33 Simulated vs. Detected Damages for Trial #13 with Hillclimbing # 3395

5.3.1.2 The Last Mode Is Omitted for Damage Detection

As expected, when the degrading error effects of the last mode are removed from the system, better results were obtained by the SDIM. Although there still were two falsely identified damage members after hillclimbing, member #5 had a relatively small damage index 0.0167 (1.67%). Member #13 was a beam at the damaged (first) floor, which localizes the damage to within the same floor level. This result is as good as any returned from shear building models, as these models can only identify damage to within story levels.

**Table 5.27 SDIM Results for 1st Story Braces Damaged Using 4 FRFs – MIMO
Case 1, The Last Mode Is Omitted**

Trial	Case	Imposed Damage	Sensor Layout	Damaged Elements	Percent
Trial #14	12 DOF-Symmetrical	1st story braces 100%	Full	1st floor brace # 21	78.74%
	Measurements are taken in y- direction			1st floor brace # 25	96.58%
				# 2	11.08%
				# 5	6.77%
				# 13	86.62%

**Table 5.28 SDIM Results for 1st Story Braces Damaged Using 4 FRFs – MIMO
Case 1, The Last Mode Is Omitted, After Hillclimbing # 1232**

Trial	Case	Imposed Damage	Sensor Layout	Damaged Elements	Percent
Trial #14	12 DOF-Symmetrical	1st story braces 100%	Full	1st floor brace # 21	76.49%
	Measurements are taken in y- direction			1st floor brace # 25	99.00%
				# 5	1.67%
				# 13	91.17%

The first floor brace member 25 was identified to be completely damaged, while a better damage indication was obtained at the brace member, #21, as 76.49% compared to Trial #13.

Tables 5.27 and 5.28 present the results in tabular format, while Figure 5.34 plots the percent damages with respect to element number.

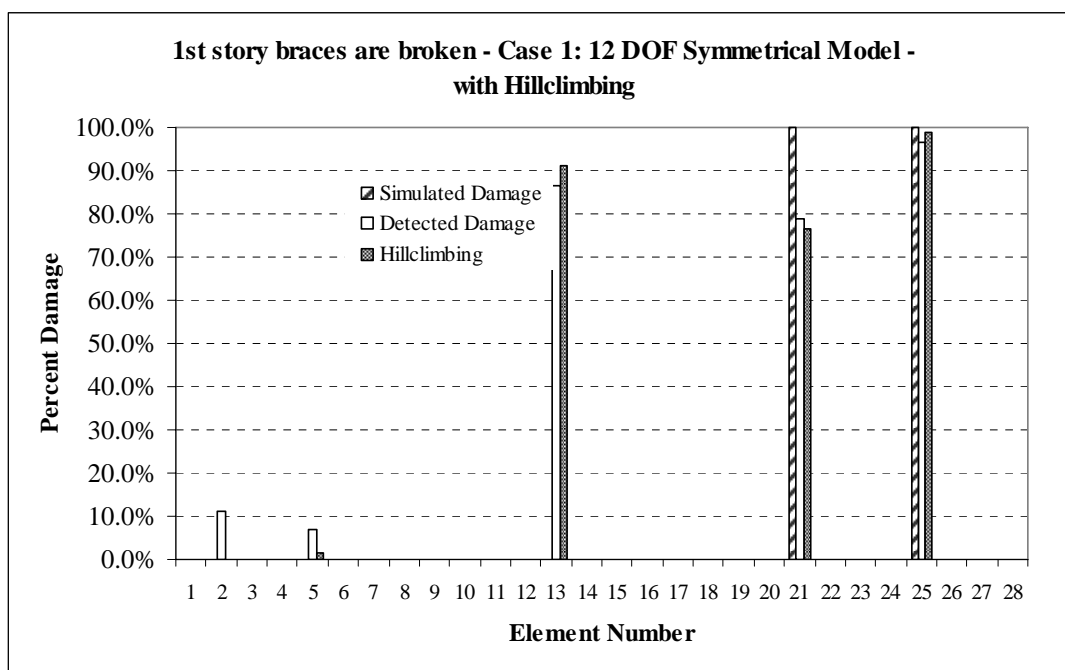
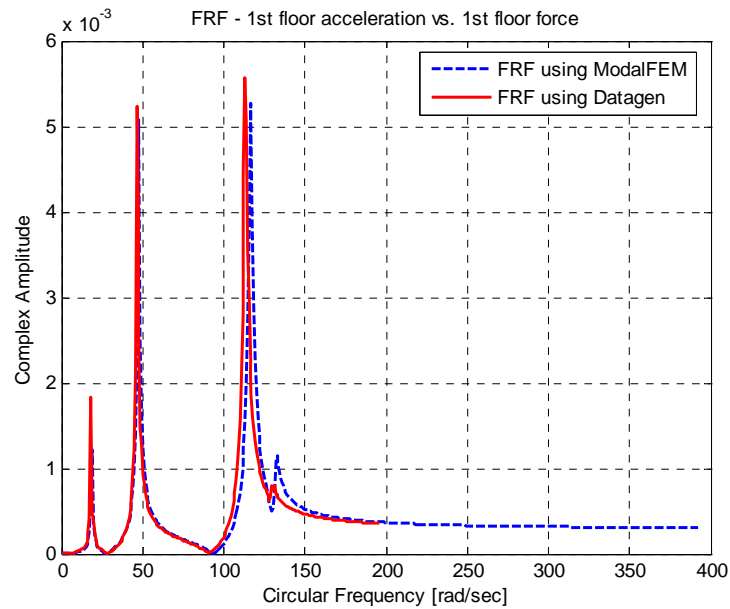


Figure 5.34 Simulated vs. Detected Damages for Trial #14 with Hillclimbing # 1232

5.3.2 Case 1: 1st – 3rd Story Braces Are Damaged

SDIM results for damage pattern two using the 12 DOF model (Case 1) will be presented in this section. Figures 5.35 to 5.38 show the comparison of the FRFs computed using ModalFEM and Datagen.



**Figure 5.35 FRF for the 1st Floor – 1st- 3rd Story Braces Are Broken
MIMO - 12 DOF Symmetric Model**

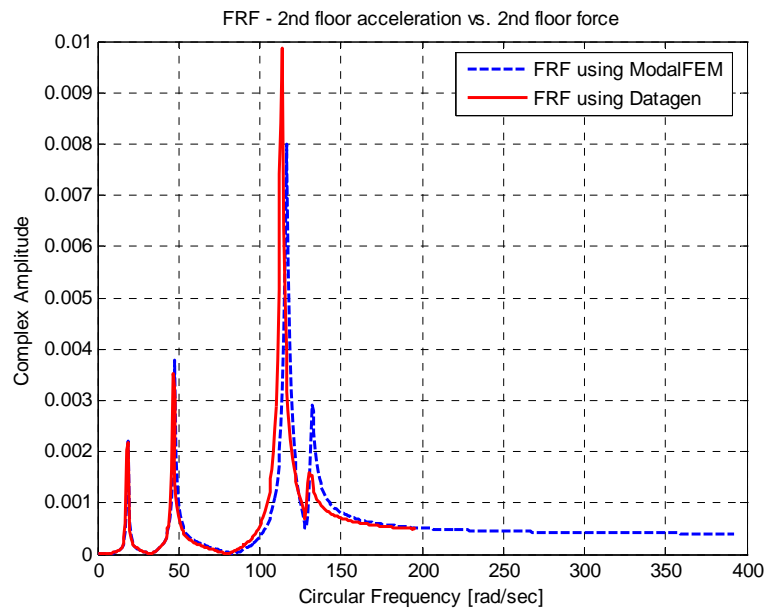


**Figure 5.36 FRF for the 2nd Floor – 1st- 3rd Story Braces Are Broken
MIMO - 12 DOF Symmetric Model**

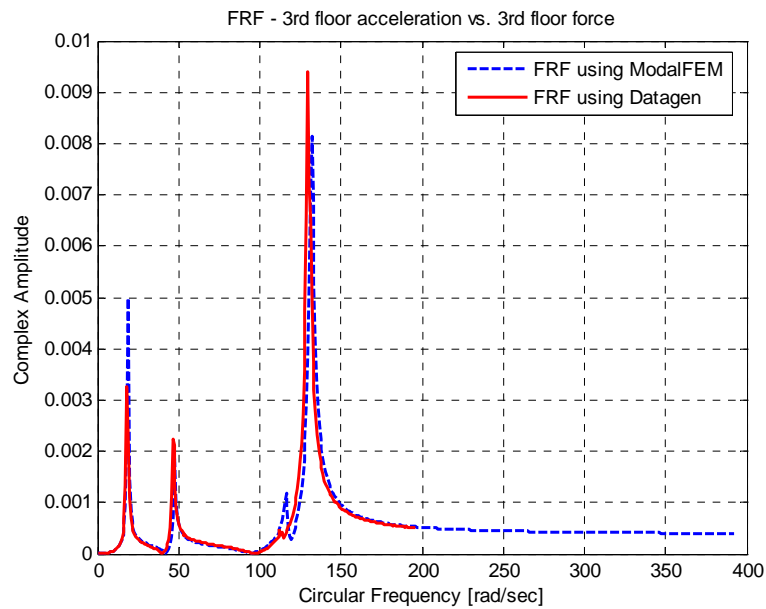


**Figure 5.37 FRF for the 3rd Floor – 1st- 3rd Story Braces Are Broken
MIMO - 12 DOF Symmetric Model**

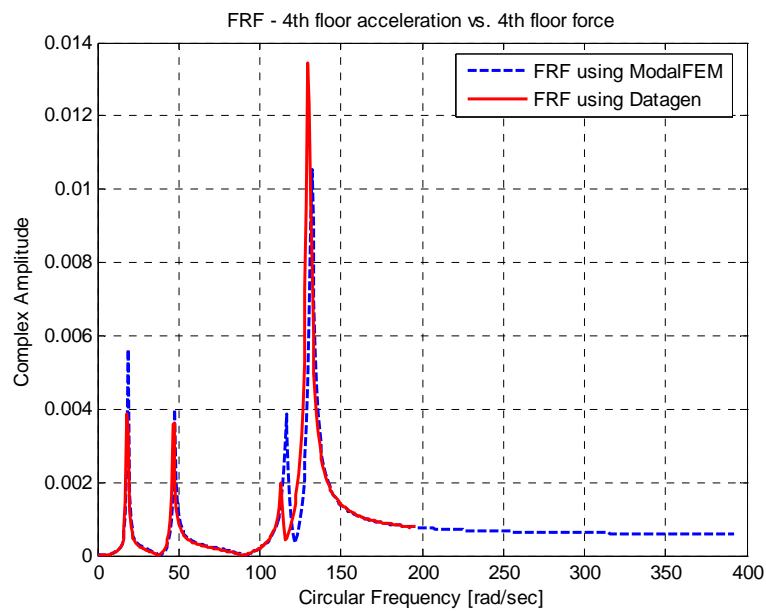


**Figure 5.38 FRF for the 4th Floor – 1st- 3rd Story Braces Are Broken
MIMO - 12 DOF Symmetric Model**

5.3.2.1 All Four Modes Are Used for Damage Detection

The problem is analyzed in two parts again: using all four modes for the FRF information provided to the SDIM and then omitting the last two modes from the FRF information provided to the SDIM. The results obtained will be compared to the results obtained by the SIMO case for the same damage pattern.

This trial gave one of the best results obtained in this research effort by identifying both the first and third story braces to be broken while only giving two falsely detected members, #11 and #22, as damaged with 51.49% and 24.77% respectively.

Tables 5.29 and 5.30 present the SDIM results for this trial before and after hillclimbing. Figure 5.39 presents these results graphically. These results will now be compared with the case where only the first two modes of the FRF were used.

**Table 5.29 SDIM Results for 1st and 3rd Story Braces Damaged Using 4 FRFs – MIMO
Case 1, All Four Modes Are Used**

Trial	Case	Imposed Damage	Sensor Layout	Damaged Elements	Percent
Trial #15	12 DOF-Symmetrical	1st - 3rd story braces 100%	Full	1st floor brace # 21	98.70%
	Measurements are taken in y-direction			1st floor brace # 25	98.47%
				3rd floor brace # 23	98.48%
				3rd floor brace # 27	90.52%
				# 11	51.49%
				# 22	24.77%

**Table 5.30 SDIM Results for 1st and 3rd Story Braces Damaged Using 4 FRFs – MIMO
Case 1, All Four Modes Are Used, After Hillclimbing # 10511**

Trial	Case	Imposed Damage	Sensor Layout	Damaged Elements	Percent
Trial #15	12 DOF-Symmetrical	1 st - 3 rd story braces 100%	Full	1 st floor brace # 21	99.00%
	Measurements are taken in y-direction			1 st floor brace # 25	99.00%
				3 rd floor brace # 23	92.84%
				3 rd floor brace # 27	94.53%
				# 11	55.11%
				# 22	21.87%

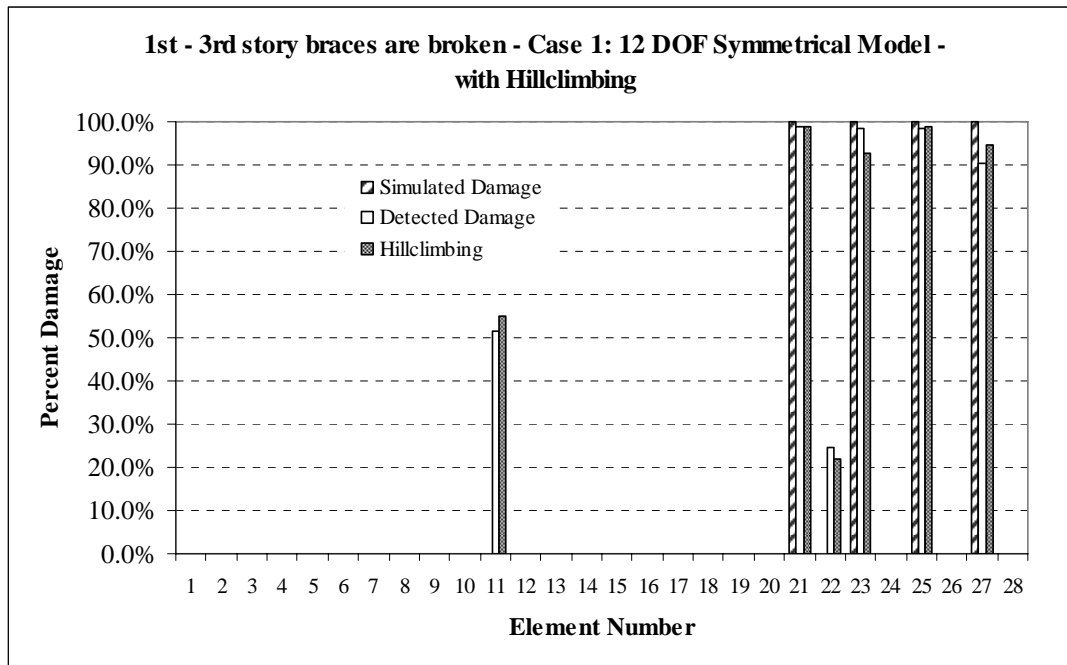


Figure 5.39 Simulated vs. Detected Damages for Trial #15 with Hillclimbing # 10511

5.3.2.2 First Two Modes Are Used for Damage Detection

Tables 5.31 and 5.32 present the results for Trial #16. Unexpected results may seem to be obtained, yet the explanation is simple if Figures 5.35 to 5.38 are examined carefully one more time. The last two modes appear to match pretty well for both programs although a slight shift is visual at the peak values. Omitting these two modes caused the system to lose some valuable information for this case.

If Tables 5.31 and 5.32 are examined, both of the first floor and one of the third floor braces were still identified to be damaged (but with degraded accuracy in identifying the value of the damage indices). However, SDIM failed to locate the damage in one of the third floor braces (namely #23) and detected more falsely damaged members with much higher severity damage indices, such as member 1 with 95.40%, member 15 with 98.58% and member 19 with 92.15%.

Figure 5.40 gives the SDIM results for Trial #16 graphically with and without hillclimbing.

**Table 5.31 SDIM Results for 1st and 3rd Story Braces Damaged Using 4 FRFs – MIMO
Case 1, First Two Modes Are Used**

Trial	Case	Imposed Damage	Sensor Layout	Damaged Elements	Percent
Trial #16	12 DOF-Symmetrical	1st - 3rd story braces 100%	Full	1st floor brace # 21	80.16%
	Measurements are taken in y-direction			1st floor brace # 25	82.93%
				3rd floor brace # 23	0.00%
				3rd floor brace # 27	99.00%
				# 1	96.50%
				# 12	35.58%
				# 15	96.58%
				# 19	71.11%

**Table 5.32 SDIM Results for 1st and 3rd Story Braces Damaged Using 4 FRFs – MIMO
Case 1, First Two Modes Are Used, After Hillclimbing # 5039**

Trial	Case	Imposed Damage	Sensor Layout	Damaged Elements	Percent
Trial #16	12 DOF-Symmetrical	1 st - 3 rd story braces 100%	Full	1 st floor brace # 21	77.67%
	Measurements are taken in y-direction			1 st floor brace # 25	88.42%
				3 rd floor brace # 23	0.00%
				3 rd floor brace # 27	99.00%
				# 1	95.40%
				# 12	67.66%
				# 15	98.58%
				# 19	92.15%

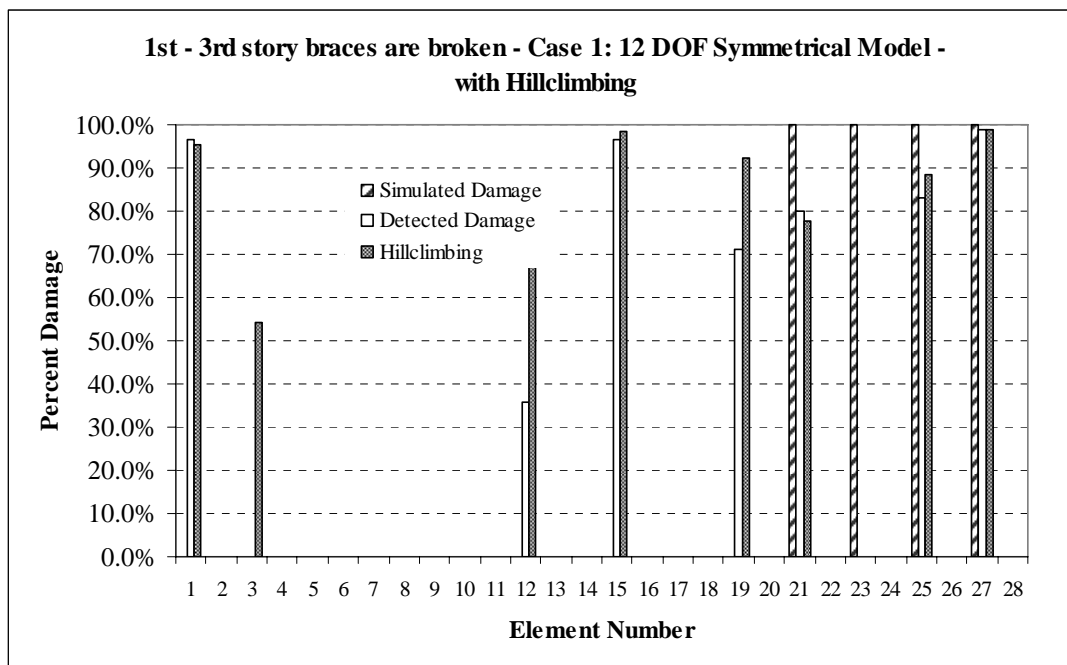


Figure 5.40 Simulated vs. Detected Damages for Trial #16 with Hillclimbing # 5039

5.3.3 Case 1: 3rd Story Braces Are Damaged

This user-defined damage pattern is the last 12-DOF trial that is analyzed as a MIMO problem. Damage is simulated by completely removing the third floor braces from the structure.

Tables 5.33 and 5.34 present the results for the SDIM before and after hillclimbing in tabular format, while Figure 5.41 shows the simulated and identified damages graphically.

The SDIM was able to identify both braces to be damaged, while hillclimbing eliminated one of the falsely detected members from the solution set.

**Table 5.33 SDIM Results for 3rd Story Braces Damaged Using 4 FRFs – MIMO
Case 1**

Trial	Case	Imposed Damage	Sensor Layout	Damaged Elements	Percent
Trial #17	12 DOF-Symmetric	3rd floor braces 100%	Full	3rd floor brace #23	94.96%
	Measurements are taken in y- direction			3rd floor brace #27	92.81%
				# 1	49.59%
				# 10	37.09%
				# 19	52.57%

**Table 5.34 SDIM Results for 3rd Story Braces Damaged Using 4 FRFs – MIMO
Case 1, After Hillclimbing #1266**

Trial	Case	Imposed Damage	Sensor Layout	Damaged Elements	Percent
Trial #17	12 DOF-Symmetric	3rd floor braces 100%	Full	3rd floor brace #23	90.49%
	Measurements are taken in y- direction			3rd floor brace #27	99%
				# 10	52.89%
				# 19	61.94%

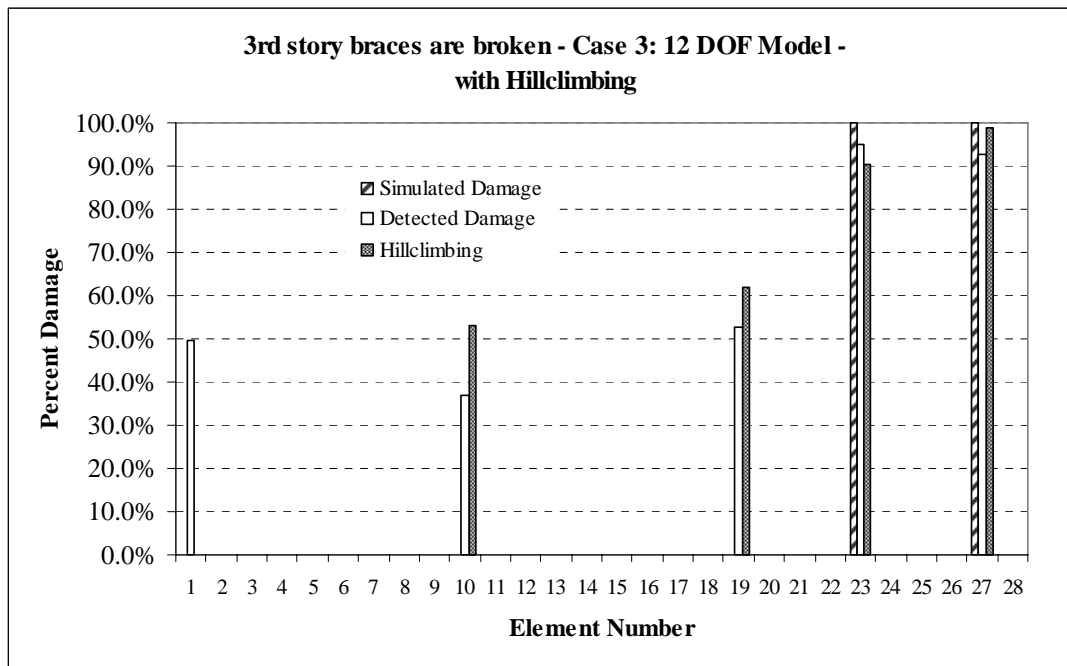


Figure 5.41 Simulated vs. Detected Damages for Trial #17 with Hillclimbing # 1266

5.3.4 Case 2: 1st Story Braces Are Damaged

This case is more complicated than the first one due to the 120-DOF model used. This finite element model combined with asymmetric mass distribution previously proved to work inefficiently for the SIMO cases analyzed in Section 5.1.

The mass distribution is kept to be symmetric in Case 1 and 2, so the effects of 120 DOF model may be analyzed solely in this particular case.

Figure 5.42 presents a demonstrative graph of the FRFs computed for the first floor acceleration/excitation pair. As expected, the shift between the graphs is more obvious in this case as it was for the problems analyzed in Case 5.

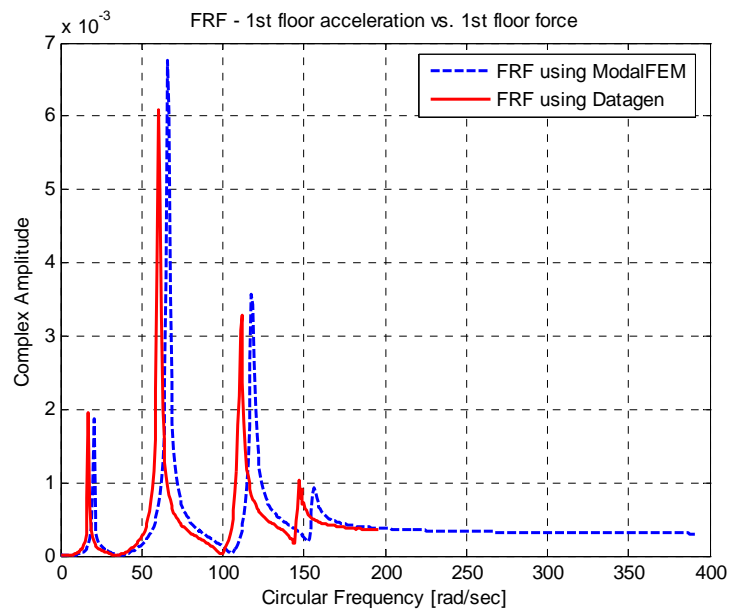


**Figure 5.42 FRF for the 1st Floor – 1st Story Braces Are Broken
MIMO - 120 DOF Symmetric Model**

However, the SDIM results were surprisingly good even when this considerable shift between the two graphs is taken into account.

**Table 5.35 SDIM Results for 1st Story Braces Damaged Using 4 FRFs – MIMO
Case 2**

Trial	Case	Imposed Damage	Sensor Layout	Damaged Elements	Percent
Trial #18	120 DOF-Symmetric	1st floor braces 100%	Full	1st floor brace #21	98.74%
	Measurements are taken in y- direction			1st floor brace #25	98.56%
				# 1	64.94%
				# 11	48.70%
				# 14	87.71%
				# 28	49.73%

**Table 5.36 SDIM Results for 1st Story Braces Damaged Using 4 FRFs – MIMO
Case 2, After Hillclimbing #309**

Trial	Case	Imposed Damage	Sensor Layout	Damaged Elements	Percent
Trial #18	120 DOF-Symmetric	1st floor braces 100%	Full	1st floor brace #21	99.00%
	Measurements are taken in y- direction			1st floor brace #25	99.00%
				# 1	63.92%
				# 11	51.25%
				# 14	88.49%
				# 28	47.95%

Tables 5.35 and 5.36 present the results for this case before and after hillclimbing.

The first floor braces were identified as 99% damaged after hillclimbing, while four undamaged members were also identified to have high severity damage indices. Members #1, #11, #14 and #28 were detected as 63.92%, 51.25%, 88.49% and 47.95% damaged respectively.

Although it may not seem to provide reasonable results, the next trial (Trial #19) is not comparable with this one where at least the actually damaged members were identified to have the highest damage severity (broken completely) in this case.

Figure 5.43 presents the SDIM results for Trial #18 graphically.

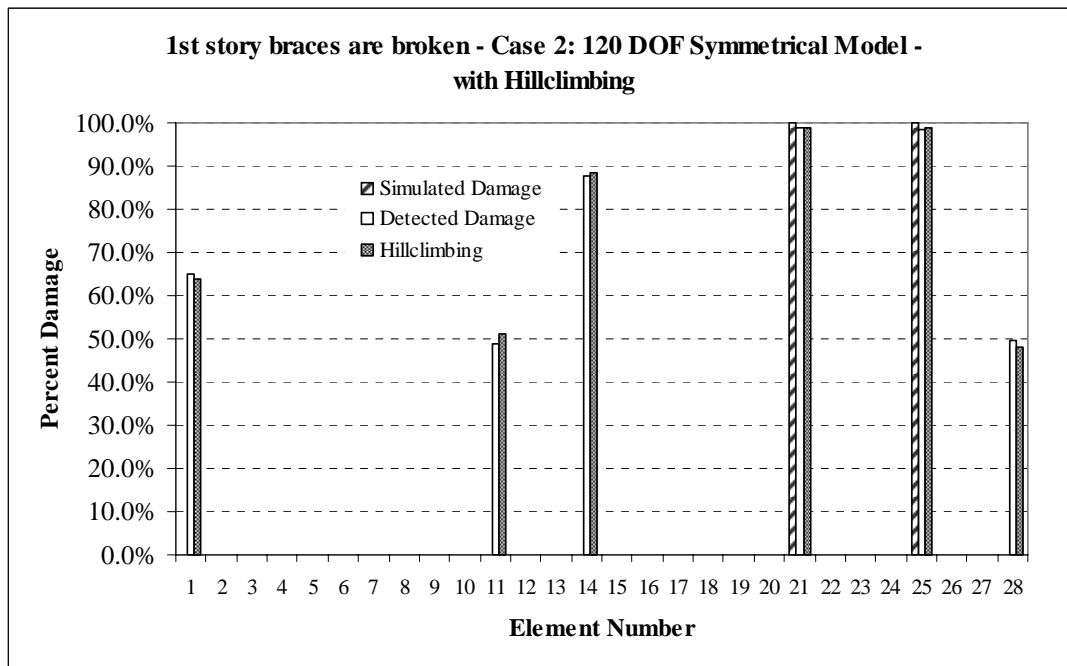
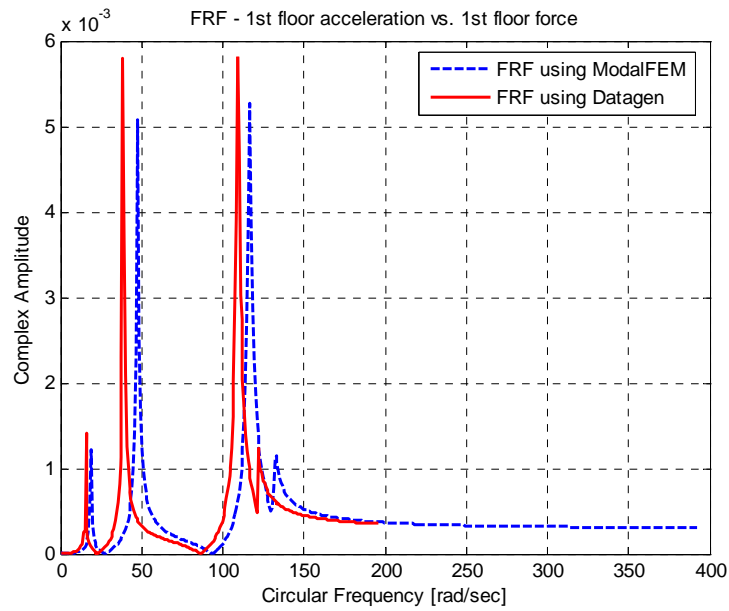


Figure 5.43 Simulated vs. Detected Damages for Trial #18 with Hillclimbing # 309

5.3.5 Case 2: 1st - 3rd Story Braces Are Damaged

After the encouraging results obtained from Trial #18, the outputs of this case were quite surprising, although they should not be if Figure 5.44 is examined. The FRFs are not completely incomparable, as they seem to reflect the behavior of the same structure. However, the shift between the two graphs is so obvious that there should be no need to apply the SDIM to this problem.

Tables 5.37 and 5.38 present the damage detection results in tabular format, where none of the actually damaged members were identified to have any damage non-zero damage indices before or after hillclimbing (although there is no need to run the hillclimber for this case at all). Three members, #1, #13 and #14, were picked as damaged elements by the SDIM with 98.61%, 12.39% and 24.75% damages respectively.



**Figure 5.44 FRF for the 1st Floor – 1st - 3rd Story Braces Are Broken
MIMO - 120 DOF Symmetric Model**

**Table 5.37 SDIM Results for 1st and 3rd Story Braces Damaged Using 4 FRFs – MIMO
Case 2**

Trial	Case	Imposed Damage	Sensor Layout	Damaged Elements	Percent
Trial #19	120 DOF-Symmetric	1st – 3rd floor braces 100%	Full	1st floor brace #21	0.00%
	Measurements are taken in y-direction			1st floor brace #25	0.00%
				3rd floor brace #23	0.00%
				3rd floor brace #27	0.00%
				# 1	98.61%
				# 13	12.39%
				# 14	24.75%

**Table 5.38 SDIM Results for 1st and 3rd Story Braces Damaged Using 4 FRFs – MIMO
Case 2, After Hillclimbing #58**

Trial	Case	Imposed Damage	Sensor Layout	Damaged Elements	Percent
Trial #19	120 DOF-Symmetric	1st – 3rd floor braces 100%	Full	1st floor brace #21	0.00%
	Measurements are taken in y-direction			1st floor brace #25	0.00%
				3rd floor brace #23	0.00%
				3rd floor brace #27	0.00%
				# 1	98.86%

Keeping this last case as an exception, the proposed SDIM provided slightly better results in MIMO problems compared to SIMO cases, especially when the 12-DOF model is used. As model uncertainties dominate the dynamic response of the structure (when the 120-DOF model is used) the credibility of damage detection decreases drastically. Figure 5.45 presents the SDIM results for Trial #19 graphically.

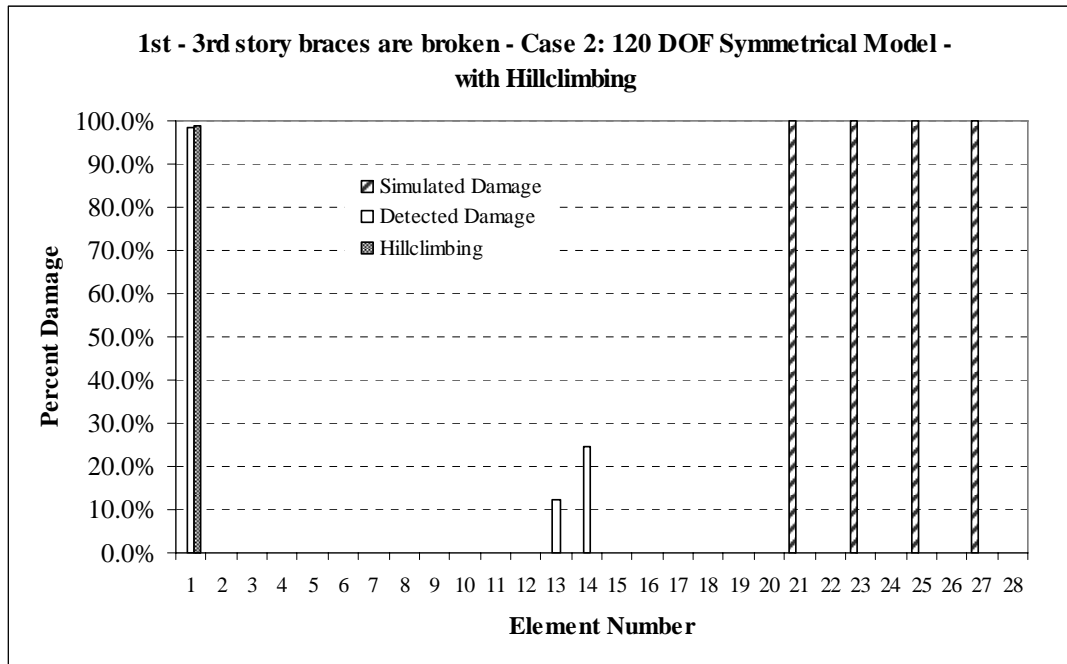


Figure 5.45 Simulated vs. Detected Damages for Trial #19 with Hillclimbing # 58

Even if the FRFs of the benchmark structure can be obtained with full confidence, the input card that currently defines the baseline structure used by the SDIM does not allow the user to work with complicated models.

5.4 Effect of Noise on Performance of the SDIM

The effect of noise on performance of the proposed SDIM is investigated in the section. The accuracy of damage detection degrades with increasing noise levels for any SDIM. Noise is defined as Gaussian pulse processes with RMS %10 of the RMS of the roof acceleration in Datagen and was introduced to system by the parameter sheet shown in Figure 2.8 in Section 2. Accelerometers return noisy sensor measurements and FRFs can be calculated using these acceleration records.

Noise was also introduced to the system in the ModalFEM and compared to the FRFs obtained by Datagen graphically before each trial as usual. The imposed noise level is 10%.

5.4.1 SIMO Model: 1st Story Braces Are Damaged Using Case 3 (10% Noise)

SDIM results for damage pattern one using the 12-DOF model (Case 3) will be presented in this section. Figure 5.46 compares the FRF graphs obtained by ModalFEM and Datagen. In addition to the obvious difference between the last modes of the FRFs, noise causes fluctuations at every frequency.

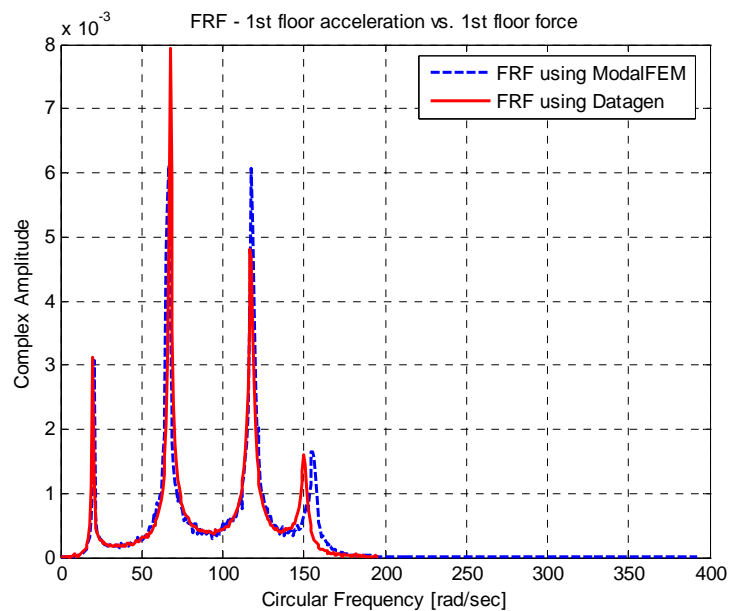


**Figure 5.46 FRF for the 1st Floor – 1st Story Braces Are Broken
SIMO - 12 DOF Symmetric Model (10% Noise)**

The first floor braces were identified as 55.49% and 98.94 % damaged, while several undamaged members were also found to have false positive damage indices. Tables 5.39 and 5.40 present the results before and after hillclimbing. 4976 hillclimbing iterations didn't improve the solution.

**Table 5.39 SDIM Results for 1st Story Braces Damaged Using 4 FRFs (10% Noise) – SIMO
Case 3**

Trial	Case	Imposed Damage	Sensor Layout	Damaged Elements	Percent
Trial #20	12 DOF-Symmetrical	1st story braces 100%	Full	1st floor brace # 21	55.49%
	Measurements are taken in y- direction			1st floor brace # 25	98.94%
				# 3	26.45%
				# 11	30.29%
				# 13	80.17%
				# 14	49.51%
				# 19	58.37%

**Table 5.40 SDIM Results for 1st Story Braces Damaged Using 4 FRFs (10% Noise) – SIMO
Case 3, After Hillclimbing # 4976**

Trial	Case	Imposed Damage	Sensor Layout	Damaged Elements	Percent
Trial #20	12 DOF-Symmetrical	1st story braces 100%	Full	1st floor brace # 21	59.80%
	Measurements are taken in y- direction			1st floor brace # 25	99.00%
				# 3	52.24%
				# 11	1.16%
				# 13	71.43%
				# 14	27.67%
				# 19	58.55%

Slightly different results were obtained in this case compared to one without noise (Trial #1). Thus, the degrading effects of noise weren't so obvious with the exception of one more falsely detected member. This is an expected result since the difference in the FRF graphs is not dominated by noise, but by the difference of the finite element models the two programs (ModalFEM and Datagen) currently use.

Figure 5.47 shows the SDIM results graphically for this trial.

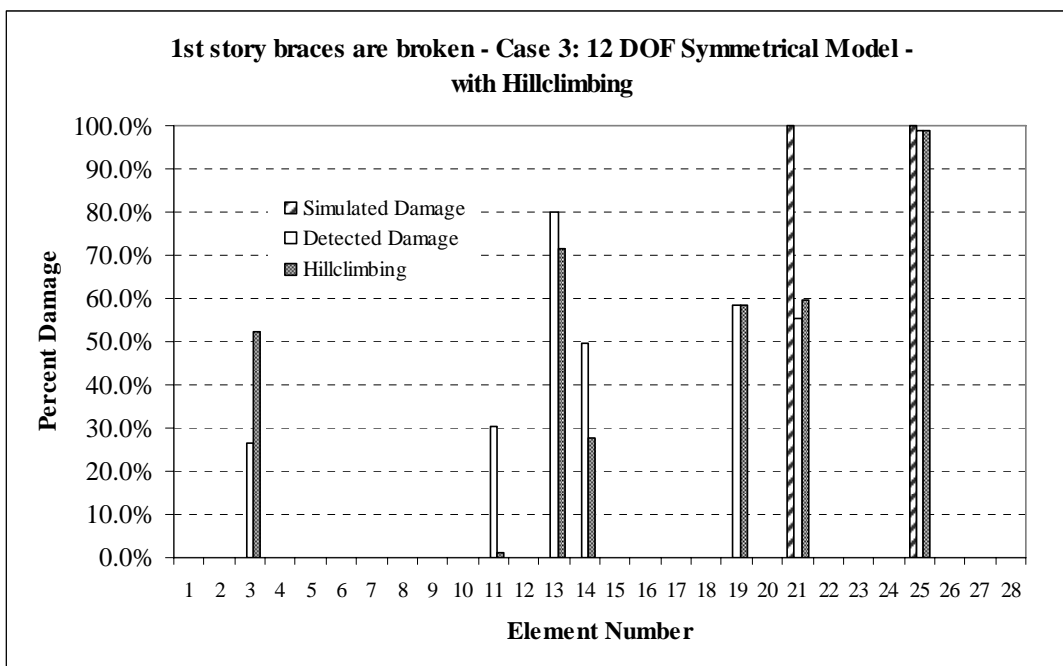
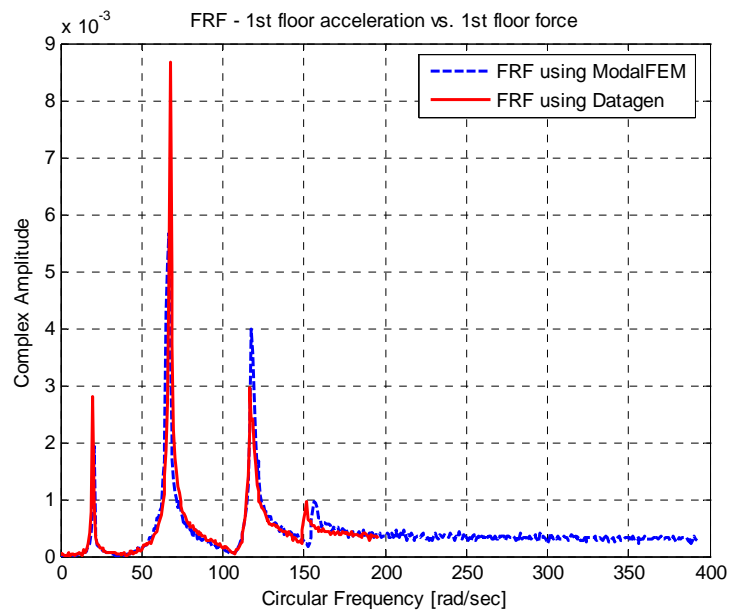


Figure 5.47 Simulated vs. Detected Damages for Trial #20 with Hillclimbing # 4976

5.4.2 MISO Model: 1st Story Braces Are Damaged Using Case 1 (10% Noise)

The SDIM results for damage pattern one using the 12-DOF model (Case 1) is presented in this section. This is the multiple input case, thus it will be analyzed using

MISO and MIMO models separately. Figure 5.48 compares the FRF graphs obtained by ModalFEM and Datagen when the accelerometer is placed at node 7. The effect of noise is more obvious in this trial if the results are compared to the results obtained using noise free measurements (Trial #10).



**Figure 5.48 FRF for the 1st Floor – 1st Story Braces Are Broken
MISO - 12 DOF Symmetric Model (10% Noise)**

Tables 5.41 and 5.42 present the results before and after hillclimbing. One of the first story braces was completely identified to be undamaged while first story column (member #9) was falsely detected as damaged with 88.68% severity instead. Trial #10 certainly provided better results by picking both of the simulated damages and giving less falsely detected members. Figure 5.49 presents the results graphically.

**Table 5.41 SDIM Results for 1st Story Braces Damaged Using 4 FRFs (10% Noise) – MISO
Case 1**

Trial	Case	Imposed Damage	Sensor Layout	Damaged Elements	Percent
Trial #21	12 DOF-Symmetrical	1st story braces 100%	First Floor	1st floor brace # 21	0.00%
	Measurements are taken in y- direction			1st floor brace # 25	97.45%
				# 9	89.72%
				# 22	25.82%
				# 23	26.80%
				# 27	9.31%

**Table 5.42 SDIM Results for 1st Story Braces Damaged Using 4 FRFs (10% Noise) – MISO
Case 1, After Hillclimbing # 4083**

Trial	Case	Imposed Damage	Sensor Layout	Damaged Elements	Percent
Trial #21	12 DOF-Symmetrical	1st story braces 100%	First Floor	1st floor brace # 21	0.00%
	Measurements are taken in y- direction			1st floor brace # 25	98.47%
				# 9	88.68%
				# 22	27.58%
				# 23	28.26%
				# 27	7.02%

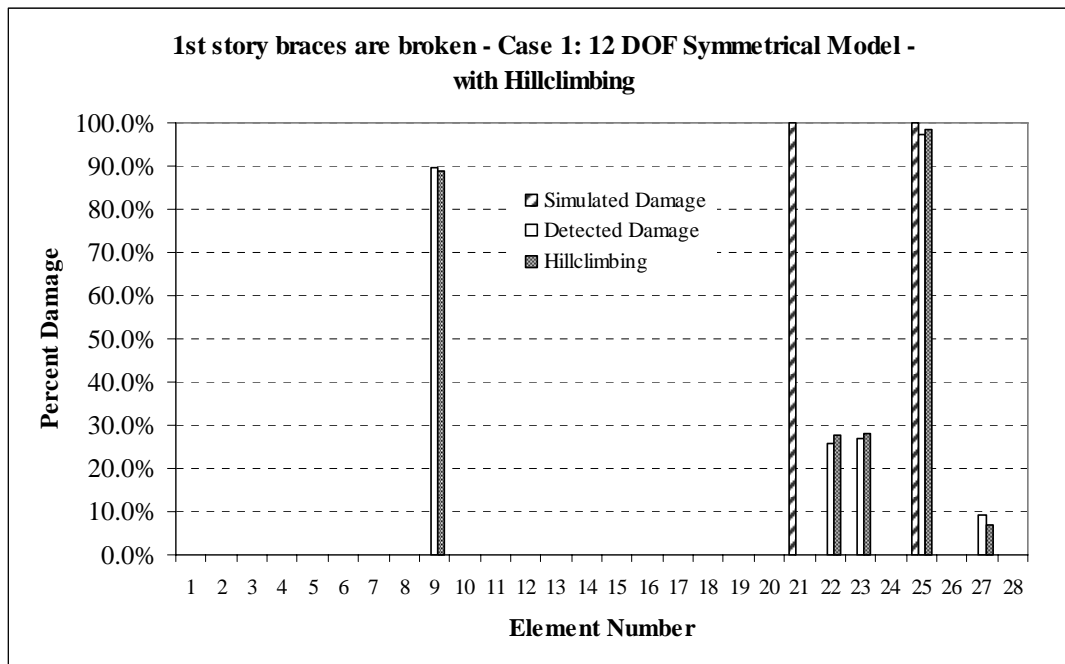
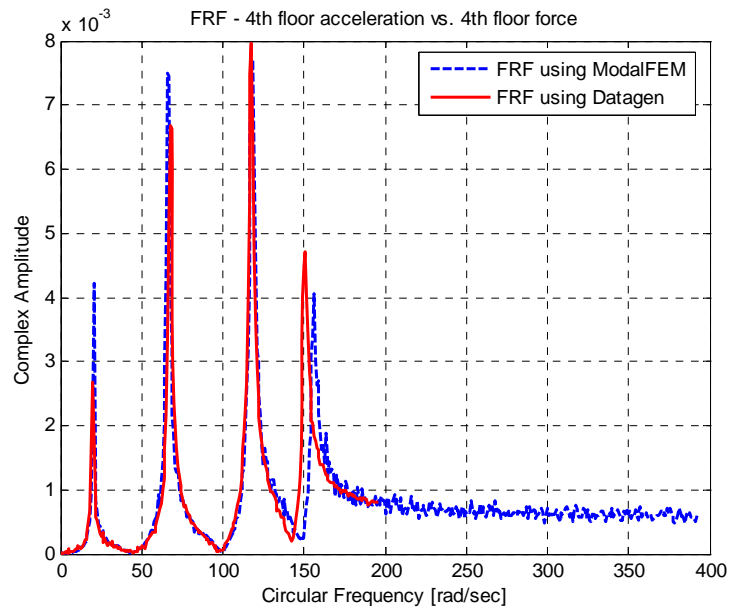


Figure 5.49 Simulated vs. Detected Damages for Trial #21 with Hillclimbing # 4083

5.4.3 MIMO Model: 1st Story Braces Are Damaged Using Case 1 (10% Noise)

The previous problem was solved using the MIMO model. Figure 5.50 compares the FRF graphs obtained by ModalFEM and Datagen. The effect of noise is undetectable if the results are compared with the trial that used noise free measurements (Trial #13).



**Figure 5.50 FRF for the 4th Floor – 4th Story Braces Are Broken
MIMO - 12 DOF Symmetric Model (10% Noise)**

Table 5.43 presents the results without using the hillclimbing feature. The actual damage indices are comparable for the noise free and noisy measurement cases. Even the same members were falsely identified as damaged with one exception (member #3 in Trial #13). It is obvious that noise is not inputting any additional uncertainty to the system. The effect will certainly be more detectable for increasing noise levels. Figure 5.51 presents the results graphically.

Table 5.43 SDIM Results for 1st Story Braces Damaged Using 4 FRFs (10% Noise) – MIMO Case 1

Trial	Case	Imposed Damage	Sensor Layout	Damaged Elements	Percent
Trial #22	12 DOF-Symmetrical	1 st story braces 100%	First Floor	1 st floor brace # 21	75.26%
	Measurements are taken in y-direction			1 st floor brace # 25	84.38%
				# 5	47.97%
				# 13	83.10%
				# 19	68.11%

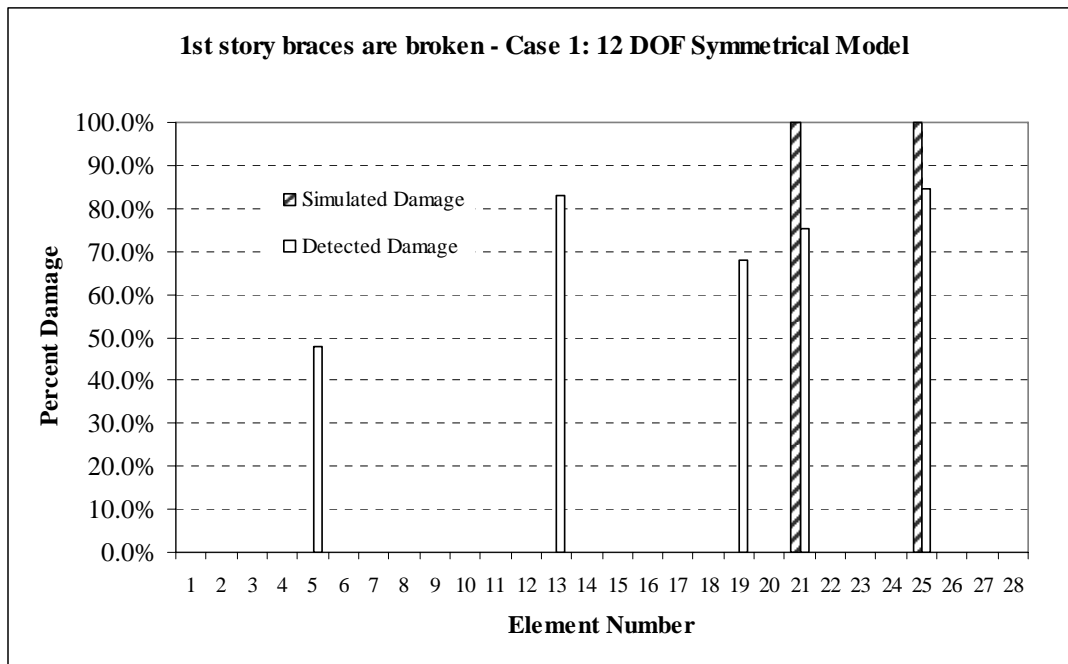


Figure 5.51 Simulated vs. Detected Damages for Trial #22

6 SUMMARY AND CONCLUSIONS

This research evaluated the performance of an existing structural damage detection method when only experimentally-obtained measurement information was available.

The existing SDIM program, GaDamDet, uses an advanced genetic algorithm, along with a two-dimensional finite element model of the structure, to identify the location and the severity of damage using the linear vibration information contained in frequency response functions (FRF) as response signatures. FRFs are obtained by using the utility program, ModalFEM, which simulates the measurement data and generates FRF input files for different finite element models.

Datagen is a Matlab program that simulates the three-dimensional dynamic response of the four-story, two-bay by two-bay UBC test structure built at University of British Columbia. The dynamic response of the structure can be obtained for a range of specific damage cases or for any user-defined damage case. Datagen can be used to provide the FRF measurement information for the three-dimensional test structure.

Instead of using the utility program ModalFEM to simulate the damaged structure's FRFs as was done in the previous research effort, the results of the ASCE Benchmark problem were used to provide the information required for the damaged structure input card by GaDamDet. In the simplest terms, ModalFEM was replaced with the simulated results obtained from the first phase of the ASCE benchmark problem. Several complex issues related to signal processing; including input/output relationships and data processing were investigated in this research.

The first phase of the benchmark problem was divided into two sections according to specific input/output parameters. Datagen provides single and multiple excitation locations at different cases. These parameters are used to obtain the spectral density functions required to perform the frequency response function calculations.

The theory and formulations of input/output relationships for single-input/multiple-output (SIMO), multiple-input/single-output (MISO) and multiple-

input/multiple-output (MIMO) problems were discussed in order to develop a method to compute FRFs from the measurement information obtained for the benchmark structure. Although solving SIMO problems was relatively straightforward, MISO and MIMO models required computations of high complexity. An easy algorithm that uses conditioned spectral density was defined in order to overcome these difficulties. Multiple-input/multiple-output models were treated as a combination of separate and simpler multiple-input/single-output problems and were solved using direct extensions of the techniques developed for MISO problems

The hybrid SDIM method was able to identify the damaged elements correctly, while giving some falsely damaged members. All calculations have been performed using the forcing and acceleration measurements in the weak direction. Since the two finite element models that GaDamDet and Datagen use are quite different (2-D versus 3-D), some falsely damaged members were obtained. The general behavior of the structure, however, seems to be captured using the proposed methodology.

The SDIM provided slightly better results for MIMO problems compared to SIMO cases; however the success of damage detection is mostly related to the accuracy of the finite element model used by the programs rather than the input/output models. Since model uncertainties dominate the dynamic response of the structure, the accuracy of damage detection decreases drastically. Thus, even if the FRFs of the benchmark structure can be obtained with full confidence, the input card that defines the baseline structure does not allow the user to work with complicated models. The degrading effects of noise weren't so obvious since difference in the FRF graphs also is not dominated by noise, but by the difference of the 2-D and 3-D finite element models that the programs use.

Previous studies on the UBC test structure proposed SDIMs that only used the information gathered from the damaged structure. Although, no records taken from the baseline is used to analyze the system in this research, an undamaged finite element model file is constructed that may vary from the original structure. The method provides reliable results in considerable amount of time due to GaDamDet's iterative nature.

The SDIM results are expected to improve as a more accurate finite element model representing the structure is developed.

6.1 Future Recommendations

Upgrading the program in order to allow it to work with 3-D models would be the most important and beneficial recommendation for future research. The main challenges faced in this thesis were related to the accuracy of the finite element model rather than signal processing. The slab elements were so heavy compared to other structural members, thus the dynamic behavior of the structure was highly dominated by the slab elements. Even though the weight of the slabs were simulated using the density card, the rigid effect created by them on the overall structure could not be captured. Using a 3-D finite element model may still have some differences compared to various other models researchers use (such as the 12 and 120 DOF models used in the benchmark problem), but the general behavior would be comparable, and definitely more accurate than using a 2-D frame model.

Although the success of damage detection is mostly related to different structural models than the input/output parameters in this research, spectral densities could only be estimated, thus they may contain random or bias errors (or both). Since the proposed SDIM is highly sensitive, errors occurred during the computation procedure of FRFs combined with the differences in the finite element models, lead to less accurate results.

ModalFEM (thus, GaDamDet) only uses the number of accelerometers to determine the size of the FRF matrices in the system. Extending this feature is also necessary when different excitation location and directions are defined with a 3-D model.

GaDamDet updates the stiffness parameters of the analytical model iteratively, thus requires significant amount of time. Alternative procedures should be considered to reduce this computation time.

The second phase of the benchmark problem applies experimental data to various SDIMs. Due to huge model uncertainties of real-life structures, the results of the second phase of studies could not be performed in this research. Important experimental features such as using hammer test or ambient vibration are not applicable to GaDamDet currently. Even working with forced excitations, the measurements taken from the benchmark structure and ModalFEM have large differences due to the highly asymmetric model of the structure. Even though the input/output algorithms are still applicable to the second phase, the finite element models (as well as the damage cases simulated) are not currently compatible.

REFERENCES

- Au S.K., Yuen K.V. and Beck J.L. (2000). "Two-stage System Identification Results for Benchmark Structure" *Proc., 14th ASCE Engineering Mechanics Conference*, Austin, Texas.
- Bendat J.S., Piersol A.G. (1980). *Engineering Applications of Correlation and Spectral Analysis*. New York, John Wiley and Sons.
- Bendat J.S., Piersol A.G. (2000). *Random Data Analysis and Measurement Procedures*, Third Edition. New York, John Wiley and Sons.
- Bernal, D. and Gunes, B. (2000). "Observer/Kalman and Subspace Identification of the UBC Benchmark Structural Model." *Proc., 14th ASCE Engineering Mechanics Conference*, Austin, Texas.
- Corbin, M., Hera, A., and Hou, Z. (2000). "Locating Damage Regions Using Wavelet Approach." *Proc., of the 14th ASCE Engineering Mechanics Conference*, Austin, Texas.
- Doebbling, S.W., Farrar, C.R., Prime, M.B., (1998). "A summary review of vibration-based damage identification methods." *The Shock and Vibration Digest*, 30(2), 91-105.
- Doebbling, S.W., Farrar, C.R., Prime, M.B., and Schevitz, D.W. (1996). "Damage Identification and Health Monitoring of Structural and Mechanical Systems from Changes in their Vibration Characteristics: A Literature Review, Los Alamos Report." Report No. *LA-13070-MS*, Los Alamos National Laboratory, University of California, Los Alamos, New Mexico.

- Dyke, S.J., Caicedo, J.M., and Johnson, E.A. (2000). "Monitoring of a Benchmark Structure for Damage Detection." *Proc., 14th ASCE Engineering Mechanics Conference*, Austin, Texas.
- Ewins, D.J., (2000). *Modal Testing: Theory, Practice and Applications*. Baldock, England, Research Studies Press Ltd.
- Johnson E.A., Lam H.F., Katafygiotis L.S., Beck J.L. (2000). "A Benchmark Problem for Structural Health Monitoring and Damage Detection" *Proc., 14th ASCE Engineering Mechanics Conference*, Austin, Texas.
- Marwala, T., and Heyns, P.S., (1998). "Multiple-criterion method for determining structural damage." *AIAA Journal*, 36(8), 1494-1501.
- Marwala, T., (2000). "Damage identification using committee of neural networks." *Journal of Engineering Meachanics*, 126(1), 43-50.
- MATLAB Signal Processing Toolbox Version 6*. (2005). Natick, MA, The Mathworks Inc.
- MATLAB user's guide*. (1999a). Natick, MA, The Mathworks Inc.
- Park S., Stubbs N. and Bolton R.W. (1998). "Damage Detection on a Steel Frame Using Simulated Modal Data." *Proc., 16th International Modal Analysis Conference (IMAC XVI)*, Santa Barbara, California.
- Rodriguez R. and Barroso L. (2002). "Stiffness-Mass Ratios Method for Baseline Determination and Damage Assessment of A Benchmark Structure." *Proc., of the American Control Conference*, Anchorage, AK
- Rytter, A., (1993). "Vibration based inspection of civil engineering structures." Doctoral dissertation, Department of Building Technology and Structural Engineering, University of Aalborg, Denmark.

- Sampaio, R.P.C., Maia, N.M.M., Silva, J.M.M., (1999). "Damage detection using the frequency-response-function curvature method." *Journal of Sound and Vibration*, 226, 1029-1042.
- Liszkai T.R. (2003). "Modern heuristics in structural damage detection using frequency response functions" Doctoral dissertation, Department of Civil Engineering, Texas A&M University.
- Lee, U., and Shin, J., (2002). "A frequency response function-based structural damage identification method." *Computers & Structures*, 80, 117-132.
- The IASC-ASCE SHM Task Group Web Site, "Structural Health Monitoring Benchmark Problem", <http://wusceel.cive.wustl.edu/asce.shm>.
- Thyagarajan, S.K., Schulz, M.J., and Pai, P.F., (1998). "Detecting structural damage using frequency response functions." *Journal of Sound and Vibration*, 210(1), 162-170.
- Wang, Z., Lin, R.M., and Lim, M.K., (1997). "Structural damage detection using measured FRF data." *Computer Methods in Applied Mechanics and Engineering*, 147, 187-197.

APPENDIX A

Table A.1. Cards That Can be Used in the Text Input File (*.inp) for the *ModalFEM* Utility Program
(Adapted from Lizskai, 2003)

Card	Usage	Explanation
*Node	*NODE Node #, X-coor, Y-coor	Defines finite element nodes. The first input is the node number followed by the x and y coordinates of the node. The input line can be repeated as many as necessary to define all nodes in the model.
*Element	*ELEMENT, TYPE = B23 Elem. #, 1 st node #, 2 nd node #	Defines finite elements. The “TYPE =” option determines the finite element type (B23 = Bernoulli frame element). The input parameters are the element number followed by the first and second node numbers enclosing that element.
*Material	*MATERIAL, NAME = STEEL	Defines a material. The option “NAME =” is used to uniquely identify this material definition. This card does not have any input parameters but it is followed by other cards defining the material behavior.
*Elastic	*ELASTIC Young’s Modulus, Poisson’s ratio	Preceded by the “*Material” card and defines a linear elastic material. Input parameters are the Young’s modulus and Poisson’s ratio.
*Density	*Density ρ	Preceded by the “*Material” card and defines the mass density of the material. The only input parameter is the mass density ρ .
*Elset	*ELSET, ELSET = NAME Elem. #, Elem. #, Elem. # *ELSET, ELSET = A, GENERATE 1 st Elem. #, Last Elem. #, Increment	Groups selected elements that share some common characteristics. The “ELSET =” option is used to uniquely identify this group of elements. Input parameters are the element numbers. Using “GENERATE” option, element numbers are generated between the first and last element with increment given in the input line.
*Beam General Section	*BEAM GENERAL SECTION, ELSET = ELS_NAME, MATERIAL = MAT_NAME Moment of Inertia, Area	Sectional properties of frame finite element. The option “ELSET =” identifies the element set for which these properties are applied. The option “MATERIAL =” identifies the material used for these set of elements. The input line contains the moment of inertia and the area of the frame element.
*Nset	*NSET, NSET = NAME Node #, Node #, Node #	Defines a set of nodes that share some common characteristics. The input line contains the node numbers in this set and can be repeated as many times as necessary to list all nodes.
*Boundary	*BOUNDARY Nset, DOF	Defines the boundary conditions. The first input identifies the set of nodes for which this boundary condition is applied. The second input parameter identifies the degree of freedom in the local coordinate system that is restrained (1 – horizontal, 2 – vertical, 3 – rotational)

Table A.1. (Continued)

Card	Usage	Explanation
*Step	*STEP	Identifies the beginning of a finite element step
*End Step	*END STEP	Identifies the end of a finite element step
*Frequency	*FREQUENCY Number of modes	Performs mode shape and eigenvalue extraction. The input parameter identifies the number of modes to be extracted.
*Node Print	*NODE PRINT Output *NODE PRINT, NSET = NAME Output	Output request associated with nodal finite element results. If the option "NSET =" is omitted then information for all nodes are output. Using "NSET =" a subset of nodes can be defined. The input line can be U (natural frequencies and mode shapes) provided that the *FREQUENCY card is used in the current step. In a *MODAL DYNAMIC step the input line can be U (displacement), V (velocity), A (acceleration), FRF1, FRF2, FRF3 (accelerance in 1, 2 or 3 DOF).
*Modal Dynamic	*MODAL DYNAMIC $\Delta t, T_{total}$	Defines a response analysis or a frequency response function calculation analysis using modal decomposition. The input line contains the time interval Δt and the total time for the analysis. For the frequency response function analysis the time data are converted into the frequency domain.
*Modal Damping	*MODAL DAMPING Start mode, Last mode, damping	Defines the modal damping ratio for different modes. The first input parameter identifies the starting mode, the second input parameter the end mode and the third input parameter the damping ratio for each mode between the starting and ending modes.
*Base Motion	*BASE MOTION, DOF = #, INPUT = file.ext, SCALE = #	Defines a base motion within a step. The option "DOF =" identifies the degree of freedom for which the base motion is defined. The option "INPUT =" identifies the input file containing acceleration information of the base motion. The option "SCALE =" multiplies (scales) the input data with the provided scale number.
*Cload	*CLOAD, INPUT = file.txt Nset, DOF, scale	Defines a load applied at a node or nodes. The option "INPUT =" identifies the input file containing load data. This parameter is omitted for frequency response function calculations. The first parameter in the input line identifies the node set for which this load is applied. The second parameter identifies the degree of freedom in which the load acts. The third parameter scales the input data (omitted for FRF calculations).
*Noise	*NOISE level, # of measurements	Introduces noise into simulated measurement (frequency response function) data. The first parameter defines the noise level and the second parameter identifies the number of simulated measurements. If the second parameter is more than 1 then the average of the generated frequency response functions are taken.

```

*Node
1,      0.,      0.
2,      0.,      0.9
3,      0.,      1.8
4,      0.,      2.7
5,      0.,      3.6
6,      1.25,    0.
7,      1.25,    0.9
8,      1.25,    1.8
9,      1.25,    2.7
10,     1.25,    3.6
11,     2.5,     0.
12,     2.5,     0.9
13,     2.5,     1.8
14,     2.5,     2.7
15,     2.5,     3.6
*Element, type=B23
1, 1, 2
2, 2, 3
3, 3, 4
4, 4, 5
5, 2, 7
6, 3, 8
7, 4, 9
8, 5, 10
9, 6, 7
10, 7, 8
11, 8, 9
12, 9, 10
13, 7, 12
14, 8, 13
15, 9, 14
16, 10, 15
17, 11, 12
18, 12, 13
19, 13, 14
20, 14, 15
21, 1, 7
22, 2, 8
23, 3, 9
24, 4, 10
25, 7, 11
26, 8, 12
27, 9, 13
28, 10, 14
*MATERIAL, NAME=STEELC
*ELASTIC
2.E11, 0.3
*DENSITY
23400.
*MATERIAL, NAME=STEEL
*ELASTIC
2.E11, 0.3
*DENSITY
7800.
*MATERIAL, NAME=DAMSTEEL
*ELASTIC
0., 0.3
*DENSITY
7800.
*MATERIAL, NAME=STEEL1

```

```

*ELASTIC
2.E11, 0.3
*DENSITY
941259.
*MATERIAL, NAME=STEEL2
*ELASTIC
2.E11, 0.3
*DENSITY
717483.
*MATERIAL, NAME=STEEL3
*ELASTIC
2.E11, 0.3
*DENSITY
493706.
*Elset, elset=BEAMS1
5, 13
*Elset, elset=BEAMS2
6, 7, 14, 15
*Elset, elset=BEAMS3
8, 16
*Elset, elset=COLUMNS
1, 2, 3, 4, 9, 10, 11, 12, 17, 18, 19, 20
*Elset, elset=BRACING
22, 23, 24, 26, 27, 28
*Elset, elset=DBRACING
21, 25
*BEAM GENERAL SECTION, ELSET=BEAMS1, MATERIAL=STEEL1
1.43E-3, 2.44E-6
*BEAM GENERAL SECTION, ELSET=BEAMS2, MATERIAL=STEEL2
1.43E-3, 2.44E-6
*BEAM GENERAL SECTION, ELSET=BEAMS3, MATERIAL=STEEL3
1.43E-3, 2.44E-6
*BEAM GENERAL SECTION, ELSET=COLUMNS, MATERIAL=STEELC
1.133E-3, 0.664E-6
*BEAM GENERAL SECTION, ELSET=BRACING, MATERIAL=STEEL
0.0705E-3, 0.
*BEAM GENERAL SECTION, ELSET=DBRACING, MATERIAL=DAMSTEEL
0.0705E-3, 0.
*Nset, nset=SUPPORT
1, 6, 11
*BOUNDARY
SUPPORT, 1
SUPPORT, 2
SUPPORT, 3
*NSET, NSET=MEAS
7, 8, 9, 10
*NSET, NSET=EXC
10
*STEP
*FREQUENCY
8
*NODE PRINT
U
*END STEP
*STEP
*MODAL DYNAMIC
0.008, 8
*MODAL DAMPING
1, 4, 0.01
5, 8, 0.012
*CLOAD, INPUT=dummy.txt

```

```
EXC, 1, 150  
*NOISE  
0.0, 0  
*NODE PRINT, NSET=MEAS  
FRF11  
*END STEP
```

Figure A.1. Sample Input File of a SIMO Problem for the *ModalFEM* Utility Program

APPENDIX B

Table B.1. List of Files in the Datagen Package
(Adapted from Structural Health Monitoring Committee Website)

M-file name	Function
datagen	The main function of this package. It helps the user to interactively enter all required input parameters for the analysis.
cal_model	Sub-function called by datagen for the formation of the system matrix of the 4-story 2-bay steel frame system.
cal_resp	Sub-function called by datagen for the calculation of the time-domain acceleration responses at measured degrees-of-freedom.
checkboxdlg2	Sub-function called by cal_model for creating an interactive checkbox on screen. It will be called if the user wants to define his/her own damage case other than the 6* damage patterns.
checkbox2	Sub-function called by checkboxdlg2 .
draw3d	The datagen main function will NOT call draw3d. This function is for users to plot the structure out after calling datagen . This function needs some of the output parameters from cal_model .
NJ_integrator**	SimuLink model which is required to do the integration in Nigham-Jennings Algorithm .

Table B.2. List of Input Parameters in the Datagen Package
(Adapted from Structural Health Monitoring Committee Website)

Variable	Representation
caseid	Case index can be 1, 2, 3, 4 or 5. Representing CASE 1 to 5 in Appendix B of the minutes of the meeting at 28-August-2000.
damageid	Damage pattern index can be 0, 1, 2, 3, 4, 5, 6 or 7. 0 stands for undamaged; 1 to 6 stand for damage pattern 1 to 6 in the above mentioned minutes; 7 is user define damage pattern.
methodid	Time-domain response calculation method index; 1 - lsim (You MUST have Control Toolbox) 2 - Nigham-Jennings Algorithm (VERY SLOW) 3 - FAST Nigham-Jennings Algorithm (You MUST have SimuLink)
e	Damping ratio. Default = 0.01
dt	Time step size (unit = second). Default = 0.001
Duration	The time duration for analysis (unit = second). Default = 40
noiselevel	Noise level to be added to the calculated responses for the simulation of measurement noise. Default = 10
S	Force intensity. Default = 150

Table B.2. (Continued)

Variable	Representation
SeedNum	Seed for random number generation. Default = 123
outfile	The name of the output data file. Default = "DATAfile"
Findx	Filter index = 1 or 0 1 - use a filter to handle the direct pass-through problem. 0 - no filter.

**Table B.3. List of Output Parameters in the Datagen Package
(Adapted from Structural Health Monitoring Committee Website)**

Variable	Representation
T	Transformation matrix for the consideration of rigid-floor effect.
force	External loading time history, which depends on the case of study: CASE 1 to 2: force(:,i) is the loading in the y-direction at the i-th floor for i = 1 to 4. CASE 3 to 5: force(:,1) is the loading in the x-direction at the root; and force(:,2) is that in y-direction.
K	System stiffness matrix (transformed).
M	System mass matrix (transformed).
node	Node coordinates and constrain index.
prop	Element group properties.
time	The corresponding time axis.
elem	Element connectivity and element group number.
acc	Simulated acceleration time history with the number of row equals to the number of time step and the number of column equals to the number of measured dofs. acc(:,1) - floor 1 of column 2 in x-direction acc(:,2) - floor 1 of column 6 in y-direction acc(:,3) - floor 1 of column 8 in x-direction acc(:,4) - floor 1 of column 4 in y-direction acc(:,5) - floor 2 of column 2 in x-direction acc(:,6) - floor 2 of column 6 in y-direction acc(:,7) - floor 2 of column 8 in x-direction acc(:,8) - floor 2 of column 4 in y-direction acc(:,9) - floor 3 of column 2 in x-direction acc(:,10) - floor 3 of column 6 in y-direction acc(:,11) - floor 3 of column 8 in x-direction acc(:,12) - floor 3 of column 4 in y-direction acc(:,13) - floor 4 of column 2 in x-direction acc(:,14) - floor 4 of column 6 in y-direction acc(:,15) - floor 4 of column 8 in x-direction acc(:,16) - floor 4 of column 4 in y-direction

VITA

Name: Selcuk Dincal

Address: Texas A&M University, Civil Engineering Department, College
Station, TX 77843

Email Address: selcukdincal@tamu.edu

Education: B.S., Civil Engineering, Osmangazi University, Eskisehir,
Turkey, 2002

M.S., Civil Engineering, Texas A&M University, U.S., 2005